The Eocambrian Valdres Group at Skarvemellen, Mellane

Field observations and sedimentpetrographical analysis

Rikke Øya Småkasin

Master Thesis in Geoscience

Petroleum Geology and Petroleum Geophysics

30 credits

Department of Geoscience

Faculty of Mathematics and Natural Science

University of Oslo

June.2017

The Eocambrian Valdres Group at Skarvemellen, Mellane

Field observations and sedimentpetrographical analysis

Rikke Øya Småkasin

Master Thesis in Geoscience

Petroleum Geology and Petroleum Geophysics

30 credits

Department of Geoscience

Faculty of Mathematics and Natural Science

University of Oslo

June.2017

Abstract

The Eocambrian Valdres Group sedimentary succession at Skarvemellen, Mellane has been studied in this thesis. The Valdres Group is a siliciclastic succession (of at least 4000 m) deposited in a continental rift basin (the Valdres Basin) on the western margin of the continent Baltica. The coarse grained succession is interpreted to have been deposited in a fluvial/alluvial environment as a braided stream deposit, controlled by an active tectonic rift phase.

The Valdres Group sedimentary rocks are one of the least understood sedimentary formations in the Southern Norwegian Caledonides. The aim of this study is to better understand the depositional conditions, way of formation and possible source for the Valdres Group sedimentary rocks, and try to say something about the relation between the Valdres Group and the more studied Hedmark Group of the Hedmark Basin in East.

Sedimentary field data combined with petrgraphical and mineralogical studies (thin section analysis, XRD, SEM and heavy minerals) have been used to interpret the depositional environment. Analysis of the sedimentary facies and facies associations is done to provide a better understanding of the depositional environment and conditions of the Valdres Group. The sedimentary facies (conglomerate, sandstone, silty-to fine-grained sandstone and breccia) represents deposits of varying flow velocity. The facies associations reflect different architectural elements in a braided stream deposit; interpreted to be longitudinal bar-, channel fill-, transverse bar- and glacial deposits.

The sediments are in general sub-rounded to rounded with a high quartz and K-feldspar content indicating a mature nature of the sediments. The heavy mineral content as well as the high content of quartz, K-feldspar and muscovite indicate moderate to long transport. The provenance area for the Valdres Group sedimentary rocks at Skarvemellen is interpreted to be gneisses and volcanic rhyolites of Sveconorwegian origin, more precise Telemark land. The paleocurrent measurements show a transport direction towards East, indicating a possible erosion and sediment transport from the southwestern basin margin of the Valdres Basin.

Acknowledgements

Table of Content

1   Introduction

1.1   Purpose of the study and project description

This master thesis is based on sedimentological logging, sampling and petrographical analysis of the Valdres Group sedimentary succession at Skarvemellen located in Mellane, Østre Slidre, Valdres (Figure 1.1). All the data for the master thesis was collected from Skarvemellen during a joint field work with Kathrine Sørhus the summer and autumn of 2016. The XRD, thin section and SEM analyses of the collected data from Skarvemellen and Rundemellen were conducted in cooperation with Kathrine Sørhus. The Rundemellen data is presented by Kathrine Sørhus (2017) and her findings from Rundemellen, which is situates approximately 2 km North of Skarvemellen (Figure 1.1), will be correlated with the Skarvemellen results. The main studied succession at Skarvemellen were the Rundemellen type sandstones and conglomerates (Figure 1.2) (Loesche and Nickelsen, 1968).

The main goal is to better understand the depositional conditions and way of formation of the Valdres Group by analyzing samples from Skarvemellen. Comparison and correlation with the Rendalen and Ring formations of the Hedmark Group (Nystuen, 1982) will be done to see if there are any relation between the sedimentary formations. The Skarvemellen is correlated with the Ring Formation to investigate if the provenance area were the same for both successions. The Rendalen Formation is interpreted to have been deposited in the continental part of the Hedmark basin (Nystuen, 1982), in a braided stream setting, which probably reflect the same depositional conditions as for the Valdres Group. Supervisor for this thesis is Professor Henning Dypvik, Department of Geoscience, University of Oslo.

The Valdres Group is probably one of the least understood sedimentary formations of the Southern Norwegian Caledonides. The approximately 4000 meter thick siliciclastic succession consists of alluvial/fluvial deposits, deposited in a continental rift basin on the western most part of Baltica in the Eocambrian age (Loesche and Nickelsen, 1968). The Valdres Group sedimentary rocks are well exposed in the study area Skarvemellen (Figures 1.1 and 3.1) and it is possible to map the Valdres Group sedimentary succession far outside the study area. The sedimentary succession is of low metamorphic grade, possible lower green schist facies (Bockelie and Nystuen, 1985, Loesche and Nickelsen, 1968, Kumpulainen and Nystuen, 1985, Heim et al., 1977).

1.1.1 Study area

Skarvemellen (Figure 1.1) is the second highest of four mountains in the Mellane area; Rundemellen (1345 m.a.s.l.), Skarvemellen (1267 m.a.s.l.), Kalvemellen (1136 m.a.s.l.) and Rabalsmellen (1111 m.a.s.l.). The sedimentary rocks were deposited in the Valdres Basin at the Baltoscandian margin, which was formed during the break-up of the supercontinent Rodinia (Lamminen et al., 2015). The sedimentary rocks found in the area today, reflect the tectonic events of the area. During the formation of the Caledonian Orogen the sediments of the Valdres Basin were compressed and transported may kilometers towards SSW in thrust sheets (Nystuen and Lamminen, 2011). Today the sedimentary rocks at Skarvemellen are part of the Skarvemellen anticline representing the overturned limb of the recumbent fold (Loesche and Nickelsen, 1968).
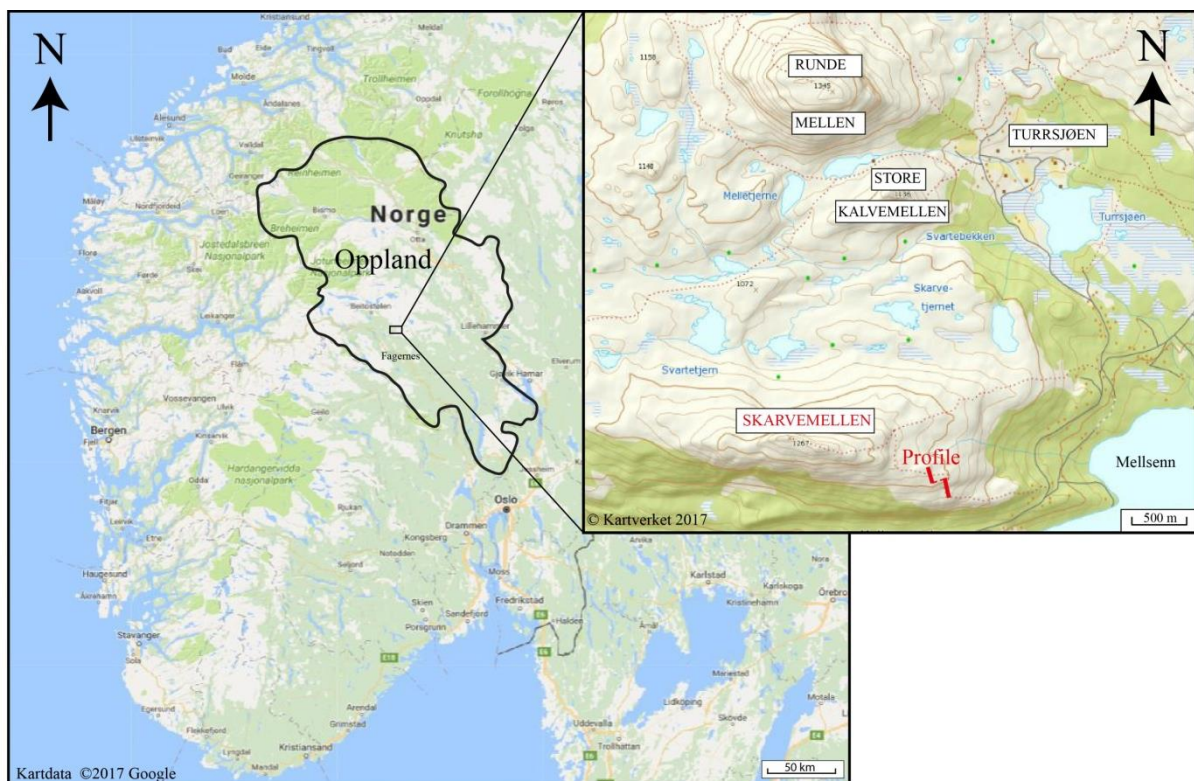
Figure 1.1: Map of the study area Skarvemellen in Mellane, Valdres. Mallane is located in central southern Norway in Østre Slidre, north of Fagernes in Oppland County. The studied profile at Skarvemellen is marked in red. Modified from Google Maps (2017) and Kartverket (2017).

The deformation from the Caledonian Orogeny is today represented in the elongated conglomerate clasts at Skarvemellen (Nickelsen et al., 1985). The elongated conglomerate clasts have partially been deformed, to their present shape, due to the pressure of the Jotun thrust sheet (Loesche, 1967). The Valdres Group sedimentary rocks at Mellene are overturned and situated above the stratigraphically younger Mellsenn Group (Figure 1.2) (Loesche and Nickelsen, 1968). The Valdres Group is separated from the Mellsenn Group by a diamictite (Figure 1.2), interpreted to be a tillite deposited during the Varangian Glaciation (Hossack et al., 1985).

1.1.2 Previous studies

The main focus of previous geological work in the Valdres area has been structural geology and influence of the deformation from the Caledonian Orogeny. The Valdres area has not been studied in detail since the 1970 – 80´s. The bedrock geology of the Valdres area first became known in 1885 when a series of papers and geological maps

Figure 1.2: Lithostratigraphic column of the Valdres Group and the Mellsenn Group sedimentary rocks at Mellane, illustrated stratigraphically right way up. The studied succession in this master thesis is the Rundemellen type up to the tillite, conglomerate 3. The tillite (conglomerate 3) separates the Valdres Group from the younger Mellsenn group. Modified from Hossack et al. (1985) and based on descriptions from (Loesche and Nickelsen, 1968).

of the area were published by Kjerulf during 1885- 1887, Kjerulf and Dahll (1866), and Törnebohm (1873, 1882). The age of the Precambrian basement rocks, the Upper Proterozoic "sparagmites" and the Silurian (Paleozoic) strata were estimated by Kjerulf (1879). "Sparagmite" is an old expression introduced by Esmark (1829) for the coarse grained feldspar rich sandstones deposited in the Baltoscandian basins. This term is no longer in use today, but in the old literature the feldspar rich sediments from the basins of the Baltoscandian margin are called "sparagmites" (Bockelie and Nystuen, 1985). Through a series of profiles,

Kjerulf (1873; 1879) showed characteristic folding characterizing the Upper Proterozoic and Silurian (Figure 1.3) strata of the Lower allochthon (Bockelie and Nystuen, 1985). The overthrust position of deformed Precambrian basement rocks and younger strata were demonstrated by Törnebohm (1888; 1896) (Bockelie and Nystuen, 1985).

The age and tectonic position of the Valdres Group was discussed by Bjørlykke (1901), Goldschmidt (1916) and Strand (1959). They suggested an Upper Ordovician or Lower Silurian age (Figure 1.3) for the Valdres Group. Kulling (1955, 1961) worked on similar sedimentary successions in Sweden, based on this work he suggested an Eocambrian age for the Valdres Group, forming a separate tectonic unit; The Valdres Nappe (Loesche and Nickelsen, 1968). Based on observations at Grønnsennknipa, located southwest of Mellane, Holtedahl (1959) agrees on an Eocambrian age for the Valdres Group. The amount of movement of the Valdres Basin due to Caledonian displacement and the direction of movement is still a debated topic and there is no agreement on the subject, but an Eocambrian age for the Valdres Group sedimentary rock is generally accepted.
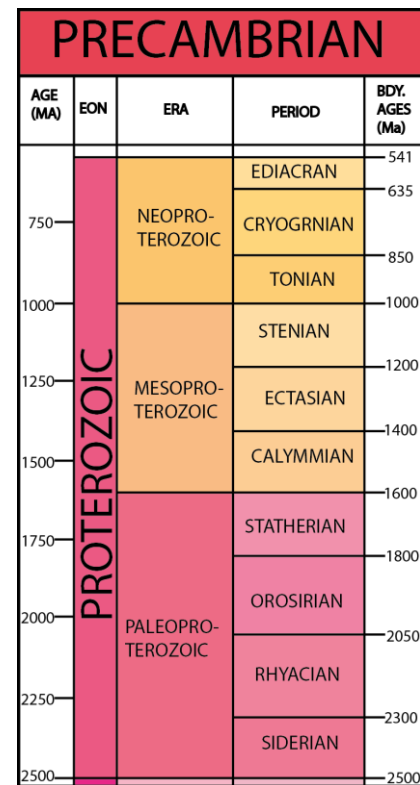
Figure 1.3: Geological time-scale of Precambrian. Modified from Walker et al. (2012).

Detailed description of the sedimentary succession at Mellane is provided by Loesche (1967), based on field observations from Rundemellen and Skarvemellen and petrographic analyses. Several papers are published by Kumpulainen and Nystuen (1985), Nickelsen et al. (1985) and Hossack et al. (1985) discussing the stratigraphy, age and tectonic position of the Valdres Group sedimentary rocks.

2   Geological framework

This chapter presents the tectonic development of the Valdres Basin, Baltoscandian basins and lithostratigraphy of the Valdres Group deposited in the Valdres Basin. The geology of the Valdres area was strongly affected by rifting during the creation of the Iapetus Ocean.

2.1   Tectonostratigraphic development

The Valdres, Hedmark, Risbäck, Engerdalen and Tonsåsfjället Basins are Neoproterozoic basins formed on the western margin of the continent Baltica (Figures 2.1 and 2.2), also called Baltoscandian basins (Lamminen et al., 2015). These basins originated as a result of rifting 750-600 Ma ago in the early stages of the opening of the Iapetus Ocean (Late Neoproterozoic to early Paleozoic times, Figure 1.3) (Lamminen et al., 2015, Nystuen, 1987). During the formation of the Caledonian Orogen the continental rift margins were damaged and the rocks in the sedimentary basins deformed and transported eastward to their present position (Lamminen et al., 2015, Nystuen, 1987). The sedimentological records in the sedimentary basins are highly variable and reflect the structure and morphology of the basin and drainage area (Lamminen et al., 2015).

2.1.1 From the supercontinent Rodinia to the formation of the Caledonian Orogen

The formation of the Baltscandian basins can be related to rift phases that occurred during the break-up of the supercontinent Rodinia (Figure 2.1) at the end of Precambrian 750-600 Ma (Lamminen et al., 2015, Kumpulainen and Nystuen, 1985). During the continental break-up the continent Baltica in the East was separated from the continent Laurentia in the West, resulting in the opening of the Iapetus Ocean.
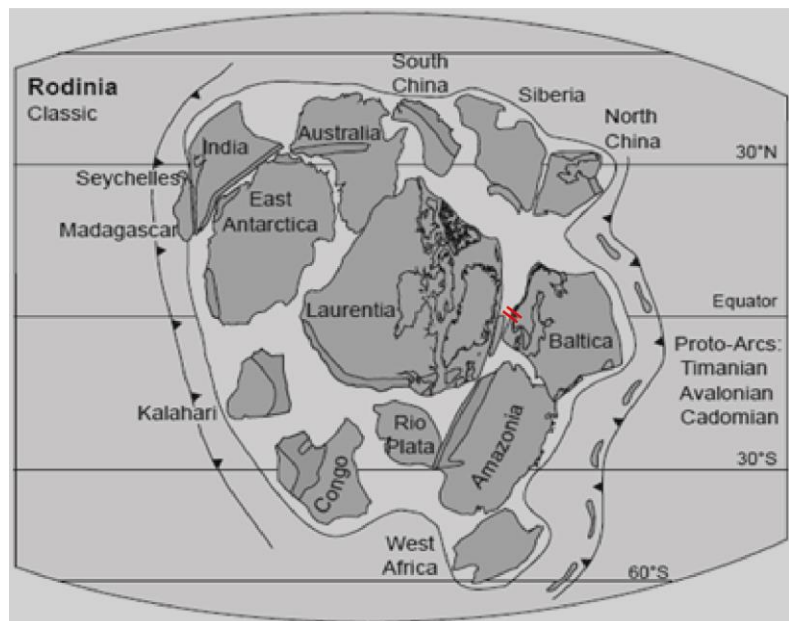
Figure 2.1: Illustration of the supercontinent Rodinia at 750 Ma. The red lines at the continent Baltica indicate the position of the Baltoscandian basins. Modified from Torsvik (2003).

5

At this time the rift basins at the Baltioscandian margin were created (Lamminen et al., 2011). Closing of the Iapetus Ocean started in the Early Ordovician, resulting in the collision of Laurentia and Baltica (400 Ma) initiating the development of the Caledonian Orogeny (490-390 Ma) (Lamminen et al., 2015).

The sedimentary rocks in the Baltoscandian basins were later thrusted and transported several hundred kilometers inland from the Baltoscandian margin (Lamminen et al., 2011, Lamminen et al., 2015). According to Kumpulainen and Nystuen (1985) the Baltoscandian basins may have been transported 100-300 km towards the east/southeast during the Caledonian Orogeny and are now found in thrust sheets, nappes and nappe complexes in southern Norway (Lamminen et al., 2015).

These thrust sheets can be subdivided into Lower, Middle, Upper and Uppermost Allochthon (Lamminen et al., 2011), these will be further explained later in this chapter 2.2. The Caledonian Orogeny is known for its well-developed thrust systems and a exposed width of 200-500km (Gee et al., 2008, Hossack and Cooper, 1986).

2.1.2 Baltoscandian rift basins

Restoration of the Caledonian displacement, strik/dip movement along plate margins and sea floor spreading is necessary to reconstruct the Baltoscandian basins (Nystuen et al., 2008). Previous work on the Baltoscandian basins have been done by Nystuen (1981, 1982) on the "Hedmark" Basin (Figure 2.2), Hossack (1978) and Nickelsen et al. (1985) on the "Valdres" Basin (Figure 2.2), Gee et al. (1978) and Kumpulainen (1980) on the "Tonssåsfjället" Basin, Nystuen (1980) on the "Engerdalen" Basin (Figure 2.2) and Kumpulainen (1982a, 1982b) on the "Risbäck" Basin.

In Neoproterozoic time (Figure 1.3) when the Valdres Basin was formed it was located along the western margin of Baltoscandia (Figure 2.2). During the early rifting stages when the Iapetus Ocean started to open, the Valdres Basin was a shallow continental basin (pers. com. Nystuen, 2017). Coarse clastic sediments started to fill the continental rift basin (Loesche and Nickelsen, 1968). The Valdres Group sedimentary rocks were deposited in an area with high relief, possibly maintained by block faulting (Nickelsen et al., 1985) which is reflected in

the immature petrographic composition, various thicknesses and lithology of the Valdres Group.
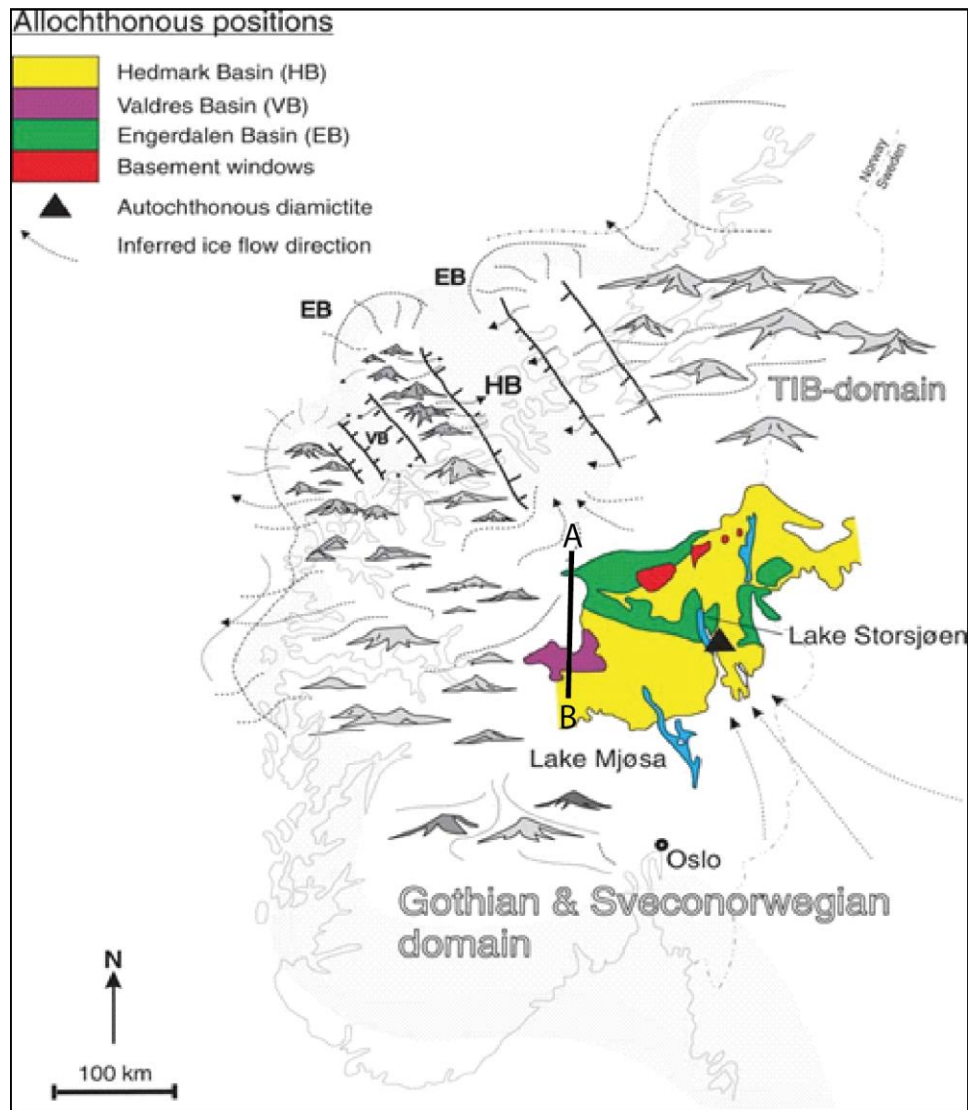
Figure 2.2: The positions of the Valdres and the Hedmark basins outside the western part of Baltica. The colors indicate the present position of the basins, after they were transported as nappes hundreds of km in SE direction during the Caledonian Orogeny (modified from Nystuen and Lamminen (2011)). TIB – Transscandinavian Igneous Belt. The inferred ice flow direction is from the Varangian Glaciation. The black A – B line marks the position of the thrust sheet cross-section Figure 2.5.

The Baltoscandian rift successions is reflected by 5000-6000 m thick sequence, with laterally large facies variations; from marginal alluvial or deep marine sandstones and shales, or alluvial plain sandstones (Kumpulainen and Nystuen, 1985). The largest and most studied Baltoscandian basinal successions are the ones of the Hedmark Basin (Figure 2.2). According to Bockelie and Nystuen (1985) the Hedmark Basin was 200-300 km wide in east-west direction and stretched a few hundred kilometers in NNE-SSW direction. The Hedmark Group consists of at least 4000 meter thick sedimentary successions, consisting of turbidite

sandstones and mud in the western part of the basin (Nystuen, 1987). In the eastern continental part of the basin the deposits of the Rendalen Formation are coarse grained sandstones of braided river system configuration (Bjørlykke et al., 1976). These deposits are overlain by approximately 2000 meter of younger Cambrian strata (Bockelie and Nystuen, 1985).

Nystuen (1987) divided the rift episodes creating the Baltoscandian basins into three thermo-mechanical phases:

1) Initial crustal stretching
2) Basin widening and eastward moving fault block systems
3) Thermal cooling

During the initial crustal stretching (1) the basins were filled with sand and gravel from the surrounding rivers (Nystuen, 1987). The opening of the Iapetus Ocean resulted in more stretching of the crust and basinal widening (2). In the Neoproterozoic time the sea level started to rise (Figure 1.3). This is thought to be related to an interglacial period when small amounts of the Earths water were tied up in glaciers. The sea level transgressed Baltica (750-650 Ma) creating huge accommodation space in the Baltoscandian basins (Nystuen, 1987). Sand and gravel-fans were deposited along the basin margins, recognized as conglomerate and coarse-grained sandstone deposits (Figure 2.6) containing fragments of surrounding litholgies. During the thermal cooling stage (3) fluvial and shallow marine siliciclastic sedimentation were deposited and glacial till from the Varangian Glaciation (650 Ma) (Nystuen, 1987). The Moelv Tillite was deposited during the Varangian Glaciation and is represented in several of the Baltoscandian rift basins, including the Valdres Basin (Figure 2.6). The transgression in early Cambrian marks the end of the Baltoscandian rifting episode (Nystuen, 1987).

During the Varangian Glaciation, ice sheets covered large areas of Baltica (Nystuen and Lamminen, 2011). The ice sheet moved towards west and into the Baltoscandian basins (Figures 2.2 and 2.3) and glacial tills where deposited in the Valdres and Hedmark basins. The tillite is an important regional stratigraphic correlation marker. According to Kumpluainen and Nystuen (1985), this tillite is not found East of the Caledonian thrust sheets in Scandinavia.
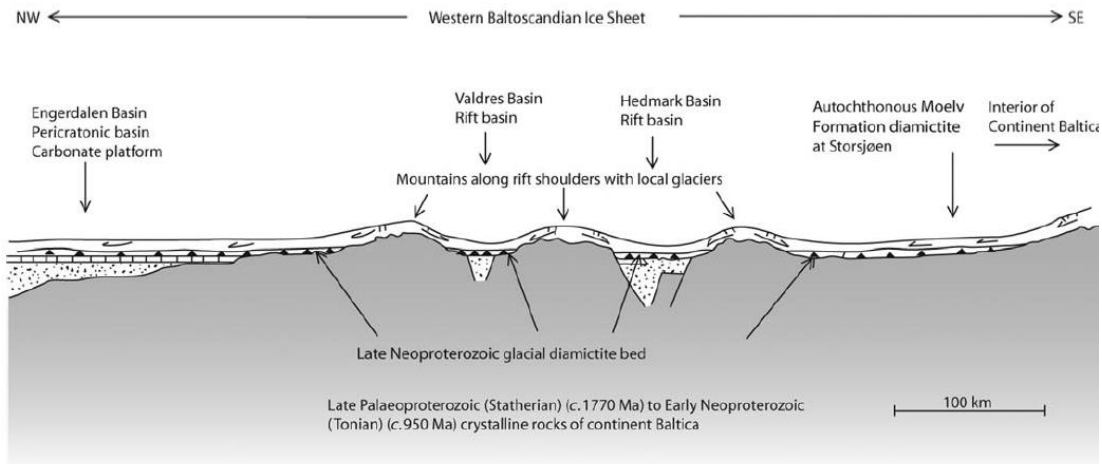
Figure 2.3: Cross section of the western Baltoscandian craton with the position of the Hedmark, Valdres and Engerdalen basins. The illustration shows the Western Baltoscandian Ice Sheet covering the Baltoscandian basins during the Varangian Glaciation. (Nystuen and Lamminen, 2011)

2.2 Thrust sheets

The Caledonian thrust sheets can be divided into the Lower, Middle, Upper and Uppermost allochthones, each consisting of several thrust sheets (Figure 2.5) (Lamminen et al., 2015). The lower allochthon consists of the Synnfjell and Osen-Røa thrust sheets (Figure 2.4), the Middle allochthon of the Jotun and Valdres thrust sheets and the Upper allochthon consist of the Trondheim thrust sheet. The Hedmark Basin is located in the lower allochthon and the Valdres and Engerdalen basins in the middle allochthon. The Lower and Middle allochthones
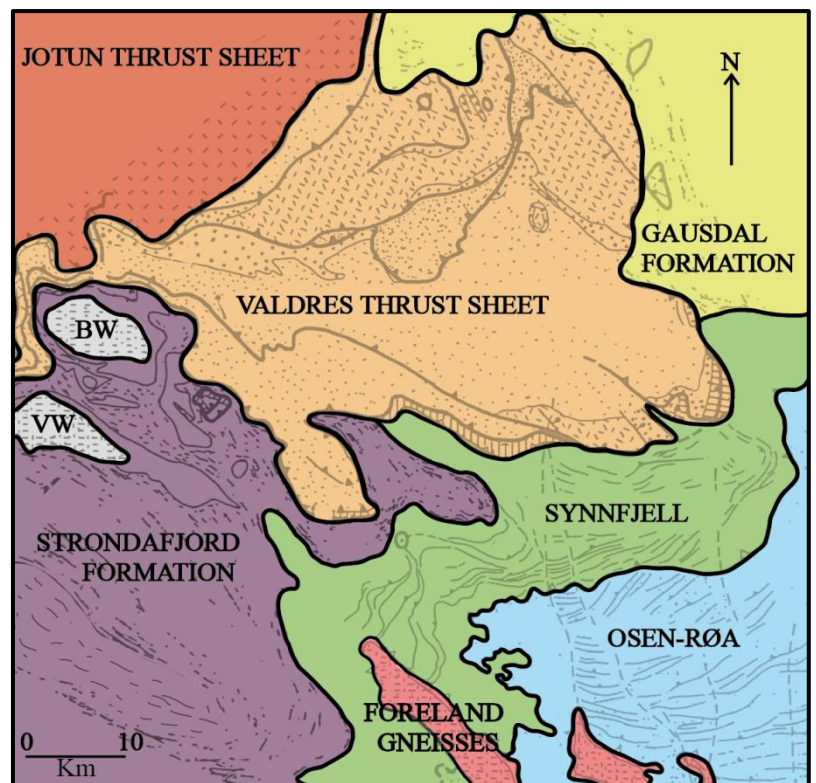
Figure 2.4: Thrust sheets of the Lower Allochthon (Synnfjell and Osen-Røa) and the Middle Allochthon (Jotun and Valdres thrust sheets). The basement windows are shown in grey color; BW is the Beito window and VW is the Vang window, modified from Nickelsen et al. (1985).

probably originate from the western Baltoscandian margin and the affinity of the Uppermost allochthon is probably Laurentian (Lamminen et al., 2015).

Lower allochthon

The lower allochthon (Figure 2.5) consists of the Synnfjell thrust sheet and the Osen-Røa thrust sheet (Figure 2.4) (Bockelie and Nystuen, 1985). Within the Synnfjellet thrust sheet (Figures 2.4 and 2.5) sedimentary rocks of the Dalselvi and the Ørneberget formations are repeated. The Dalselvi Formation has been correlated with the sedimentary rocks of the Valdres Group, and the Ørneberget Formation with the sedimentary rocks of the Mellsenn Group (Nickelsen et al., 1985). The Hedmark Group sedimentary rocks of Upper Proterozoic to Lowermost Cambrian age are located in the Osen-Røs thrust sheet (Figures 2.4 and 2.5).
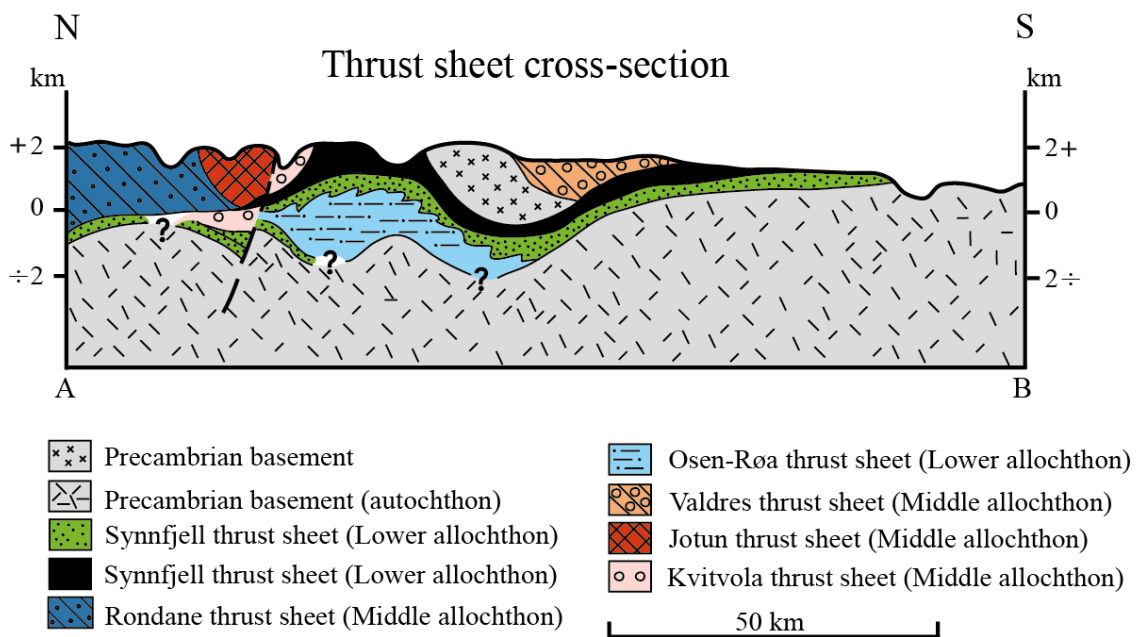
Figure 2.5: Thrust sheet cross-section of the southeastern part of the Scandinavian Caledoniedes. Position of the cross-section is seen in Figure 2.2. Modified from Bockelie and Nystuen (1985).

Middle allochthon

The Middle allochthon consists of the Jotun and the Valdres thrust sheets (Figures 2.4 and 2.5). The Jotun thrust sheet has been thrusted over the Valdres trust sheet. This resulted in deformation of the Valdres Group sedimentary rocks within the Valdres thrust sheet (Figure 2.5). The Jotun thrust sheet consists of basement rocks, where the oldest are the basement gneisses (Hossack et al., 1985), these are also present in the Valdres thrust sheet. According to Hossack et al. (1985) there is no agreement on the transport length of the Jotun thrust sheet. The Valdres thrust sheet consists of Precambrian gneisses overlain by the Valdres Group, which in turn is overlain by the youngest sequence within the thrust sheet, the Mellsenn Group (Hossack et al., 1985). An equivalent to the Valdres thrust sheet is the Kvitvola thrust sheet in the East.

2.3   Lithostratigraphy of the Valdres and Hedmark Basin.

2.3.1 Mellsenn Group

The Mellsenn Group is described by Loesche (1967) and consists of a 240 meters thick sequence of quartzites and slates (Figures 1.2 and 2.6). The occurrence of *graptolites* and *dictyonema* in the sedimentary rocks suggest an Cambrian-Ordovician age for the Mellsenn Group (Nickelsen et al., 1985). The tillite separates the Mellsenn Group from the Valdres Group (Figures 1.2 and 2.6).

2.3.2 Valdres Group

The sedimentary rocks of the Valdres Group make up a sequence of a thickness of at least 4000 meters and is characterized by coarse clastic arkosic sandstones and conglomerates (Figure 2.6) (Nickelsen et al., 1985). This coarse grained formation is thought to have been deposited by a braided stream, on braided plain, alluvial fan or alluvial flood plains, in response to tectonic activity along the marinas of the basin (Kumpulainen and Nystuen, 1985).

During the Late Precambrian (Figure 1.3) the sediments were generally deposited in fining-upward successions. They display massive or planar cross bedded feldspathic arenites and conglomerates (Figure 1.2) (Nickelsen et al., 1985). Two main conglomerate units occur within the Valdres Group, a quartzite conglomerate and a conglomerate containing volcanic clasts (conglomerate 2 and 3, Figure 1.2) (Loesche, 1967). The quartzite conglomerate is situated at the top of Skarvemellen and north at Rundemellen (Loesche, 1967). The conglomerate clasts have been post-depositionally elongated due to the pressure from the overlying Jotun thrust sheet and the thickness of the sedimentary rocks at Mellane is probably tectonically reduced (Loesche, 1967). The Valdres Group sedimentary rocks can be divided into three feldspatic arkoses, each given their name according to where they have been discovered and described: Rabalsmellen type, the Rognslifjell type and the Rundemellen type (Nickelsen, 1967), as seen in Figure 1.2.

The *Rabalsmellen type* is the oldest of the three types of arkoses and represents the most common arkose found at Mellane (Figure 1.2) (Loesche, 1967). Coarse and fine-grained layers alternate and the color vary from green and pink towards gray. Conglomerates have not

been found within the Rabalsmellen type arkose (Figure 1.2). Dark stripes are often enriched in heavy minerals, probably formed due to hydrothermal activity before deposition, now found as clastic grains (Loesche, 1967). The thickness is suggested to be around 1000 meter (Loesche and Nickelsen, 1968).

The *Rognslifjell type* arkose is very coarse grained and poorly sorted. The color is green gray, dark gray and pink or red and is known as the "tricolor sandstone". It consists of normal arkose and quartzites. The Rabalsmellen type is approximately 130 m thick with quartzite and quartz-feldspar conglomerate (10-30m) (Conglomerate 1, Figure 1.2) at the top separating the Rognslifjell type from the Rundemellen type (Loesche, 1967).

The *Rundemellen type* arkose covers large areas at Mellene and is the most common type at Skarvemellen and Rundemellen. It is a medium-grained, feldspathic sandstone ranging in color from pink to red and purple, approximately 650 meters thick (Loesche, 1967). The Rundemellen arkose alternates with conglomerate layers, as seen in Figure 1.2 (Conglomerate 2). Volcanic fragments of rhyolite have been found in the conglomerates within the Rundemellen type sandstone (Figure 1.2) (Loesche, 1967).

Tillite (Conglomerate 3, Figure 1.2): Is a poorly sorted glacial moraine containing rock fragments of different sizes and shapes as described previously. Thickness of the tillite in the Valdres Group ranges from 0.5 – 3 meter (Loesche, 1967) and separates the Valdres Group from the Mellsenn Group (Figures 1.2 and 2.6).

2.3.3 Hedmark Group

Ring Formation

The Ring Formation is a marine succession of the Neoproterozoic Hedmark Basin (Figure 2.6), with sediments interpreted to be deposited on the *Ring submarine fan* (Bockelie and Nystuen, 1985). The Ring Formation consists of an 300 meter thick unit of coarse clastic arkoses and conglomerates (Nystuen, 1999). Bjørlykke et al. (1976) suggested that the top of the Ring Formation included fluvial facies as well as sub-marine facies, whereas Nystuen (1987) interpreted the Ring Formation as mainly representing submarine gravity flow.

Rendalen Formation

The Rendalen Formation consists of at least 2500 m thick fluvial arkosic sandstone interbedded with conglomerates and mudstone (Figure 1.2) (Nystuen, 1982). The Rendalen Formation is interpreted to be deposited in braided plains on the eastern continental part of the Hedmark Basin (Figure 2.6) (Nystuen, 1982). The succession is composed of coarse-grained sandstone ranging in color from red to light gray (Nystuen, 1982). The fluvial sandstones of the Rendalen Formation are interpreted as the eastern equivalent to the turbidities of the Brøttum Formation in the western Hedmark Basin (Figure 2.6) (Nystuen, 1982). Based on zircon dating from Bingen et al. (2005a) the age of the Rendalen formation is of Meso-proterozoic age 1600-1500 Ma.
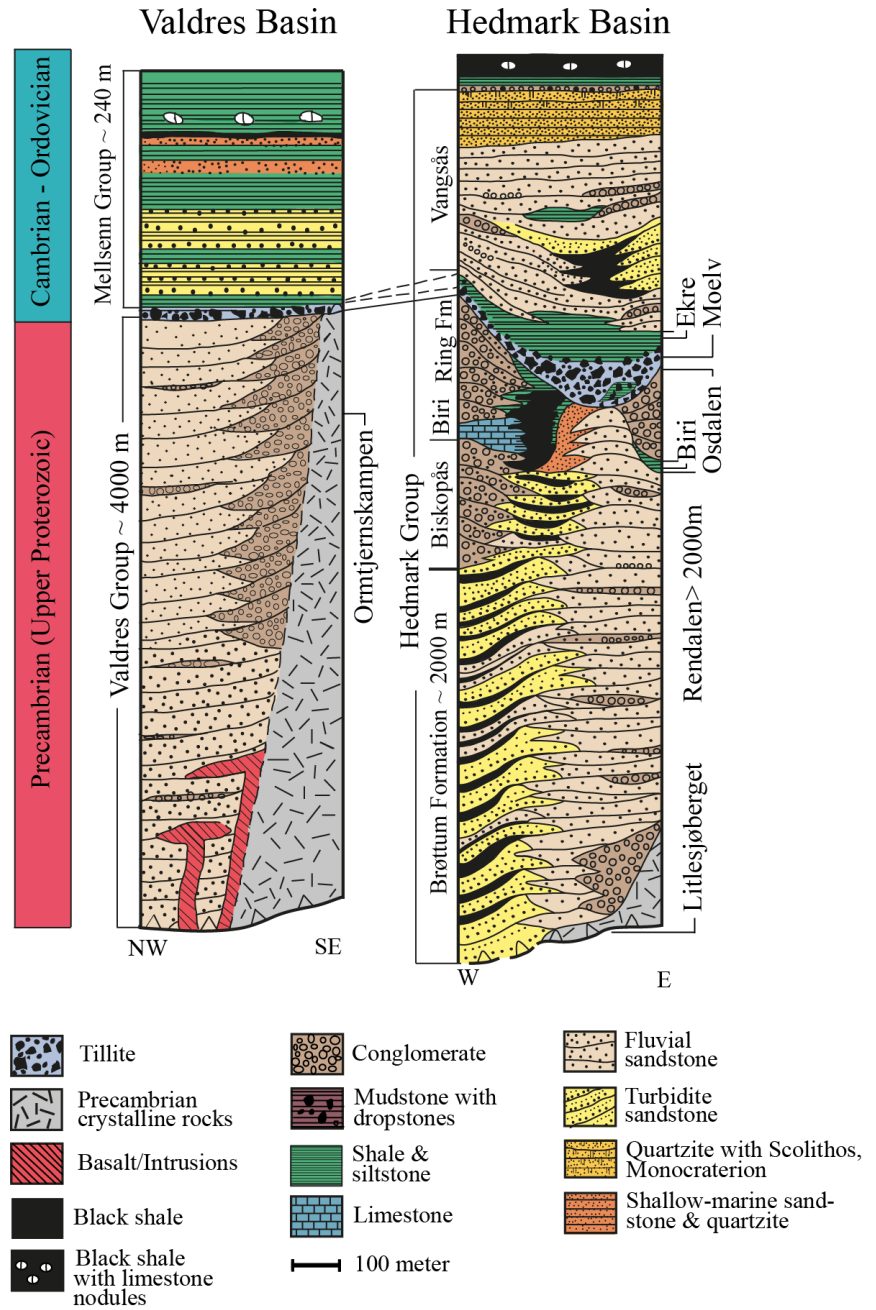
Figure 2.6: Simplified lithostratigraphic section of the Valdres and Hedmark basins. The thickness is according to the scale bar, if not otherwise stated. Left column shows geological time scale. Modified from Bockelie and Nystuen (1985) and Kumpulainen and Nystuen (1985).

13

3   Methodology

3.1   Field work

Field work and sedimentological logging of Rundemellen and Skarvemellen at Mellane in Østre Slidre, Valdres was carried out from July 18th to 30th and September 9th and 10th. The field work was done together with Kathrine Sørhus, under the supervision and guidance of Professor Henning Dypvik (UiO). The localities visited included Rundemellen and Skarvemellen (Figure 1.1) where sampling and logging was performed (Figure 3.1). Kathrine Sørhus and the author logged approximately 240 m at Rundemellen and 170 m at Skarvemellen. The Rundemellen section is presented by Sørhus (2017). The samples collected were given the locality names of "Rund" and "Ska" referring to Rundemellen and Skarvemellen, respectively. When naming the samples, the locality reference was used followed by the sample number and the year the samples were collected. To separate the samples when collecting them in field some of the samples were marked with a 2- in front of the sample number, e.g. Ska 2-2-16. The samples collected in the field were brought back to the University of Oslo where they were prepared for thin section-, XRD- and geochemical analyses (SEM and heavy mineral).

A standard logging sheet was used with a scale of 1:100 at both localities, and some detailed logs in the scale of 1:20 were performed. During logging, several characteristic features of the lithological units were taken into consideration; e.g. bed thickness, grain size and shape, color, sedimentological structures, geometry of the beds, counting of the clasts in the conglomerates, paleocurrent direction and strike/dip. Wentworth (1922) classification system was used to determine the different grain sizes (Table 3.1). Pictures and samples were collected during logging of the field area. Collected field measurements were plotted in stereonet to reconstruct the transport direction of the sediments. A summary figure of the methodology steps is presented at the end of this chapter (Figure 3.6).
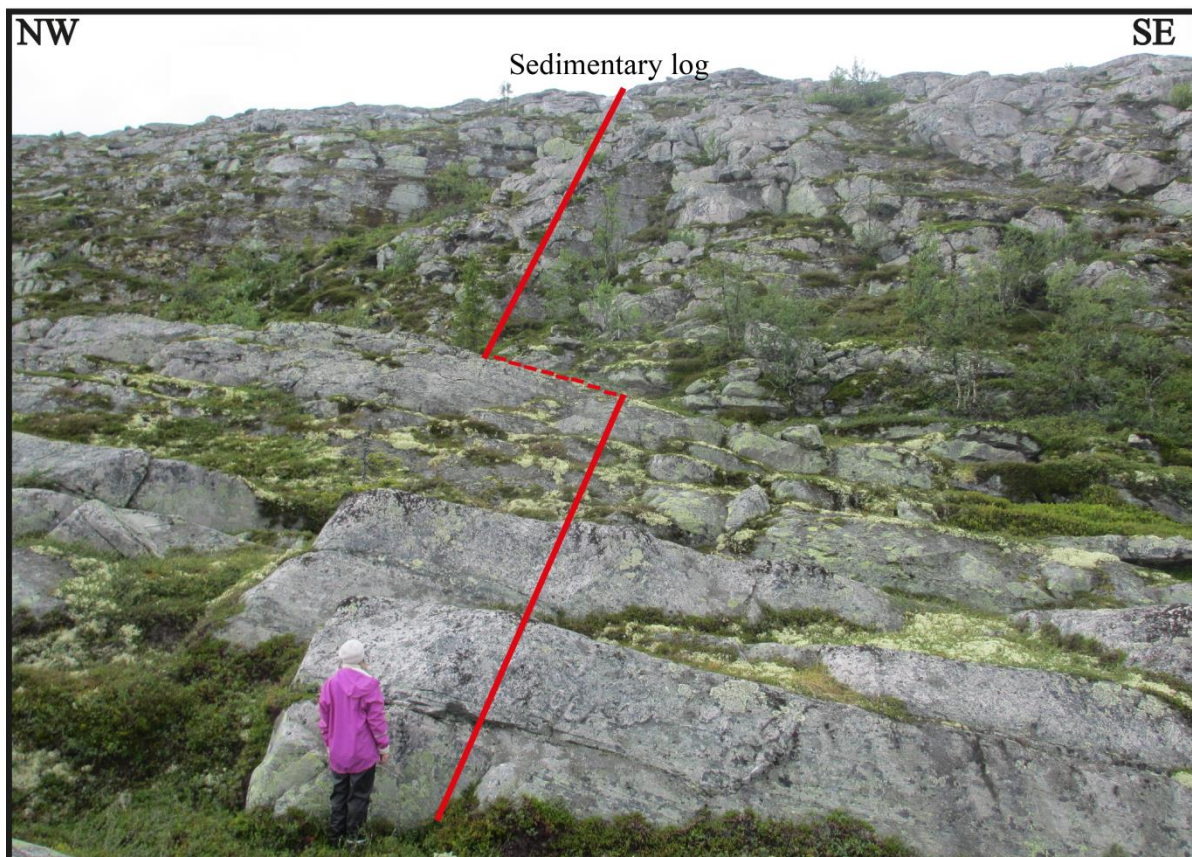
Figure 3.1: Part of the studied profile (red) at Skarvemellen, marked in map Figure 1.1.

Table 3.1: The table shows the Wentworth (1922) grain size classification. The grain sizes are given in millimeter (mm) and phi (φ).

Wentworth size class	Phi (φ) units	Size in mm
Boulder	-8	> 256 mm
Cobble	-6	64-256 mm
Pebble	-4	4-64 mm
Granule	-2	2-4 mm
Very coarse sand	-1	1-2 mm
Coarse sand	0	0.5-1 mm
Medium sand	1	0.25-0.5 mm
Fine sand	2	0.125-0.25 mm
Very fine sand	3	0.063-0.125 mm
Silt	4	0.004-0.063 mm
Clay	8	< 0.004 mm

3.2   Facies description and facies associations

To determine the sedimentary facies field observations, field logs, pictures and thin sections were used. The sedimentary succession was divided into facies based on the lithology, texture and sedimentary structure. Sedimentary facies reflect the environmental conditions at the time of deposition. Facies that are genetically related and represent a specific environment are grouped together in facies associations (Reading and Levell, 2009).

3.3   Mineralogical and Petrophysical analysis

Petrophysical and mineralogical analysis were performed on the collected samples by the use of thin section observations (Appendix A), point counting (Appendix B), X-ray diffraction (XRD) (Appendix C), scanning electron microscopy (SEM) and heavy mineral analyses (Appendix E). The petrophysical and mineralogical analyses were performed under the guidance and supervision of Professor Henning Dypvik (UiO), Katrine Fossum (*Diffrac.EVA*), Lars Riber (Siroquant) and Berit Løken Berg (SEM). A summary figure of the methodology steps is presented at the end of this chapter (Figure 3.6).

The field samples were split into four pieces; one for thin section analyses, one for XRD - analyses, one for heavy mineral analyses and the rest of the samples were placed at the Department of Geoscience storage room for future work.

3.3.1 Thin section analysis

Salahalldin Akhavan of the petro-technical department at the Department of Geoscience (UiO) prepared 22 thin sections from the Skarvemellen samples collected in the field. The rock samples were impregnated in blue epoxy and glued after drying onto a 2.5 cm x 4.5 cm glass slide and then polished down to a thickness of about 30 μm. A *Nikon Labophot-Pol* petrographic microscope was used to study the thin sections in detail, in order to give information about the mineralogy and rock texture.

All the 22 thin sections were studied under plane polarized light (ppl) and cross polarized light (xpl) to collect information about mineralogy, lithology, sorting, structures, average grain size, grain shape, sorting and the degree of feldspar weathering (Figure 3.4). To

determine the degree of rounding the terminology from Powers (1953) was used (Figure 3.2) and the degree of sorting is based on Compton`s (1962) classification scheme (Figure 3.3).
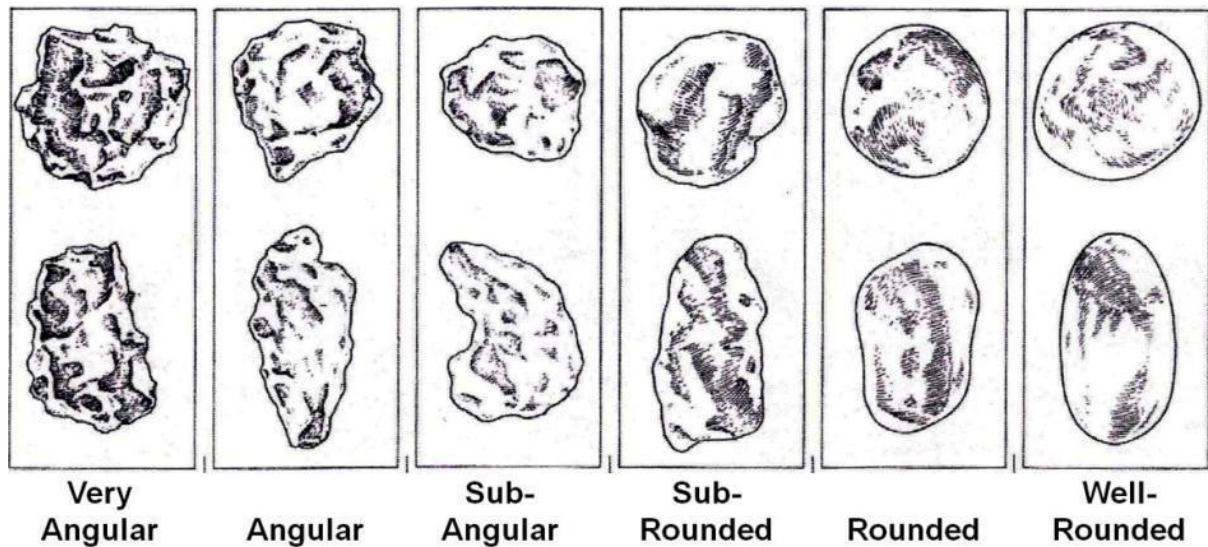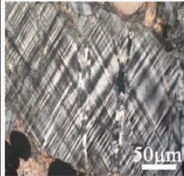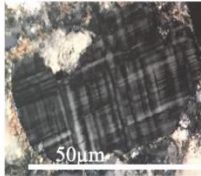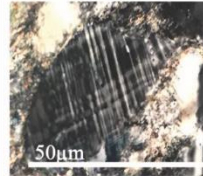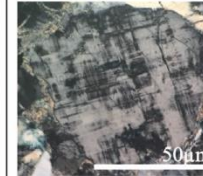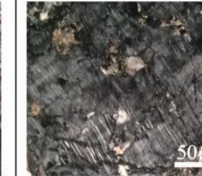
Figure 3.2: Terminology of the degree of rounding of detrital grains (Powers, 1953).
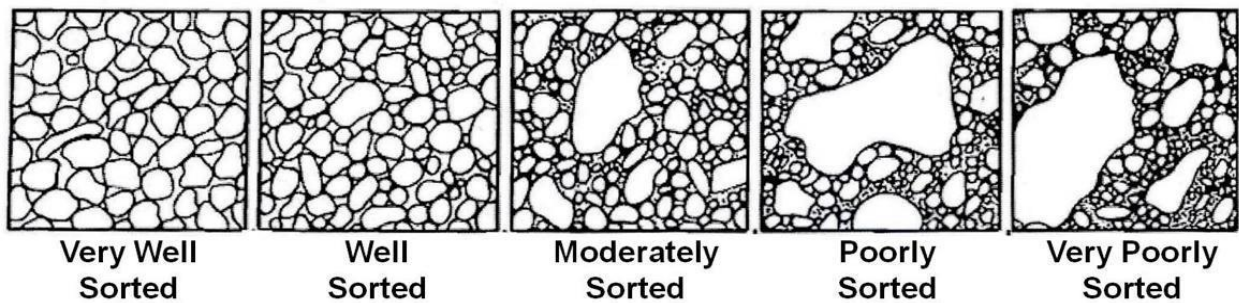
Figure 3.3: Classification regarding the degree of sorting (Compton, 1962).

The feldspar grains were categorized based on the degree of preservation from I to V and described in Figure 3.4. Each of the categories represent specific feldspar preservation, where category I represents perfect preservation of the feldspar and category V represents dissolved and barely recognizable feldspar grains, as seen in Figure 3.4.

Figure 3.4: Examples and description of feldspar preservation, categorized from I to V. Modified from Fossum (2012) with examples from Skarvemellen and Rundemellen.

3.3.2 Point counting

To estimate the average mineral content, 400 points have been counted on each of 16 selected thin sections from the Skarvemellen samples (Table 3.2 and Appendix B). This was done by optically quantifying the mineral content in each of the chosen samples. A *Swift* point counter (with automatic top frame sample holder) installed on a standard *Nikon Labophot-Pol* petrographical microscope was used. The samples were studied under plain polarized light (ppl) and cross polarized light (cpl) to identify and count the minerals.

Table 3.2: Samples prepared for thin section analysis. Samples selected for point counting marked in bold font.

Thin section summary table	
Ska 4-16	Ska 18-16
Ska 5-16	Ska 21-16
Ska 6-16	Ska 2-2-16
Ska 7-16	**Ska 2-4-16**
Ska 8-16	**Ska 2-5-16**
Ska 9-16	**Ska 2-7-16**
Ska 10-16	**Ska 2-8-16**
Ska 11-16	**Ska 2-9-16**
Ska 13-16	**Ska 2-11-16**
Ska 15-16	**Ska 2-12-16**
Ska 16-16	**Ska 2-13-15**

The quartz grains were divided into monocrystalline and polycrystalline grains during the point counting. When the extinction angle of the quartz grains was above 5 degrees, it was noted as undulatory extinction. The feldspar grains were separated into plagioclase and K-feldspar. Other features counted were rock fragments, heavy minerals, pore filling cement, iron oxides, matrix and porosity. After point counting the samples were plotted in a standard Quartz-Plagioclase-Alkalifeldspar diagram (Figure 5.6) (Streckeisen, 1976).

3.3.3   X-ray diffraction (XRD)

22 samples (Appendix C) were prepared for X-ray diffraction (XRD) by M.Sc. student Chloé Marcilly and Professor Henning Dypvik (UiO) and run by Beyene Girma Haile at the Department of Geoscience, UiO. XRD analysis is a useful tool for mineralogical analysis and the main goal is to get an overview of the rock composition. XRD is applicable for quantitative studies particularly when studying clay sized particles, since these are too small for microscope analysis and point counting. The XRD analyses were run on a *Bruker D8 advanced (40kV and 40mA)* diffractometer with *Lynxeye XE High-Resolution Energy Dispersice 1D Detectore,* using CuKα radiation located at Department of Geoscience, UiO.

XRD analysis makes it possible to determine the mineralogical composition since each mineral has a specific unit cell and a characteristic *d-spacing*. The *d-spacing* is the distance between two crystallographic planes in the mineral lattice and the distance is given in Ångström ($1Å = 10^{-1}m$) (Goldstein et al., 2003). Each mineral emits a specific signature, a diffraction pattern, when the sample is bombarded with X-ray beams. The diffraction pattern will be different for each mineral since each mineral has a specific unit cell and characteristic *d-spacing* (Moore and Reynolds, 1997).

The peaks in the diffractogram represent the measured diffraction angles of the X-ray beam, according to their specific Ångström values. The software *Diffrac EVA (Bruker, 2011)* was used to determine the mineralogical composition of the samples and *Siroquant (Sietronics Pty Ltd, 2017)* for semi-quantitative analysis.

Bulk analysis preparation for XRD
The grain size of the samples was reduced to less than 500 μm, by grounding the rocks into powder by using a slinging mill. To avoid contamination of the samples, the slinging mill was cleaned with ethanol between every sample.

To further reduce the grain size, the next step was to run the rock powder from the slinging mill in a *McCrone* micronizer machine. The *McCrone* micronizer reduced the grain size to less than 10 μm. This is done by mixing approximately 3 g of the rock powder from one sample and 8 ml of ethanol in a small container filled with 48 pieces of agate. The container is

placed in the micronizer machine and run for approximately 10 minutes. The micronized dispersion was put into an oven to dry, with a temperature of 40-50°C.

The dry fine-grained rock powder was put on to a small plastic holder by using the front-loading technique. This was done with care to avoid artificial orientation of the preparations. The XRD analysis has a detection limit of approximately 5 %, which means that if a mineral contribute to less than 5 % it is not detected.

Mineral identification

The peak at 3.34 Å is a common peak for several minerals and was therefore not used for mineral identification. To accurately identify those minerals, the second largest peak have been used, e.g. quartz. Orthoclase has a peak that is too close to the 3.34 Å peak, and the second largest peak is used instead of the 3.34 Å peak. Table 3.3 display the peaks used for identification of the different minerals in this thesis.

Table 3.3: The peak values in Å (Ångström) for the minerals of interest.
*= the second most intensive peak after 3.34 Å

Mineral	*d*-value (Å)	Mineral	*d*-value (Å)
Quartz	*4.26	Illite	10.00
Microcline	3.24	Chlorite	3.54
Orthoclase	*3.77	Hematite	2.69/2.51
Plagioclase	3.18	Rutile	3.48
Muscovite	9.90	Pyrite	2.71

Diffrac Eva Program

The Bruker software *Diffrac.EVA (Bruker, 2011)* was used to analyze X-ray diffraction data and identify the mineral phases that were present in the diffractograms, according to methods by Moore and Reynolds (1997). The *d*-spacing and the 2θ-values of the minerals were used to identify the respective peaks in the diffractogram (Table). To help identify the right minerals accurately, PDF (Powder Diffraction File) 2002 database published by the International Center for Diffraction Data (ICDD) was used. Figure 3.5 shows the identification of the primary minerals that were present in most of the samples. Semi-quantitative analysis of the mineral content was provided using the *Diffrac.EVA* software.
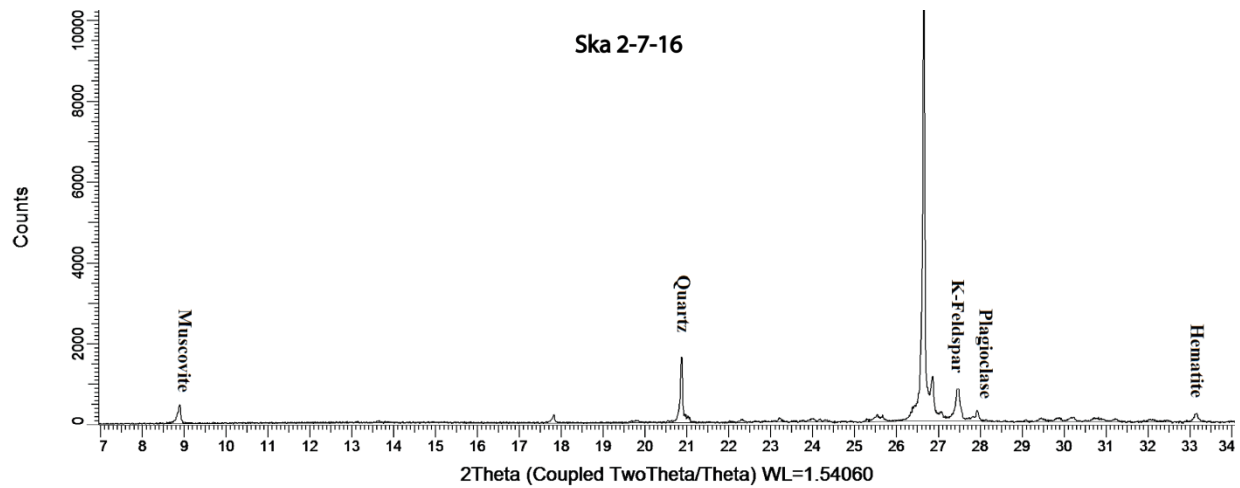
Figure 3.5: Typical diffractogram from software *Diffrac.Eva* (Bruker, 2011) show identification of the primary minerals from sample Ska 2-7-16.

Siroquant program

Siroquant by Sietronics (Sietronics Pty Ltd, 2017) was used for quantitative analysis of the rock samples. The main goal is to make a synthetic diffractogram with the same mineral phases as the original diffractogram to estimate the percentage of each mineral in the sample. During quantification the Rietveld`s method were used (Rietveld, 1969). To optimize the fit between the synthetic and original diffractogram a six stages refinement procedure was followed, the first five-stages were provided by Hillier (2000) with an additional sixth stage (Table 3.4). It is important to notice that these estimations are not true percentages, only estimations of the mineral content in the samples (Appendix C). For minerals that have been interpreted on the second largest peak as e.g. quartz, it is worth keeping in mind that these percentages are likely higher than presented in this thesis (Appendix C).

Table 3.4: Refinement steps used in Siroquant. * steps from Hillier (2000).

Stage	Cycles	Damping factor	Target
1*	6	0.4	Phase scales
2*	6	0.4	Phase scales + instrument zero refinement
3*	6	0.8	Phase scales
4*	6	0.2	Half-width
5*	6	0.2	Uni-cell dimentions
6	6	0.4	Orientation

3.3.4   Scanning electron microscope (SEM)

Scanning electron microscope (SEM) analyses were performed on four samples from Skarvemellen and one from the Ring Formation (Hedmark Group) at the Department of Geoscience, UiO, with a *HITACHI SU5000 Scanning Electron Microscope*. *Bruker Quantax 800* was used to identify the selected grains. The analyses were carried out by Kathrine Sørhus and the author under supervision of Berit Løken Berg. The thin sections were coated in carbon before they were placed in the machine and backscatter electron image (BEI) were used. The main purpose with the SEM analyses was to identify minerals, look at zonation within the feldspar and mineral overgrowth.

3.3.5   Heavy mineral analysis

17 samples were prepared for heavy mineral analyses and run by Andrew C. Morton, six samples from Skarvemellen, six samples from Rundemellen and four samples from the Ring Formation (Hedmark Group) (Table 4.3 and Appendix E). The Rundemellen samples are presented by Sørhus (2017). Heavy mineral analysis is a procedure of five stages: sampling, preparation, separation, counting and data treatment (Morton, 1985). The samples were gently disaggregated in a mortar; the grains were not ground or crushed. The heavy minerals were separated using a high density liquid by gravity settling or centrifugation (Morton, 1985). To ensure complete separation from quartz and feldspar, the high density liquids used were tribromomethane (bromoform) (2.89 g/cm^3) and tetrabromoethane (2.97 g/cm^3) (Morton, 1985). When the heavy minerals were separated they were placed on a glass slide and examined using a petrographic microscope. Mineral estimation was done by grain counting. It is preferred to count a total of 200-300 detrital mineral grains in order to give a good estimation of the percentage of heavy minerals present in the sample (Morton, 1985).

Field Work

Sedimentological logging
Sampling
Measure bed thickness
Paleocurrent measurements
Strike/dip measurements
Clast counting

Thin Sections

Samples impregnated in blue epoxy, glued onto a 2.5 x 4.5 cm glass slide and polished down to a thickness of 30 μm.

University of Oslo
Thin section laboratory
Salahalldin Akhavan
Sem Sælandvei 1
0871 Oslo

Thin section analysis:
Petrographic Microscope
Nikon Labophot-Pol

Point counting
Swift point counter
installed on the microscope

XRD-analysis

Slinging mill

Bulk analysis:
McCrone Micronizer (10 min)
Drying
Preparation for XRD in sample holders

Run in the *Bruker* XRD machine with CuKα radiation

XRD-analysis:
-Quantitative Diffrac.*EVA*
-Semi-quantitative *Siroquant*

SEM-analysis

Scanning electron microscope:
HITACHI SU5000 Scanning Electron Microscope
Identification: *Bruker Quantax 800*
Carbon coating on thin sections
Back-scattered electron image (BEI)

Heavy minerals

- Sampling
- Preparation→ disaggregation
- Separation using heavy liquids
- Counting
- Andrew C. Morton, HM Research, Great Britain

Figure 3.6: Methodology summary table. Modified from Oberhardt (2013).

4 Results

This chapter contains field observations, facies descriptions, facies associations, XRD-results, SEM and heavy mineral analyses from Skarvemellen.

4.1 Paleocurrent measurements

During the field work, paleocurrent data were collected from the cross-bedding at Skarvemellen. When reconstructing the paleocurrent measurements a horizontal fold axis is assumed, Skarvemellen is part of the overturned limb of the fold and the fold axis is not reconstructed. The measurements, as seen in Figure 4.1, strongly indicate a transport direction towards E.
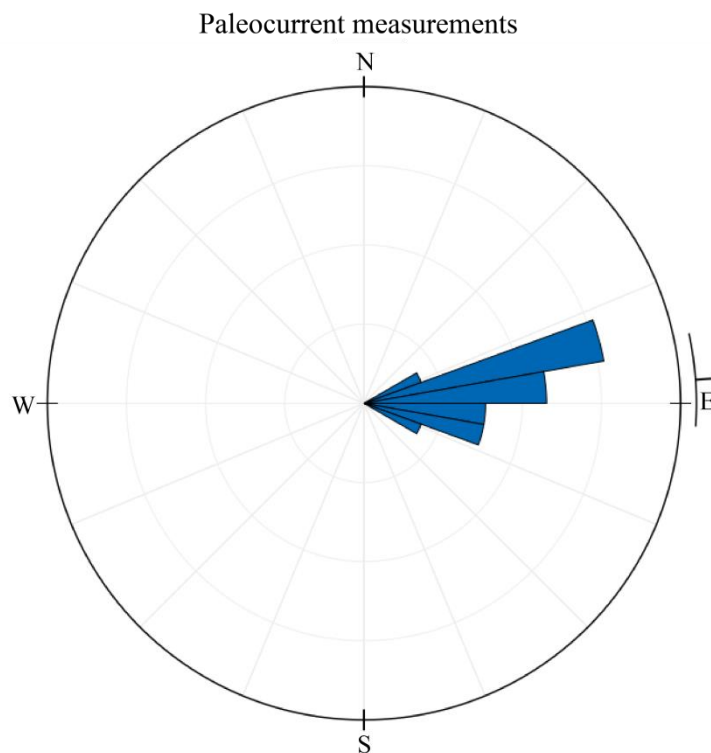
Figure 4.1: Reconstruction of the paleocurrent measurement of cross-bedding from Skarvemellen presented in a Rose diagram, indicating a transport direction towards E. A horizontal folds axis is assumed during reconstruction.

4.2 Facies description

The sedimentary succession at Skarvemellen have been divided into facies based on sedimentological structures observed in the different sandstones in field (Table 4.1), which reflect the environmental conditions during deposition.

Table 4.1: Sedimentological facies found at Skarvemellen

| Facies no.	Facies	Grain size	Physical appearance	Samples
1	Conglomerate	Coarse sand to gravel	Grain supported, polymict conglomerate. Clasts of quartzites, feldspar and jasper/vulcanites. Grains are well-rounded to sub-rounded.	Ska 10-16 Ska 2-9-16 Ska 2-8-16 Ska 2-7-16 Ska 2-5-16
2	Sandstone	Medium to coarse sand	Light pink towards red and purple in color with cross bedding, parallel lamination, structureless or through cross bedding.	Ska 8-16
2a	Cross bedding	Medium to coarse sand	Cross bedding can be observed, indicating unidirectional flow. Size of the crossbedding varies from 10 cm to 1 m. Light pink towards red and purple in color. Clasts of quartz, feldspar or clay can be observed in some of the layers.	Ska 6-16 Ska 2-12-16 Ska 8-16
2b	Parallel lamination	Medium to coarse sand	Clasts of quartz, feldspar or clay can be observed in some of the layers. Light pink towards red and purple color. Mineral precipitation can be observed in some layers.	Ska 4-16 Ska 18-16 Ska 9-16 Ska 7-16
2c	Homogenous/ structureless	Medium to coarse sand	No sedimentary structures visible. Light pink towards red and purple color. Clasts of quartz, feldspar or clay can be observed in some of the layers.	Ska 2-13-16 Ska 16-16
2d	Through cross bedding	Medium to coarse sand	Through cross bedding in light pink towards red and purple sandstone beds.	
2e	Pebbly sandstone	Medium to coarse sand	Pebbles of quartzites, clay, feldspar and rock fragments randomly spread through the layer.	
3	Silty- to fine-grained sandstone	Very fine to fine sand	Parallel lamination, Fine-grained andstone alternates between reddish brown to gray in color. Lateral extension and some layers that pinches out.	Ska 21-16 Ska 5-16 Ska 2-11-16 Ska 2-4-16 Ska 2-2-16
4	Breccia	Coarse sand	Poorly sorted, matrix supported with angular fragments.	Ska 15-16 Ska 13-16

Facies 1: Conglomerate

Five conglomerate units were observed at Skarvemellen and are shown in the sedimentary log (Figure 4.3), with an erosional base towards the underlying strata. The conglomerates are grain supported, moderately sorted and vary in thickness from about 5 to 10 meter. The conglomerates at Skarvemellen are polymict and consist of well-rounded to sub-rounded clasts varying in size from 0.5 to 10 cm.

The variations in clast composition are shown in Figure 4.2. The conglomerates consist of approximately 50% clast material. The clasts are mainly quartzite and feldspar, but some rock fragments of rhyolite (easily mistaken for jasper in field) and granite can be observed. The quartzite clasts are most abundant, well rounded and represent the largest clasts in the conglomerate units with varying color; gray, white and pink. The feldspar clasts are smaller than the quartzite clasts and more angular. The largest clasts are clearly elongated, ellipsoid shaped, as seen in Figure 4.2b. Figure 4.2a shows a conglomerate unit with smaller clasts, which are more spherical in shape. The grain size of the matrix varies from coarse sand to gravel and has the same color as the adjacent sandstone units and varies in color from light pink towards red and purple. This is seen in Figure 4.2 where the color of the matrix changes from reddish in Figure 4.2a to more light pink matrix in Figure 4.2b.
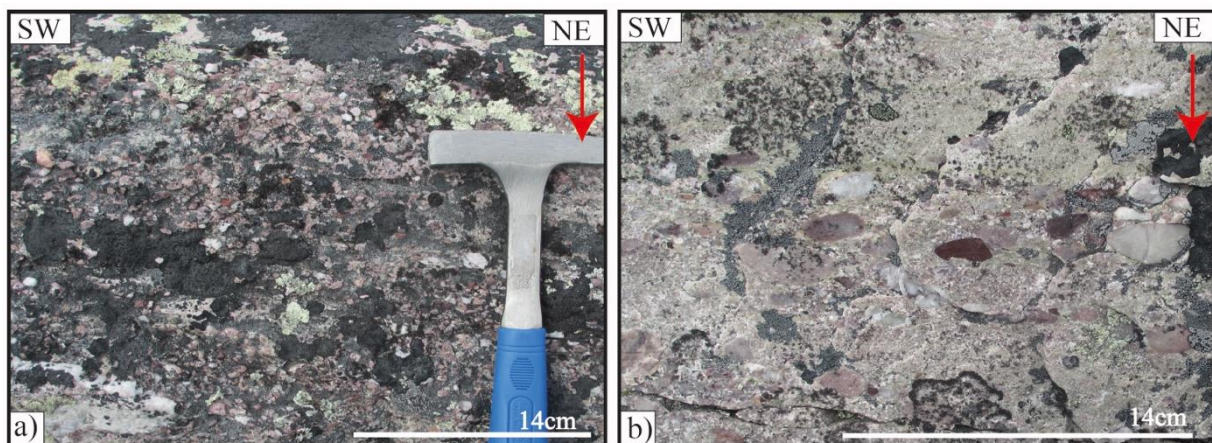
Figure 4.2: Examples of the conglomerates from Facies 1 found at Skarvemellen, red arrow indicates right way up. **a)** conglomerate with a large amounts of small clasts found at level 24 meters (Figure 4.3), clasts of quartz, feldspar, clay and rock fragments, **b)** from the lowermost conglomerate at level 7.5 meters (Figure 4.3), showing a zone with accumulation of larger pebbles.

The conglomerate units have a great lateral extent and it is possible to follow them over large distances. The sandstones from Facies 2 and the silty- to fine-grained sandstones of Facies 3 separate the conglomerates (Figure 4.3). All the conglomerate units are upwards fining, but the uppermost conglomerate at level 142 m (Figure 4.3) has minor grain size variations towards the top, with an erosional top surface. This conglomerate, at level 142 m, has an erosional contact towards the overlying breccia deposit, as seen in Figure 4.3. The transition from conglomerate to sandstone is often gradual, from conglomerates with loads of clasts to layers of pebbly sandstones of Facies 2e to sandstones with varying sedimentary structures.
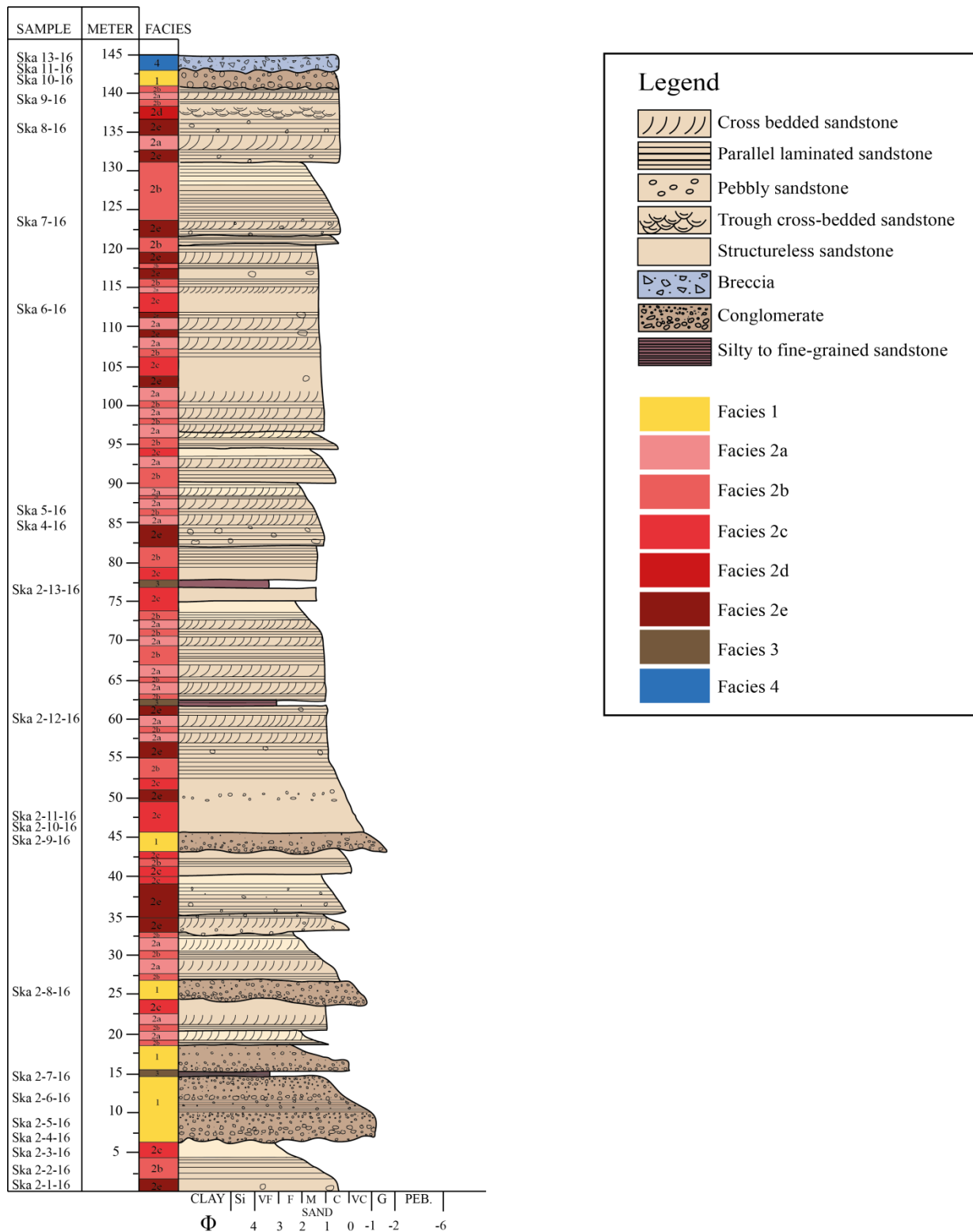
Figure 4.3: Sedimentary log presented with facies from the studied section at Skarvemellen, in the scale of 1:100. The left column shows where the samples have been collected in the sedimentary succession. The placement of the logged profile at Skarvemellen is seen in Figure 1.1.

Facies 2: Sandstone

The sandstones representing Facies 2 have been observed throughout the entire section (Figure 4.3), alternating with silty- to fine-grained sandstones and conglomerates. The sandstone facies have been divided into five separate units based on their sedimentological structures. The grain size of these facies varies from medium to coarse sand (Appendix A). Field observations indicate that the transition from sandstone to conglomerate is erosional. The transition between sandstones of Facies 2 towards silty- to fine-grained sandstone layers of Facies 3 is sharp, as seen in Figure 4.6a.

Facies 2a: Cross-bedded sandstone

Cross-bedded sandstones can be observed throughout the entire section (Figure 4.3) and all the cross-beds display uni-directional flow, towards East (Figure 4.1). They are often eroded by parallel laminated sandstone, as seen in Figure 4.4c. The cross-beds are seen upside down and hence show evidence of overturning (Figure 4.4c). The size of the cross-bedding is not consistent and varies from 10 to 40 cm in thickness. The dominating grain size is medium sand and the color varies from light pink to red. The cross-bedding in the light pink colored sandstone is often tabular or wedge shaped. In some of the layers the cross-beds show minor internal grain size variations.

Facies 2b: Parallel laminated sandstone

Parallel lamination is seen throughout the entire section (Figures 4.3 and 4.4a), often as an erosional surface cutting the cross-bedded sandstone of Facies 2a as seen in Figure 4.4c or as plain parallel lamination through the entire layer as seen in Figure 4.4a. The grain size varies from medium to coarse sand and the color changes from light pink towards red and purple as in the other sandstone facies. In the parallel laminated sandstone, no evidence of internal grain size variation has been observed.

Facies 2c: Structureless sandstone

This is a sandstone unit without any clear-cut sedimentary structures. The dominating grain size is medium to coarse sand and the dominating color is light pink towards red and purple. A few of the sandstone units show zones of coarser material with a darker pink to red color possibly a result of mineral precipitation/separation (Figure 4.4b).
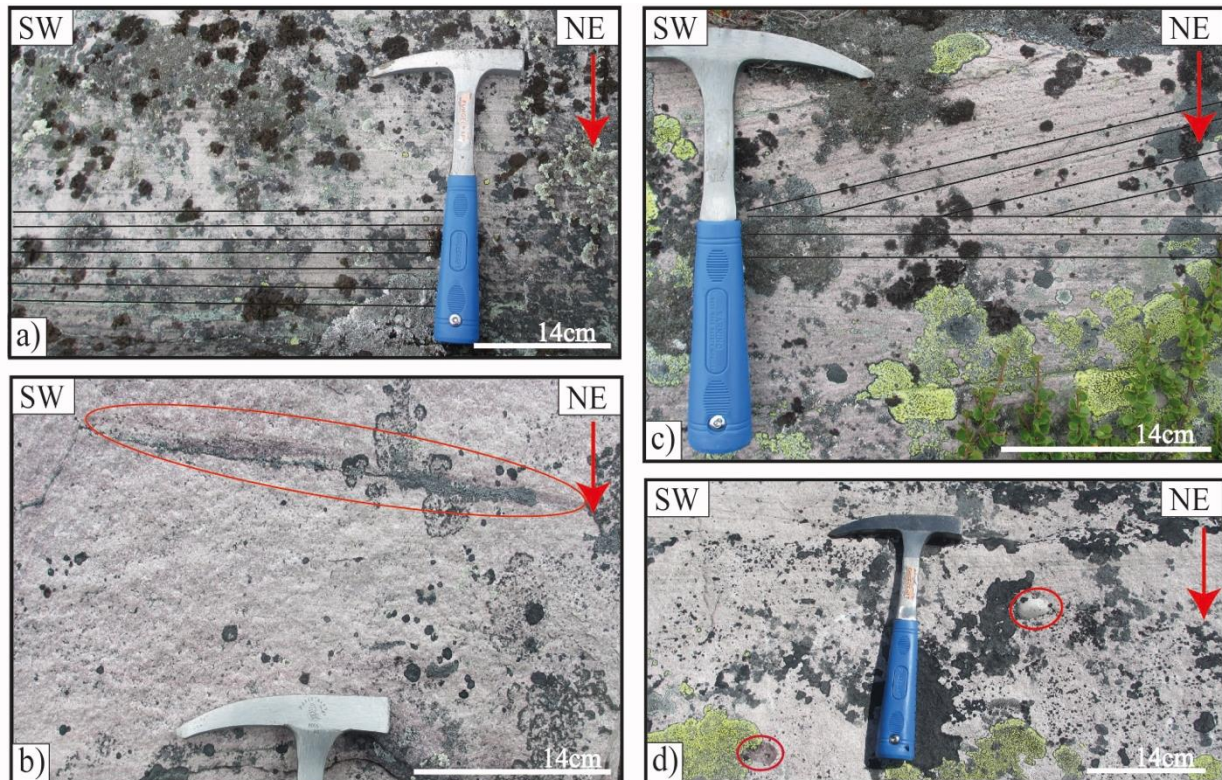
Figure 4.4: Examples of different structures found in the sandstone facies, the red arrow indicates right way up, **a)** parallel lamination of Facies 2b, level 127 m (Figure 4.3), **b)** structureless sandstone of Facies 2c, the red ellipse shows a coarser grained, dark pink zone (possible result of mineral precipitation/separation), at level 39 m (Figure 4.3), **c)** cross bedded sandstone of Facies 2a, level 27 m (Figure 4.3), **d)** cross-bedded sandstone with pebbles (Facies 2e), level 63 m (Figure 4.3), the red circles mark the pebbles, the bottom left circle show a mudstone pebble and the upper right circle show a white quartzite pebble.

Facies 2d: Trough cross-bedded sandstone

Trough cross-bedding can be observed in the section at level 138 m (Figure 4.3). The grain-size varies between medium and coarse sand and the color varies from light pink towards red and purple. Trough cross-bedding is seen as cross-beds where one or both bounding surfaces are curved. The curved lamina seems to merge tangential towards the base, but it is difficult to see because of the vegetation.
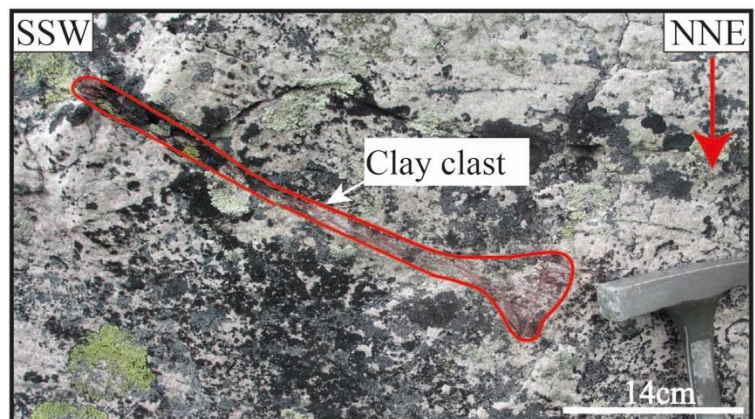
Figure 4.5: Squeezed clay clast in parallel laminated sandstone of Facies 2b, level 47 m (Figure 4.3). The red outline shows a squeezed clay filling, that is 30 cm long and 6.5 cm at the wide. The clay filling is squeezed out towards left. Red arrow indicates right way up.

Facies 2e: Pebbly sandstone

This facies consist of sandstone units with randomly distributed clasts of quartzite, feldspar, mudstones and squeezed clay clasts (Figure 4.5). The pebbly sandstone facies contain a concentration of clasts that is less than 30% and should not be confused with the conglomerate of Facies 1. The clasts vary in size from 0.5 cm to 30 cm. The quartzite clasts are well rounded and the feldspar clasts are more angular. The mudstone clasts are angular to rounded, and the clay clasts are squeezed into different structures, as seen in Figure 4.5. These mudstone clasts and clay filling structures occur in beds with parallel lamination, cross stratification and in structureless layers. The dominant clast type is quartzite, which seems to occur within the cross-bedded layers (Figure 4.4d). The clasts that occur within cross-bedding are randomly distributed and seem to be situated at the bottom of the individual cross stratified layers. Clasts of quartzite, feldspar, mudstone and clay structures seem to be occurring randomly throughout the layers. The mudstone clasts are mostly found at the bottom of the layers, as mudstone clasts or squeezed clay, randomly distributed (Figure 4.3).

Facies 3: Silty- to fine-grained sandstone

Silty- to fine-grained sandstone can be observed alternating with conglomerates (Facies 1) and sandstones (Facies 2) through the entire section (Figure 4.3). The fine-grained sandstones are laminated, but no other sedimentary structures were observed. The color alternates between dark brownish-red and grey (Figure 4.6). Some of the layers pinches out, other have a large lateral extension. The boundary between thin fine-grained sandstones, conglomerates (Facies 1) and sandstones (Facies 2) is erosional, marked with red lines in Figure 4.6.

Facies 4: Breccia

The breccia (Figure 4.3) representing Facies 4 is a poorly sorted, matrix supported deposit with angular clasts (Figure 4.7). The clasts found in the breccia are mainly quartz and feldspar, where feldspar is the most abundant clast composition and the grain size varies from 0.3 cm to approximately 4 cm. This breccia is found in an outcrop at Skarvemellen and has a thickness of approximately 20 cm. It is also found in several loose boulders some meters below. The breccia matrix consists of coarse sand and the color is grayish green (Figure 4.7).
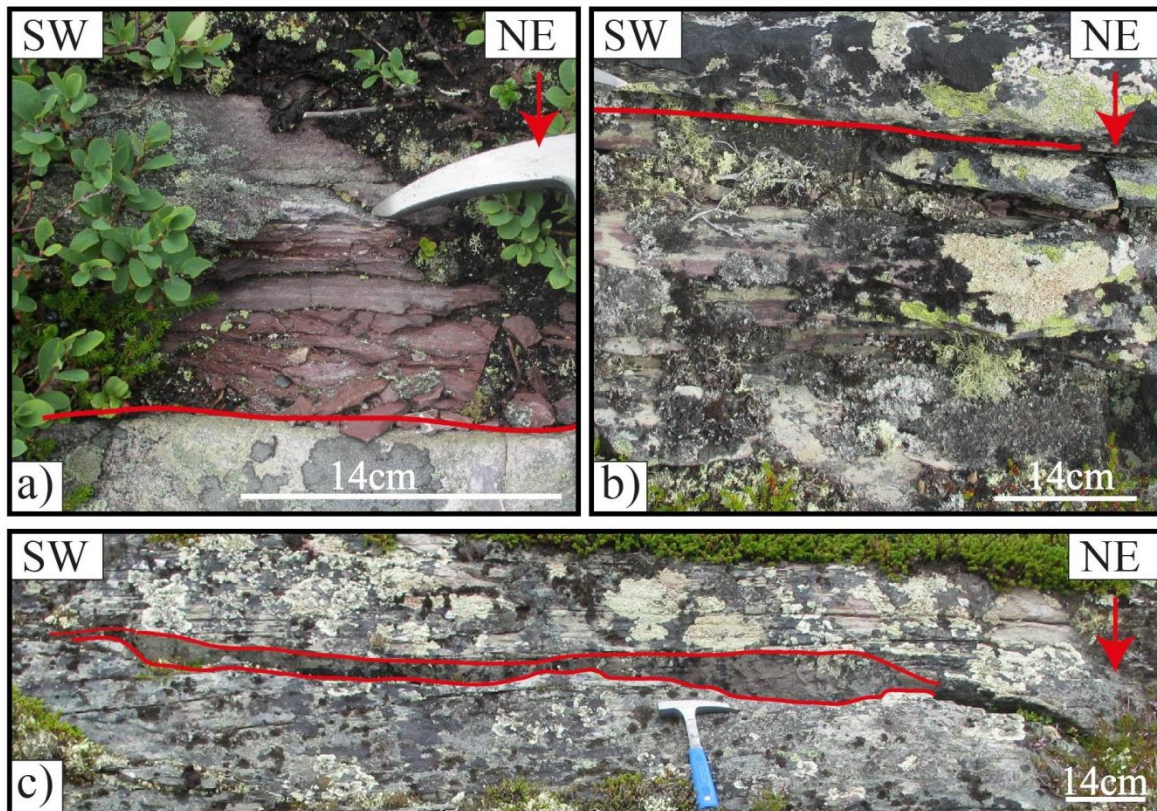
Figure 4.6: Examples of how the silty- to fine-grained sandstone occurs at Skarvemellen, **a)** thin silt layers, dark brownish-red in color, the red line shows the sharp/erosional transition towards the underlying sandstone of Facies 2, level 21 m (Figure 4.3), **b)** brownish red silty layer that alternates with gray fine-grained sandstone, the red line show the sharp/erosional transition between Facies 3 and Facies 2, level 4 m (Figure 4.3), c) red lines indicate how the silty layer pinch out in the parallel laminated sandstone of Facies 2b, level 111 m (Figure 4.3). Red arrow indicates right way up.

Figure 4.7: Breccia from Skarvemellen found in the outcrop at 1050 m.a.s.l., level 144 m in the sedimentary log (Figure 4.3). The red lines indicate the thickness of the layer (approximately 20 cm). The clasts vary in size (0.3 mm to 4 cm) floating in a finer grained greenish matrix. The pink clasts seen in the picture are K-feldspar. Red arrow indicates right way up.

4.3 Facies association

The facies have been divided into facies associations reflecting a specific depositional environment.

FA 1: Conglomerate and sandstone association

- Grain-supported conglomerate (Facies 1)
- Cross-bedded sandstone (Facies 2a)
- Parallel laminated sandstone (Facies 2b)
- Structureless sandstone (Facies 2c)
- Pebbly sandstone (Facies 2e)
- Silty- to fine-grained sandstone (Facies 3)

FA 2: Upwards fining sandstone association

- Cross-bedded sandstone (Facies 2a)
- Parallel laminated sandstone (Facies 2b)
- Structureless sandstone (Facies 2c)
- Pebbly sandstone (Facies 2e)
- Silty- to fine-grained sandstone (Facies 3)

FA 3: Sandstone association

- Cross-bedded sandstone (Facies 2a)
- Parallel laminated sandstone (Facies 2b)
- Structureless sandstone (Facies 2c)
- Trough cross-bedded sandstone (Facies 2d)
- Pebbly sandstone (Facies 2e)

FA 4: Poorly sorted feldspar rich breccia association

- Breccia (Facies 4)
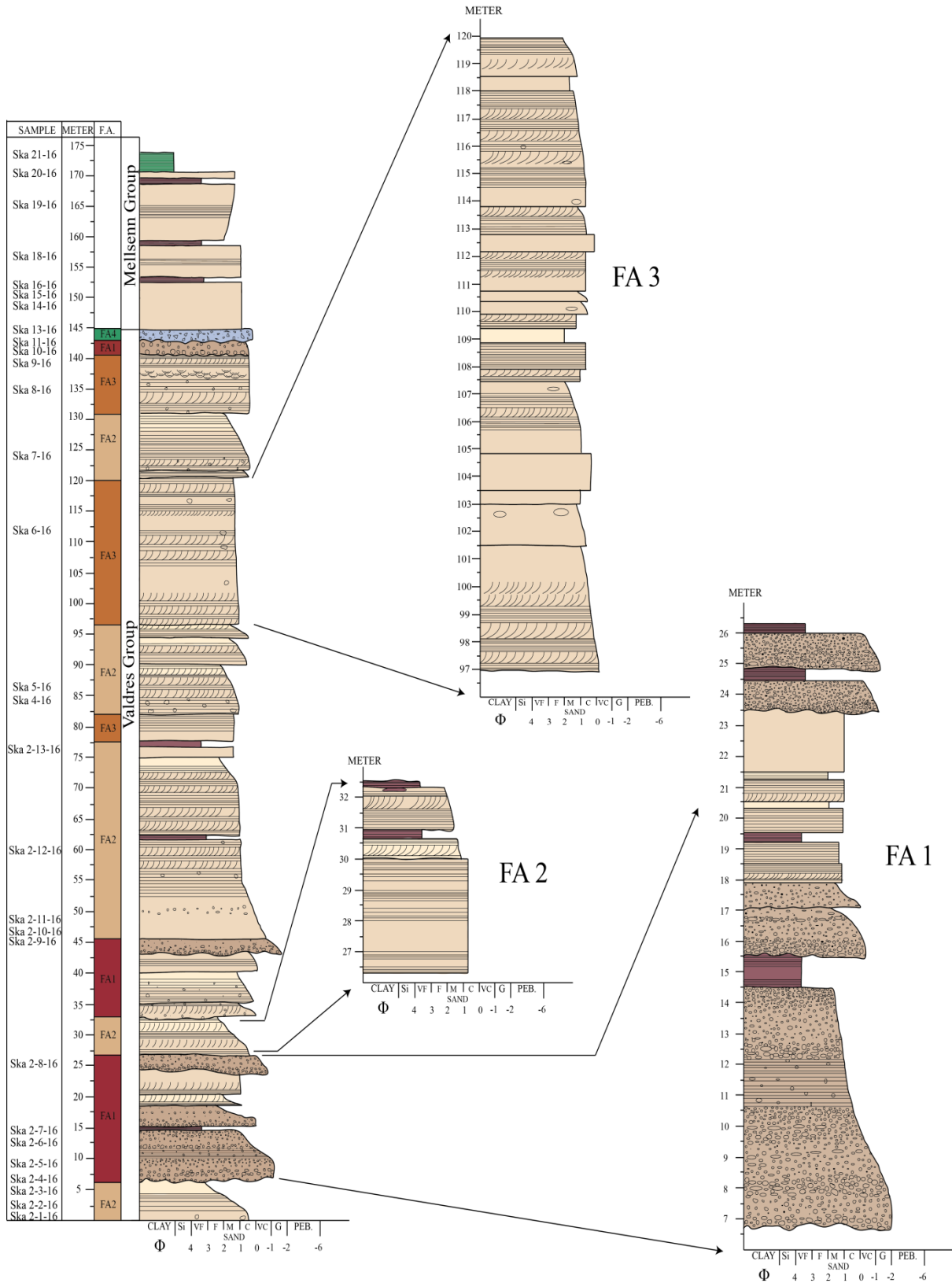
Figure 4.8: The Skarvemellen section divided into facies associations. FA1 show a more detailed log of facies association 1 with alternating conglomerate, sandstone and silty- to fine-grained sandstone sequences, FA 2 show a more detailed log of facies association 2 and FA 3 show a detail log of faces association 3. Legend is found in Figure 4.3. The green layer at the top of the main log (left) represents a phyllite in the Mellsenn Group.

FA 1: Conglomerate and sandstone association

Facies association 1 (Figures 4.8 and 4.9) from the study area, consists of alternating sequences of grain-supported conglomerates (Facies 1), sandstones (Facies 2) and silty- to fine-grained sandstones (Facies 3) (Table 4.1). The mineralogical composition and color of the matrix is similar to the surrounding sandstones. The conglomerates display an upwards fining development towards sandstones or silty- to fine-grained sandstones on top, as seen in Figure 4.9. The silty- to fine-grained sandstones occur more frequently towards the top of FA 1 (Figure 4.9). The contact between the conglomerate base, sandstones or silty- to fine-grained sandstones is always erosional (Figure 4.9).

The conglomerate found at level 6.5 to 14.5 meters (Figure 4.9), has an upwards fining development. The lowermost conglomerate at level 10.5 to 12 m (Figure 4.9) alternates into a sequence of parallel lamination with pebbles. Small erosional channels with quartzite clasts have been observed at level 11 m (Figure 4.9c). The lowermost conglomerate has larger pebbles than the uppermost conglomerates (levels 23.5 – 24.5 m and 25-25 m, respectively) (Figure 4.9). The conglomerates change from being dominated by feldspar, rock fragments (granite and rhyolite) and quartzite clasts at the bottom of FA 1 to containing more clay clasts in the upper part of FA 1 at level 24 meter (Figure 4.9). The conglomerate ranging from level 13.5 to 14.5 meters (Figure 4.9) contain smaller clasts (0.5 to 1 cm) than the other conglomerates in FA 1 (Figure 4.9).

The sandstones of FA 1 display some structureless units which appear to be massive. As seen in Figure 4.9b the structureless sandstone unit at levels 19 meter and 22-23 meter (Figure 4.9b) consists of zones of coarser material with a darker pink color than the rest of the structureless sandstone layers. The rest of the sandstone layers show parallel lamination and cross-bedding and some of the units of FA 1 may consist of pebbly sandstones (Facies 2e, Table 4.1). Silty- to fine-grained sandstones occur as fine laminated beds (Figure 4.9a). Conglomerates dominate facies association 1 and the thickness of the conglomerate units decrease towards the top of FA 1 displaying an overall upwards fining trend.
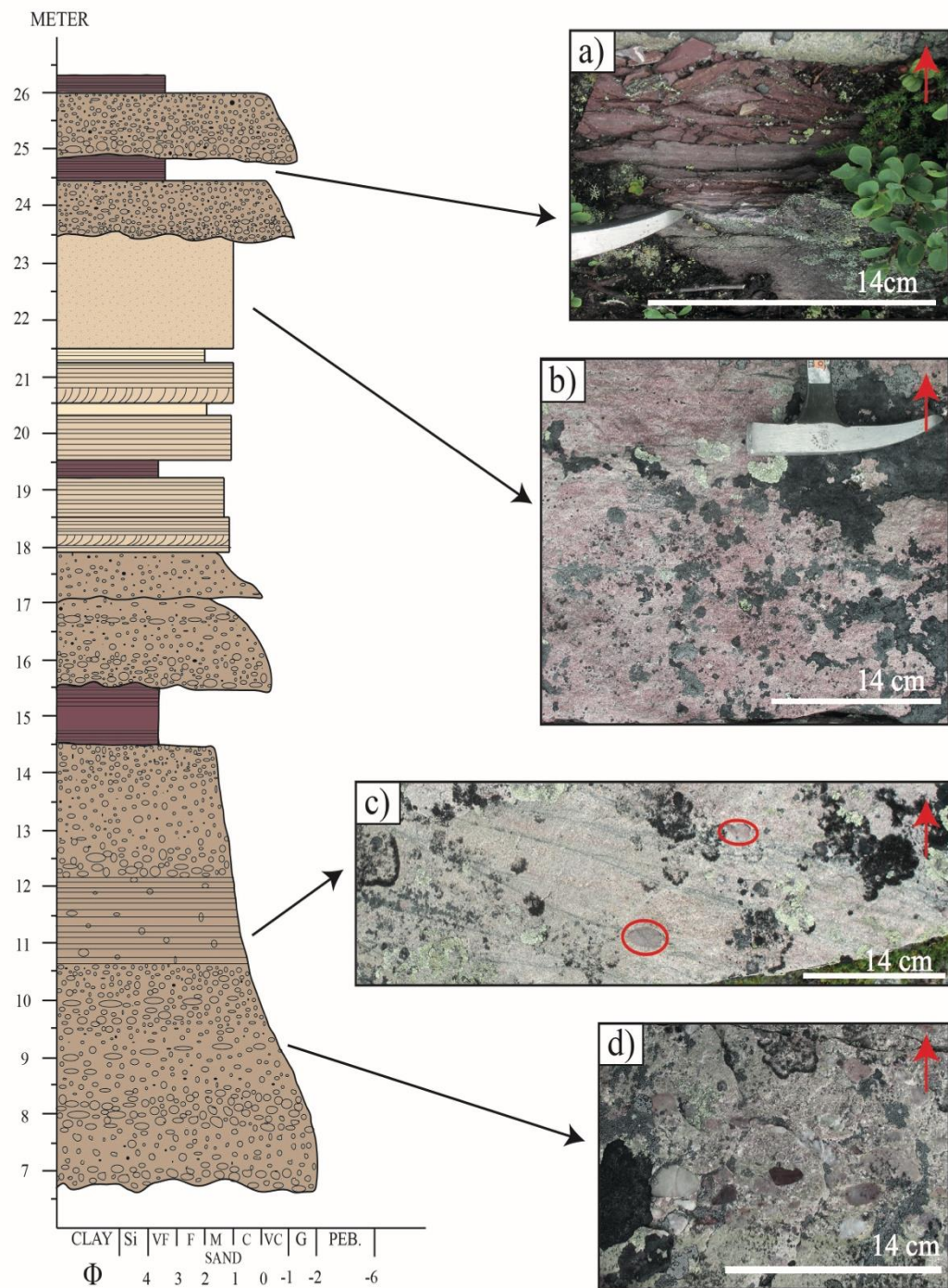
Figure 4.9: A more detailed log of facies association 1 from the studied section at Skarvemellen, Mellane. **a)** Silty- to fine-grained layer (Facies 3), **b)** structureless sandstone (Facies 2c) with darker pink zones in light pink sandstone, **c)** erosional channels with quartzite clasts (marked in red) at the base of the erosional channels, **d)** conglomerate zone (Facies 1). Legend is found in Figure 4.3. The red arrow indicates right way up.

FA 2: Upwards fining sandstone association

Facies association 2 is composed of alternating sequences of sandstones (Facies 2) and silty- to fine-grained sandstones (Facies 3) (Figure 4.8). The sandstones show parallel lamination, cross-bedding and structureless developments (Figure 4.8). FA 2 consists of upwards fining

sandstone units with a silty- to fine-grained sandstone layer on top; an overall upwards fining trend (Figure 4.8). The transitions from sandstones to overlying silty- to fine-grained sandstones layers are erosional. The parallel laminated sandstone dominates in FA 2 (Figure 4.8). The size of the cross-bedding varies from 15 to 30 cm. Pebbly sandstone (Facies 2e, Table 4.1) may occur but is not so common in this facies association. The grain size of the sandstone beds varies from medium to coarse sand (0.5 – 1 mm) (Table 3.1 and Appendix A).

FA 3: Sandstone association

The change from FA 2 to FA 3 is often abrupt, with a sudden change in grain size from very fine to fine sand (0.063-0.25 mm, Table 3.1) of Facies 3 (silty- to fine-grained sandstone) to sandstones of Facies 2 with a grain size of medium to coarse sand (0.5 – 1 mm) (Table 3.1 and Appendix A). FA 3 consists of sandstones from Facies 2 with minor grain size variations throughout the sequence. As seen in Figure 4.8 at 109 meter one unit with a grain size 0.4 mm (fine sand) (Table 3.1) is observed. No silty- to fine-grained sandstones have been observed in this facies association. Facies association 3 shows an overall slightly upwards fining trend (Figure 4.8). FA 3 consists of structureless, parallel and cross-bedded sandstone in alternating development. Some of the layers also contain randomly distributed pebbles (Facies 2e) (Figure 4.8), occurring dispersed through FA 3.

FA 4: Poorly sorted feldspar rich breccia association

This facies association consists only of breccia Facies 4. At Skarvemellen this facies association (FA 4) is found in a small outcrop, presented at page 30. FA 4 is seen in Figure 4.8 at level 145 meter.

4.4 Mineralogical and Petrophysical description

4.4.1 Thin section and point counting

A detailed description of the thin sections and the point counting results can be found in Appendix A and Appendix B respectively. These results will be described together, related to facies. The thin sections were studied in detail in the microscope and are presented here. The grain sizes of the samples were measured along the longest axis of the individual mineral grains. Minerals, grain contacts and feldspar preservation were studied.

Facies 1: Conglomerate

Five thin sections of matrix from Facies 1 were studied in detail, each representing individual conglomerates from the study area. Detailed results from optical thin section analyses are found in Appendix A. Detailed descriptions of the different rock fragments found in the conglomerates is presented below, followed by descriptions of the conglomerate matrix.

Rhyolite - rock fragment

The rhyolite rock fragments are sub-rounded with salt and pepper texture, as seen in Figure 4.10a. The clasts vary in size from 4 to 8 mm.
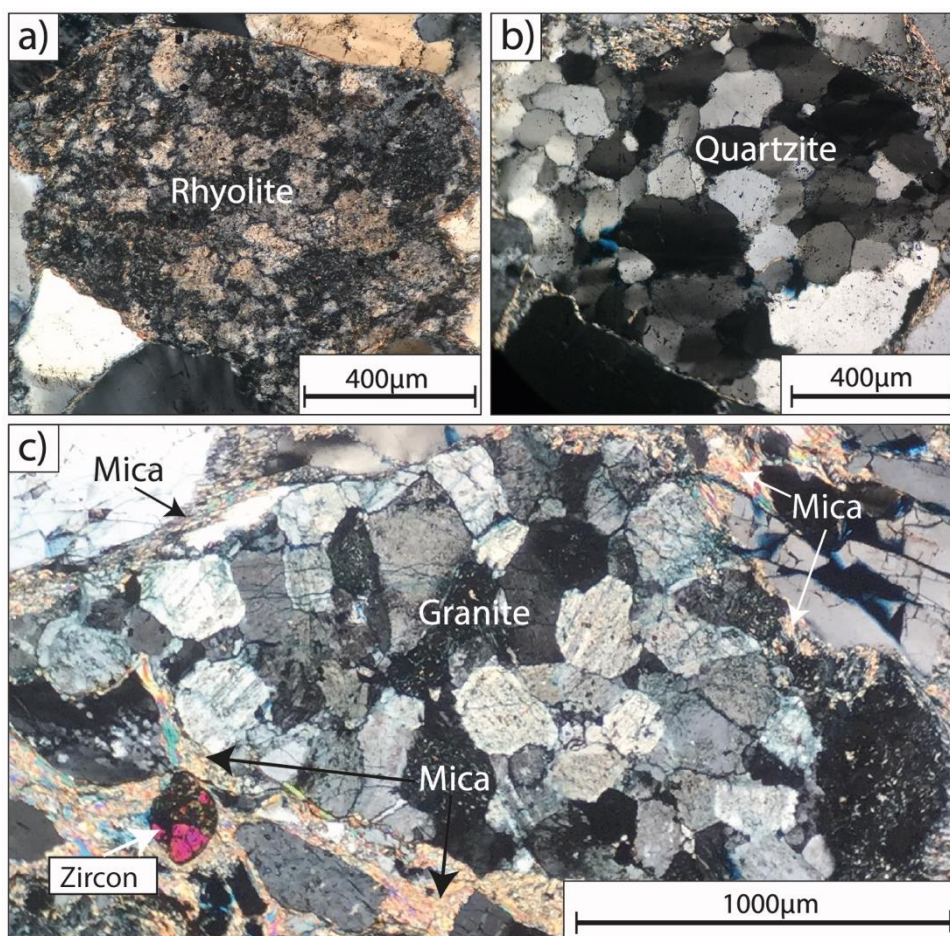
Figure 4.10: Rock fragments of **a)** rhyolite (Ska 10-16), **b)** quartzite (Ska 11-16) and **c)** granite (Ska 11-16) found in the conglomerates (Facies 1). Rhyolite with salt and pepper texture, with a thin film of mica around the rock fragment**, b)** quartzite showing polygonal simple grain contacts inside the rock fragment and **c)** granite rock fragment with mica around the rock fragment, interdigitating and sutured grain contacts within the granite rock fragment, and a pink fractured zircon grain in the bottom left corner of picture **c.**

Granitic – rock fragment

The granitic rock fragments are generally sub-angular (Figure 4.10c) and vary in size from 1.5 cm to 2.25 cm. These rock fragments consist of undulatory quartz and poorly preserved feldspar (V) (Figure 3.4) that makes it difficult to distinguish the feldspar grains from the quartz grains. The grains contacts are sutured, concavo-convex, long and tangential. Mica was observed around the grains in small amounts, mainly around the feldspar. Zircons were observed in or in close contact with the granite fragment in sample Ska 10-16, as seen in Figure 4.10c.

Quartzite – rock fragment

The quartzite rock fragments are sub-rounded and vary in size from 4 to 15 mm. They consist of small quartz grains often cemented together with a thin mica film or as polygonal simple contacts, seen in Figure 4.10b. Undulatory and non-undulatory quartz are observed in all clasts, undulatory quartz is most abundant in the quartzite clasts. The individual minerals within the quartzite rock fragment are angular too sub-angular in shape (Figure 4.10b). Minor amounts of feldspar have been observed in some of the quartzite fragments, with dominating category III preservation.

Conglomerate matrix

The conglomerate matrix contains mostly sub-rounded to well-rounded grains and the sorting ranges from well to very poorly sorted (Appendix A, Figure 4.11). The average grain size ranges from medium sand (0.47 mm) in Ska 2-7-16 to very coarse sand (1.94 mm) in Ska 2-8-16. Rock fragments are responsible for the poorly sorting in the samples and the increases in the average grains size. Quartz represents the largest grains in the conglomerate matrix and is generally sub-rounded to rounded. The K-feldspar grains are in general smaller than the quartz grains and more sub-rounded. The preservation of feldspar is on average category III (Figure 3.4 and Appendix A). The plagioclase is sub-rounded and is generally smaller than the K-feldspar grains. Figure 4.11 demonstrates the different grain contacts found in the conglomerate matrix. The matrix in Ska 11-16 is poorly sorted and the grain contacts are mainly straight and tangential or floating in the matrix (Figure 4.11a and 4.11b), reflecting a low degree of compaction. The grain contacts in the well sorted conglomerate matrix are more sutured and concavo-convex than the poorly sorted conglomerate matrix (Figure 4.11b). In samples with a high amount of quartz, polycrystalline quartz is the main pore filling material. Fractures are often filled with polycrystalline quartz, muscovite or sericite. Hematite is

observed as fine grained material around minerals in the matrix (Ska 2-9-16, Ska 2-8-16 and Ska 2-7-16) primarily in connection with or around opaque minerals (further analyzed in SEM). Opaque minerals are often found in separate zones; zircon and hematite in particular. The opaque grains make up an average of 2 % of the conglomerates (Appendix B). This is also observed in the sandstone samples as seen in Figure 4.14. The conglomerate matrix is grain supported, in Ska 2-7-16 and 2-8-16 the amount of pore filling minerals (mica, quartz, sericite) is considerably higher (on average 28 %) than in the other conglomerates, reaching an average of 16 % (Appendix B). Quartz and feldspar intergrowth has been observed in all the samples (Figure 4.12a).
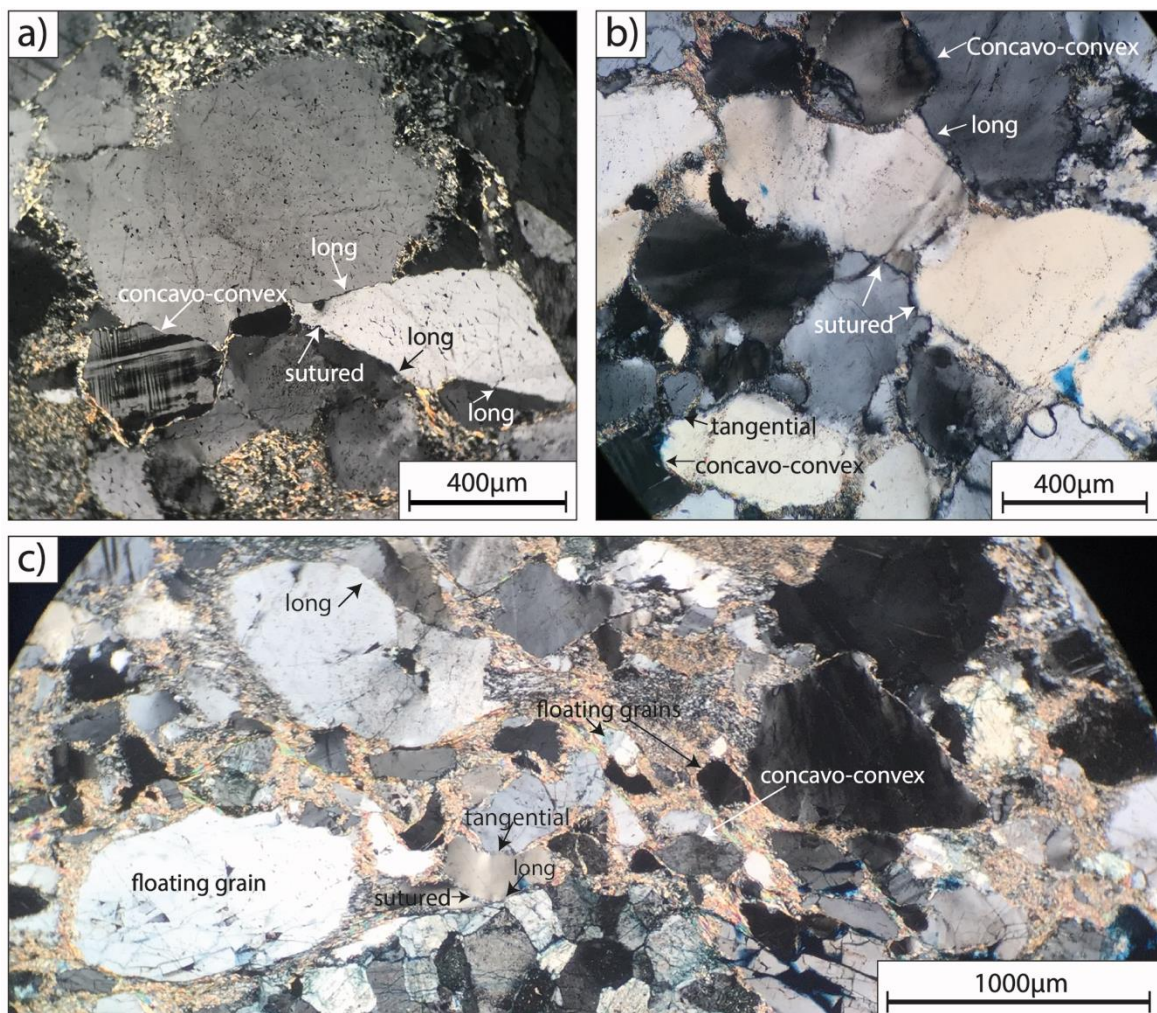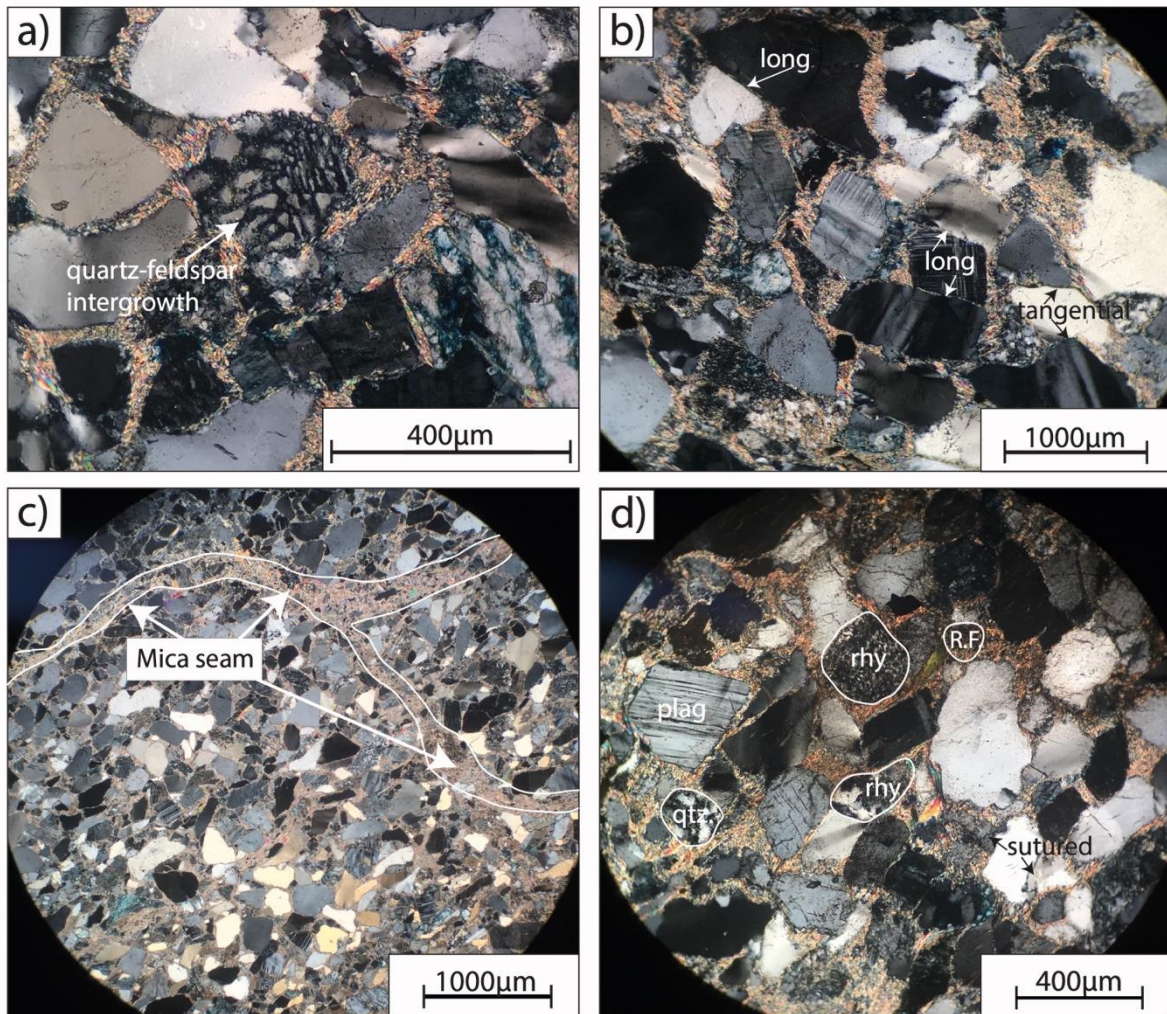

Figure 4.11: Thin section pictures taken with cpl of the grain contacts found in the conglomerate matrix. **a)** Grain contacts in Ska 11-16, showing four different contacts; long, concavo-convex and sutured. Some of the grains have a thin mica film and is not in direct contact with other grains. **b)** Grain contacts in Ska 2-9-16, less mica between the grains showing long, concavo-convex, sutured and tangential grain contacts. **c)** Show more floating grains in Ska 11-16, with tangential, long, sutured, concavo-convex and floating grain contacts, is poorly sorted.

Point counting (Appendix B) shows that quartz is the most abundant mineral in the conglomerates (Facies 1) and the average quartz content is 59 %. The average feldspar content is 13 %. Monocrystalline undulatory extinction dominates with an average of 36 % (Appendix B). All the samples except Ska 2-5-16 have an average polycrystalline quartz content of 14 % (Appendix B), Ska 2-5-16 stands out with a polycrystalline quartz content of 24 % (Appendix B).

Facies 2: Sandstone

Seven thin sections from Facies 2 were studied, each representing grain supported sandstones located between the conglomerates (Figures 4.3 and 4.8). The average grain sizes range from medium to coarse sand (0.41-0.75 mm) (Table 3.1). The grains are sub-angular to sub-rounded (Figure 3.2) (Appendix A) and the sorting ranges from well to moderate (Figure 3.3) (Appendix A). The grain contacts are mostly long and tangential (Figure 4.12b). Rock fragments (quartzite, granite and felsic fragments with salt and pepper texture) are found in all of the samples and have the same grain size as the rest of the samples, as seen in Figure 4.12d. The rock fragments seem to be more angular than the rest of the grains in the sandstones. Mica, sericite and polycrystalline quartz are pore filling. K-feldspar perthites were observed (Figure 5.7). Veins of polycrystalline quartz are observed in Ska 4-16 crossing the thin section as seen in Figure 4.13. Quartz feldspar intergrowth was discovered in all the thin sections of this facies (Figure 4.12a). Figure 4.12c demonstrates the assemblage of mica in veins found in some of the sandstone samples. Zones of opaque minerals arranged in veins were found in Ska 2-12-16, Ska 4-16 and Ska 6-16. They occur as fairly straight seams which run through the entire thin section, often with enrichment of zircon, other heavy minerals (further described in SEM and heavy mineral analyses) and hematite (Figures 4.13 and 4.14). In Ska 2-13-16 and Ska 2-12-16 the grains are more fractured than in the rest of the samples. Veins of polycrystalline quartz crossing the sample are found in some of the samples (Figure 4.13).

Feldspar grains are smaller and less rounded compared to the quartz grains. Feldspar preservation shows an average category III (Figure 3.4) for the K-feldspar and category II (Figure 3.4) for the plagioclase (Appendix A). The feldspar preservation in some of the grains was so poor (category IV/V, Figure 3.4) that it is sometime possibly mistaken for quartz in the point counting results (Appendix B).

Figure 4.12: Thin section pictures taken in cpl of sandstones (Facies 2) **a)** show a quartz feldspar intergrowth in Ska 8-16. The grains are floating in the surrounding mica matrix and some grains are in direct contact with each other, with tangential, long and sutured contacts. **b)** shows the dominating grain contacts found in the sandstone of Facies 2, long and tangential, (example from Ska 8-16). **c)** In Ska 7-16 mica is found as a seam and the general grain shape, sorting and grains contacts found in the sandstone Facies 2. **d)** shows how the rock fragments occur in the sandstone samples, picture from Ska 8-16.

Point counting (Appendix B) shows that the total percentage of framework grains (quartz, feldspar and rock fragments) is 75 % and the average matrix content is 23 % in the sandstone (Facies 2). The dominating grain type is quartz, with an average of 55 %. The average total feldspar content is found to be lower than in the other samples, only 15 %. K- Feldspar is more abundant than the plagioclase and constitutes to an average of 56 % of the total feldspar content. Monocrystalline undulatory quartz dominates (Appendix B) with an average content of 34 % and average polycrystalline quartz of 9 %.
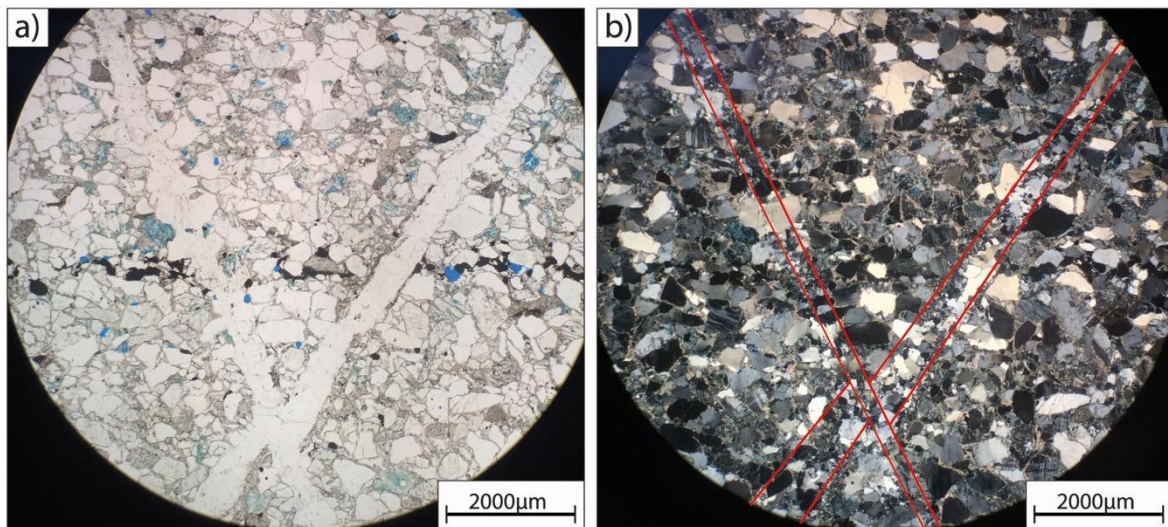
Figure 4.13: a) Show how the polycrystalline quartz veins and heavy mineral zone look in ppl in Ska 4-16. **b)** The red lines show the polycrystalline quartz veins in cpl. The polycrystalline quartz veins are crossing each other and the right vain demonstrate a small displacement.
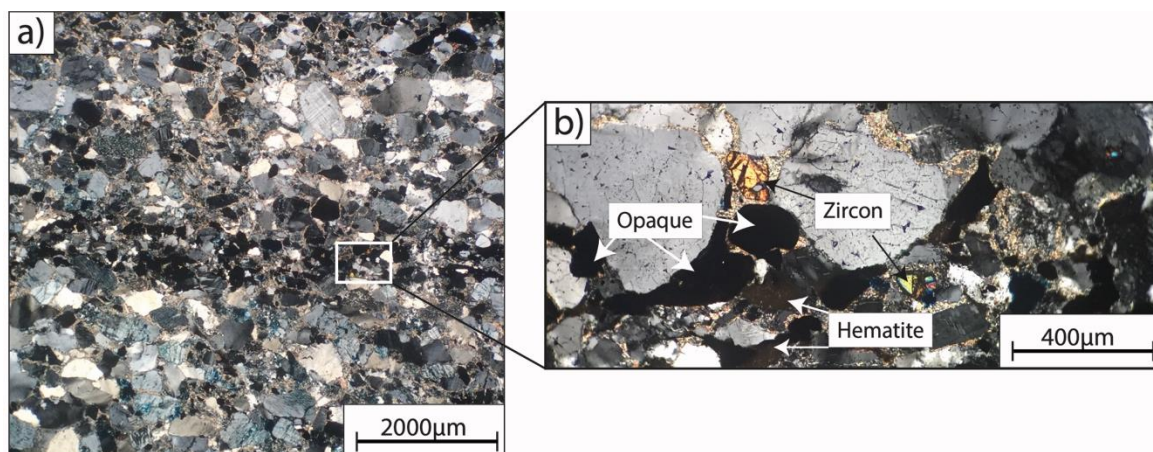
Figure 4.14: a) picture of sample Ska 2-12-16 showing a straight opaque seam in the middle with enrichments of hematite, zircon and heavy minerals, **b)** show a close up of the seam with opaque grains, zircon and hematite (see SEM results, chapter 4.4.3).
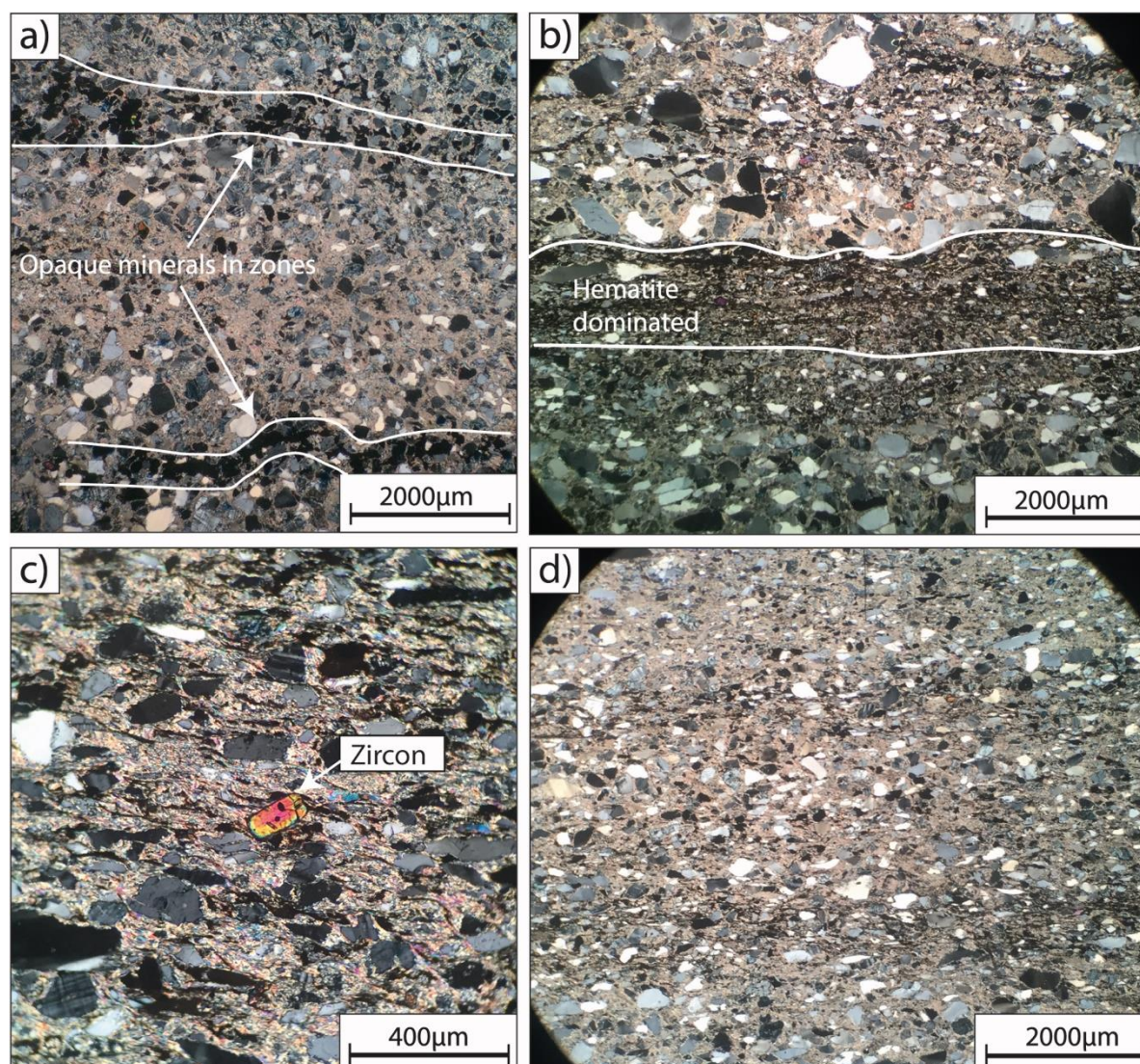
Facies 3: Silty- to fine-grained sandstone

Four thin sections were studied from Facies 3 and point counting was performed on three of the samples (Table 3.2). The silty- to fine-grained sandstone facies is matrix supported and fine grained (0.125-0.25mm) (Appendix A). The grains are sub-angular to sub-rounded (Figure 3.2) and moderately to poorly sorted (Figure 3.3) (Appendix A). Zircon, rock fragments and heavy minerals were observed in thin sections in small amounts, represented in the point counting result (Appendix B). Rock fragments were only observed in small amounts, most of the grains are floating in the matrix (Figure 4.15). The matrix consists of mica, sericite, quartz (mainly polycrystalline) and possibly other minerals of clay/silt fraction that is

difficult to optically identify in the thin sections. Mica occurs in finer grained zones as cement between grains (Figure 4.15d).

Preservation of feldspar varies within the samples, where plagioclase is generally better preserved than the K-feldspar. The average K-feldspar preservation represents category III (Figure 3.4) and plagioclase preservation category II (Figure 3.4). The silty- to fine-grained sandstones show alternating zones with variation in grain size (silt to fine sand), which is seen in Figure 4.15a. The quartz and feldspar grains are situated in the coarser zones and the heavy minerals are commonly found in the mica-rich, finer-grained zones. Ska 2-4-16 has a much higher concentration of hematite than other samples, with an enrichment of hematite in zones as seen in Figure 4.15b. In many of the silty- to fine-grained sandstone samples there are zones with opaque mineral grains, as seen in Figure 4.15a. Within these zones hematite and zircon (Figure 4.15c) are most abundant. These opaque zones are further studied in SEM (chapter 4.4.3).

Point counting (Appendix B) shows that the total percentage of framework grains (quartz, feldspar and rock fragments) is 35 %. Matrix (mica, sericite, quartz and other minerals) dominates these samples and contributes to an average of 54 %. The quartz content is much lower than in other facies and contributes to only 27 %. The average total feldspar content is only 6.7%. With a hematite content of 2 %, Ska 2-4-16 differ from the other samples with a hematite content of approximately 1 % (Appendix B).

Figure 4.15: Distribution of minerals in the silty- to fine-grained sandstone samples. **a)** Shows how the opaque grains occur in seams in Ska 2-11-16. There is an enrichment of mica between the seams. In close contact with the opaque seams the grains are larger than in the mica rich zone. **b)** A hematite dominated zone shown between the two white lines, Ska 2-4-16. **c)** White arrow pointing at a zircon grain floating in the mica-rich matrix. **d)** Show alternating zones of coarser and finer grained material thorough the thin section, Ska 2-2-16.

Facies 4: Breccia

One thin section from Facies 4 were optically analyzed in microscope and point counted (Appendix A and B). Very coarse sand (1.06 mm) (Table 3.1) is the dominating grain size in the sample (Appendix A). The grains are sub-angular to angular (Figure 3.2, Appendix A) and the breccia is poorly sorted (Figure 3.3, Appendix A). The rock fragments in the sample display the poor sorting and increased average grain size. Polycrystalline quartz, monocrystalline quartz and feldspar make up the largest grains in this sample (Figure 4.16a). The breccia sample is matrix supported, with a matrix of mica, sericite and polycrystalline

quartz (Figure 4.16). The smallest grains in the sample are more fractured than the larger grains. Opaque grains, heavy minerals and zircon are observed in this sample, but in smaller amounts than in the other facies. The preservation of feldspar varies within the sample, K-feldspar with an average preservation category II/III and plagioclase was category II (Figure 3.5 and Appendix A). Equal amounts of plagioclase and K-feldspar were observed in thin section. The K-feldspar grains are in most cases larger than the plagioclase.

The point counting analysis (Appendix B) revealed that the total percentage of framework grains (quartz, feldspar and rock fragments) is 58 % and the average matrix content is 39 %. The dominating grains are quartz, with an average of 58 %. The feldspar content is low, about 10 % (Appendix B).
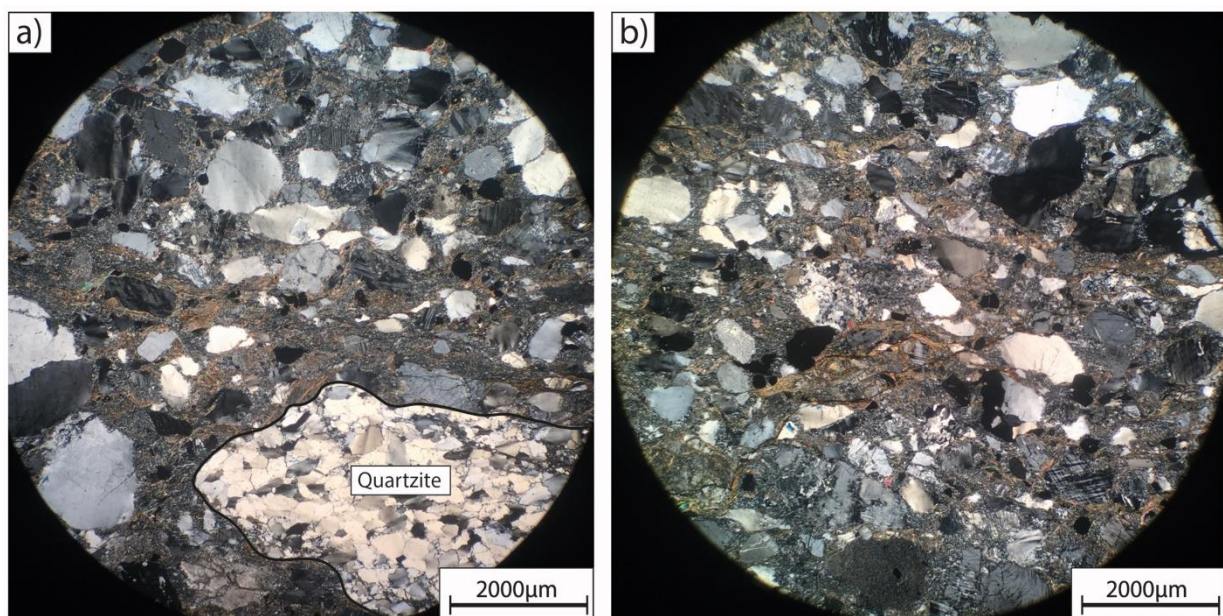
Figure 4.16: Pictures of the breccia of Facies 4 taken in cpl. **a)** Shows the poor sorting of the breccia and distribution of grains, black line around quartzite grain in Ska 13-16, **b)** show the poor sorting of the braccia, Ska 13-16.

4.4.2 XRD results

22 XRD diffractograms were analyzed with Siroquant to estimate the weight % of the minerals in the samples, the results are found in Figure 4.18 and Appendix C. Detailed description and the results are presented below according to their representative facies. Feldspar types identified were plagioclase (albite), and the K-feldspars microcline and orthoclase. The mica minerals found in the samples were muscovite, biotite and lepodolite.

45

Facies 1: Conglomerate

The samples collected from the conglomerates are mainly from the conglomerate matrix. Based on the XRD analyses, quartz, K-feldspar, plagioclase and mica are the most common minerals found in the conglomerates at Skarvemellen. Hematite is present in two of the samples (Ska 2-7-16 and 2-9-16) (Figure 4.18) (Appendix C). Quartz is the dominating mineral with a wt. % of 75 in the lowermost conglomerate (Ska 2-5-16) (Figure 4.9, 7.5 m) and 62 % in the uppermost conglomerate (Figure 4.9, 44 m) (Ska 10-16, Figure 4.18). The wt. % of K-feldspar is quite similar in all the samples and varies between 16-20 % (Figure 4.18, Appendix C). The plagioclase content increase significantly, from 3 % in the lowermost conglomerate (Ska 2-5-16) to 28 % in the uppermost conglomerate (Ska 11-16), as seen in Figure 4.18. Mica represents in this case muscovite and sericite, with a wt. % that varies from 3 % (Ska 2-9-16) to 21 % (Ska 2-7-16). The average quartz/total feldspar ratio for Facies 1 is 2.57 (Figure 4.17).

Facies 2: Sandstone

The sandstone samples from Skarvemellen (Figure 4.18) (Appendix C) are rich in quartz, K-feldspar and plagioclase. The quartz content varies from 48 wt. % (Ska 8-16) to 65 % (Ska 2-16-16) (Figure 4.18). The quartz content decreases from sample Ska 2-12-15 (65.5 wt. %) up to Ska 8-16 (48 %) before it increases to a wt. % of 53.6 at Ska 9-16 (Figure 4.18). The K-feldspar makes up an average of 21 % and varies between 13.8 % and 28.9 % (Figure 4.18, Appendix C). Plagioclase is present in varying amounts from 2.4 to 7.5 % in all the samples, with an average amount of 5 %. Mica content varies from 1.5 % (Ska 2-12-16) to 28 % (Ska 9-16), with an average wt. % of 13 (Figure 4.18, Appendix C). Mica represents muscovite, biotite and sericite in the sandstone samples (Figure 4.18, Appendix C). Traces of hematite are present in three of the samples (Figure 4.18) with a wt. % that varies from 0.1 to 3.6 %. The average quartz/total feldspar ratio for facies 2 sandstone is 2.46. The quartz/total feldspar for the individual samples can be observed in Figure 4.17.

Facies 3: Silty- to fine-grained sandstone

The dominating minerals are quartz and mica. Mica represents the total count of muscovite, biotite and sericite. Mica is the dominating mineral in these samples and constitutes an average of 43 wt. %. Quartz make up on average 41 %, and K-feldspar 9 %. Ska 21-16 (Figure 4.18 and Appendix C) is the only sample that contain chlorite and rutile, 11 % and 3 % respectively (this samples is a part of the Mellsenn Group). Plagioclase is present in small

amounts in most samples, except Ska 2-2-16. Plagioclase contributes to an average of less than 1 % (Figure 4.18). Hematite is present in three of the samples (Figure 4.18). The average quartz/total feldspar ratio is 4.30 for Facies 3. The quartz/total feldspar for the individual samples can be observed in Figure 4.17.

Facies 4: Breccia

Quartz, K-feldspar and plagioclase are the most common minerals detected in the breccia matrix from Skarvemellen, Ska 13-16 (Figure 4.18, Appendix C). Quartz is the dominant mineral and makes up 54 % (Figure 4.18, Appendix C). K-feldspar and plagioclase both make up a total of 40 %. Mica is represented by muscovite and sericite with a wt. % of 4.2. Hematite make up approximately 1 % in sample Ska 13-16, as seen in Figure 4.18 and Appendix C.
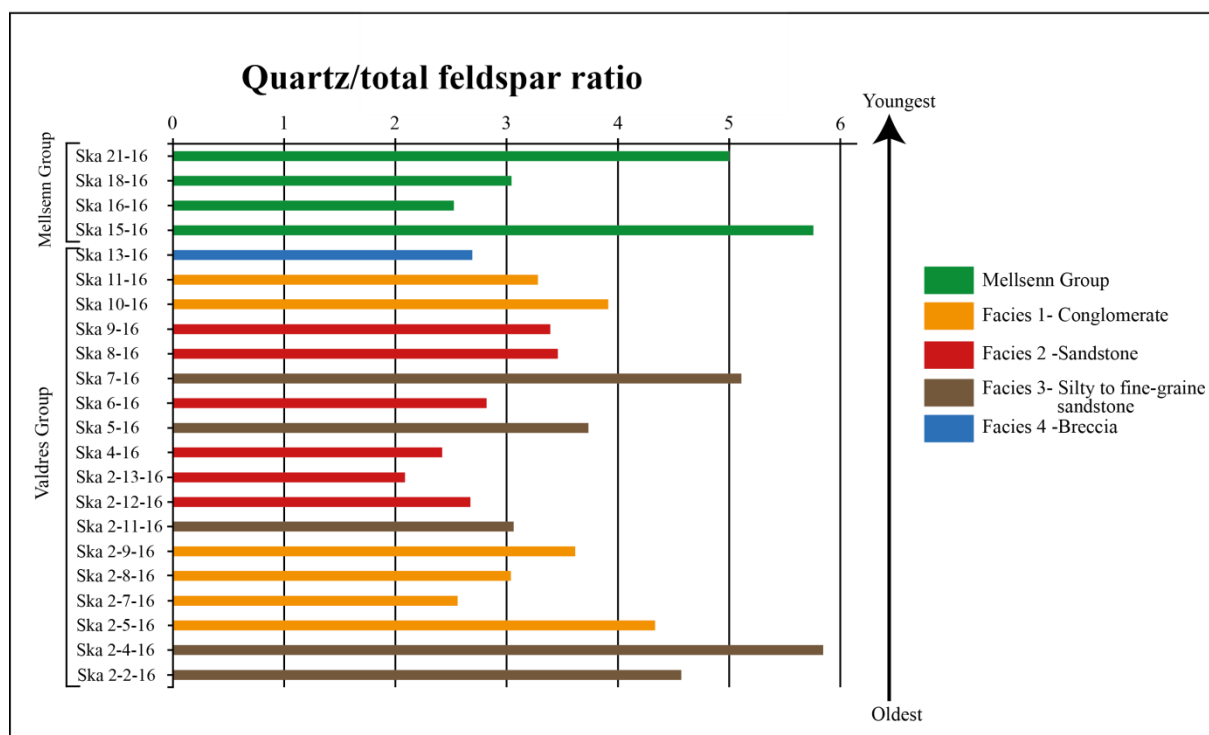
Figure 4.17: Quartz/total feldspar ratio based on results from the XRD analyses (Appendix D) from Skarvemellen. Plotted stratigraphically.
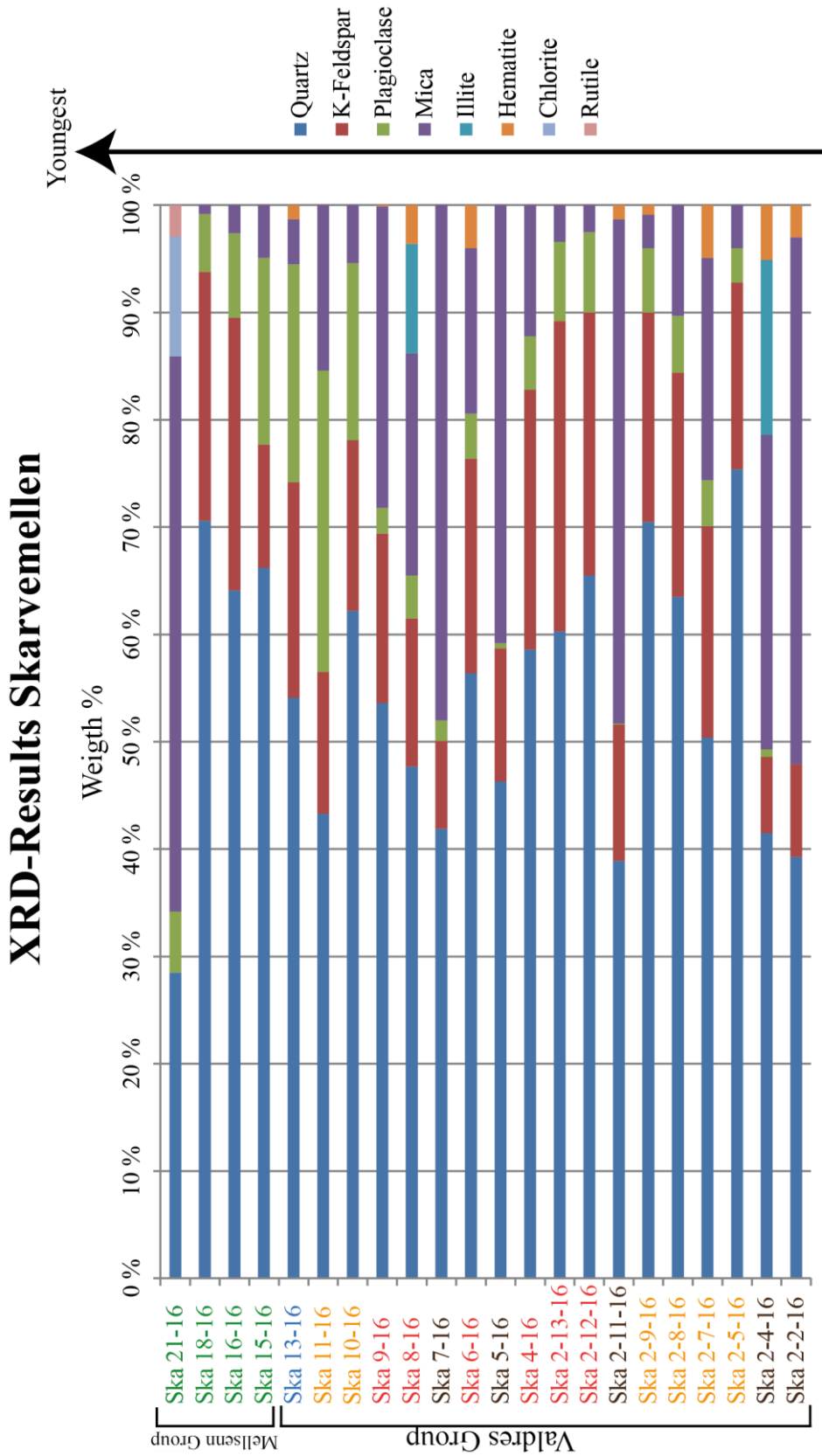
Figure 4.18: The weight % of the bulk composition from the samples collected at Skarvemellen plotted in facies, with a legend of the minerals present in the sample to the right. The x-axis shows the weight % and the y-axis shows the sample numbers. Stratigraphic plot of the wt. % are found in Appendix C. Legend for the sample colors are found in Figure 4.17.

### 4.4.3 Scanning electron microscope analysis (SEM)

A total of five thin sections were studied in the scanning electron microscope (SEM), four samples from the Skarvemellen profile and one sample from the Ring Formation (Hedmark). The results were utilized using backscattering electron images (BSE) on carbon coated thin sections. Low vacuum was used to detect feldspar overgrowth. The main focus during SEM analyses was to identify opaque grains found in the thin sections, feldspar overgrowth, feldspar zonation, intergrowth of quartz and other features possible to detect in SEM. The opaque grains turned out to be heavy minerals and iron oxides. None of the conglomerate samples (Facies 1) were studied in SEM.

Facies 2: Sandstone

Two samples from Facies 2 were studied in SEM; Ska 2-12-16 and Ska 8-16. Several K-feldspar and plagioclase grains were studied in detail, none of the samples showed zonation within the feldspar or feldspar overgrowth. Feldspar intergrowths have been observed in the sandstone samples, as seen in Figure 4.19, where K-feldspar is the host grain and albite is seen as irregular albite perthite lamellas within the K-feldspar grain. The albite grains are in general more fractured than the K-feldspar (Figure 4.20b). The grains in the samples were primarily well rounded and showed clastic grain contacts (Figures 4.19 and 4.20). The boundary between the matrix and the grains are clearly exposed in all the samples. Some grains appear fringy or with irregular edges. The matrix is primarily muscovite and some sericite, and act as the pore filling material. Several heavy minerals were identified; ilmenite, zircon, monazite and apatite (Figure 4.20a). They seem to be randomly scattered in the sandstone samples, but may also be organized in clusters or seams (Figure 4.20a).
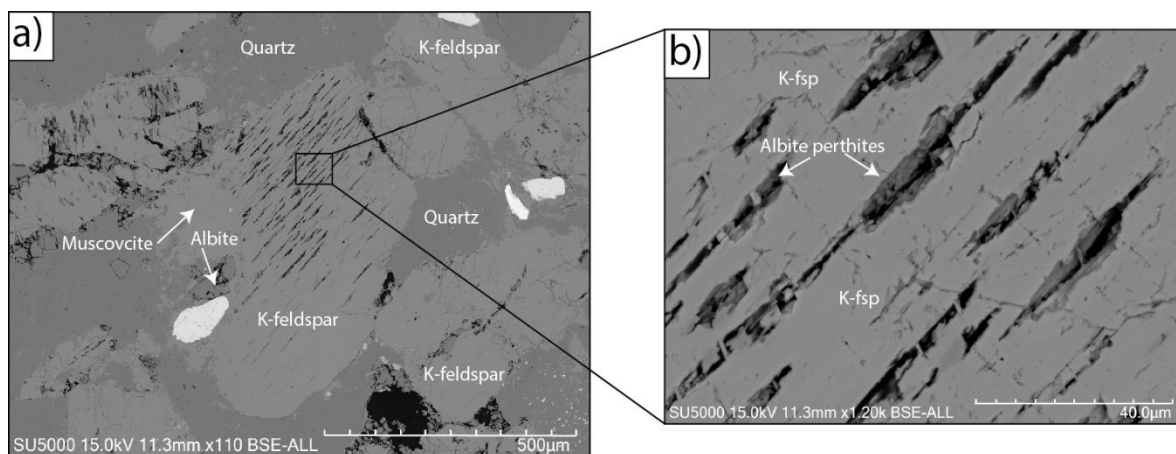

Figure 4.19: Example from Ska 2-12-16 **a)** K-feldspar with albite perthite lamella, **b)** close up of the K-feldspar and albite perthite lamella.
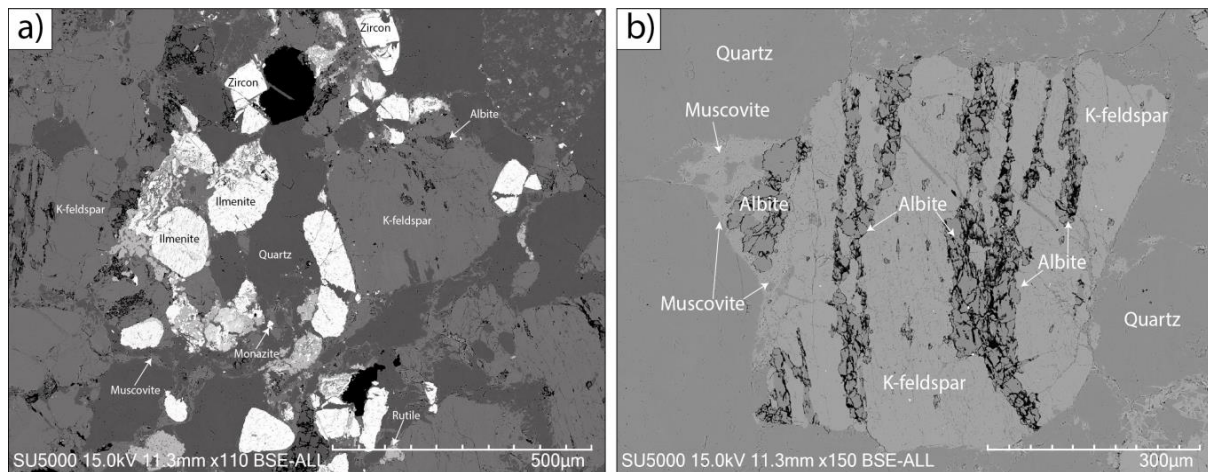
Figure 4.20: a) Assemblage of heavy minerals in Ska 2-12-16, **b)** Feldspar intergrowth of K-feldspar and plagioclase, Ska 2-12-16.

Hematite and ilmenite are the most common iron oxides found in the samples, where hematite is most abundant. Quatz-feldspar intergrowths have been observed in Ska 8-16 (Figure 4.21). Rutile was often seen as small grains arranged in clusters in the matrix surrounding the grains (Figure 4.21). K-feldspar overgrowths were discovered using low vaccum image on Ska 8-16. The original grain was seen as a rounded grain and the K-feldspar overgrowth was exposed in backscatter as an irregular surface.
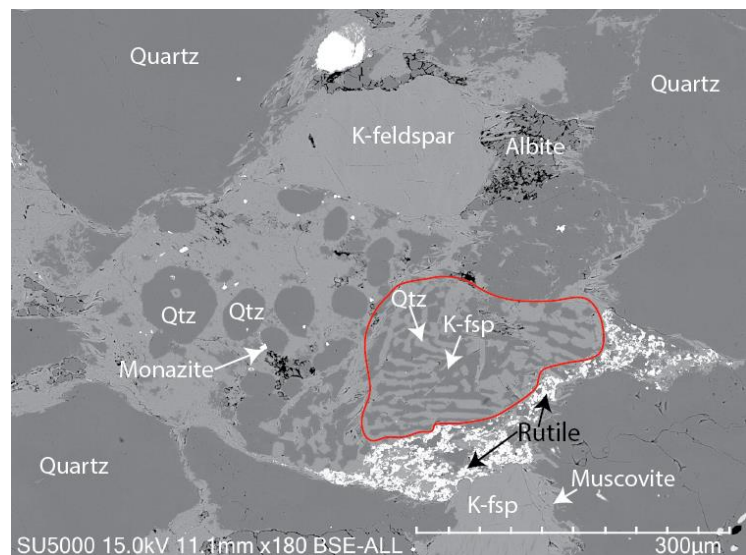
Figure 4.21: Example of an intergrowth of quartz and K-feldspar (marked with a red line), with rutile occurring as small grains arranged in clusters in the matrix surrounding the grains, in sample 8-16. Monazite, quartz, muscovite and albite are also found.

The mineral composition was identified in both of the phases, displaying that they both were K-feldspars. During detailed analyses the original K-feldspar grain appear to contain a small amount of Na, which was absent in the K-feldspar overgrowth.

Facies 3: Silty- to fine-grained sandstone

One sample from the silty- to fine-grained sandstone facies was studied in SEM; Ska 2-4-16. The sample shows a gradual transition from coarser to finer material. Heavy minerals are often arranged in seams marking a transition between the finer- and coarser-grained materials or randomly scattered in the sample as seen in Figure 4.22c. The scattering often applies to

the smallest heavy minerals in the sample, while the larger ones seem to be arranged in zones. The heavy minerals identified were apatite, zircon and rutile (Figure 4.22c). A significant amount of apatite was found and apatite overgrowth was identified on several apatite grains (Figure 4.22a). The original apatite grain has a smooth surface, while the overgrowth appears fringy or irregular (Figure 4.22a). The apatite grain is floating in the micaceous matrix, with muscovite needles interfingering the overgrowth (Figure 4.22a). Hematite was found in the heavy mineral zones, randomly scattered in the sample or as an assemblage of many small grains in a cluster (Figures 4.22b and 4.22c).
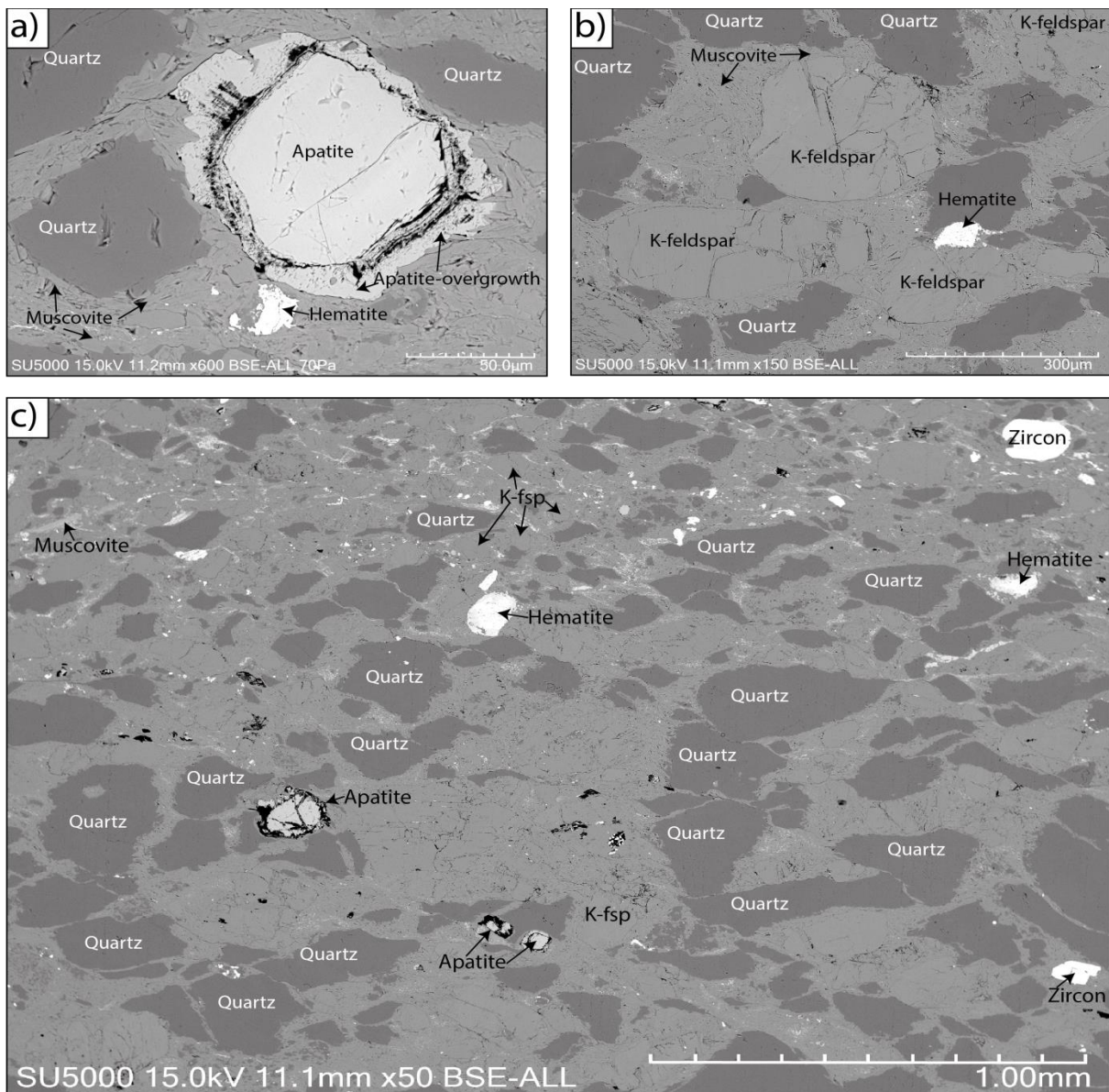
Figure 4.22: Examples from Ska 2-4-16 **a)** apatite overgrowth, **b)** shows how mica occur around the grains and a cluster of hematite, c) distribution of mineral grains in Ska 2-4-16.

Facies 4: Breccia

One breccia sample was studied in SEM; Ska 13-16. Most of the grains in this sample appear to be floating in a mica (muscovite) dominated matrix. Mica and sericite act as pore filling in fractures or around grains (Figure 4.23). The grains in this sample are more fractured than the other facies (Figure 4.23). The K-feldspar grains were found to be fractured and have irregular surfaces, with interfingering muscovite needles. Perthites where K-feldspar is the host grain with albite lamellas, also occur in this sample. Heavy minerals were found to be mainly organized in clusters or randomly scattered in the samples. Heavy minerals identified were: apatite, monazite and barite (Figure 4.23b). Hematite was identified and occur in considerable amounts, the largest grains were often fractured (Figure 4.23a).
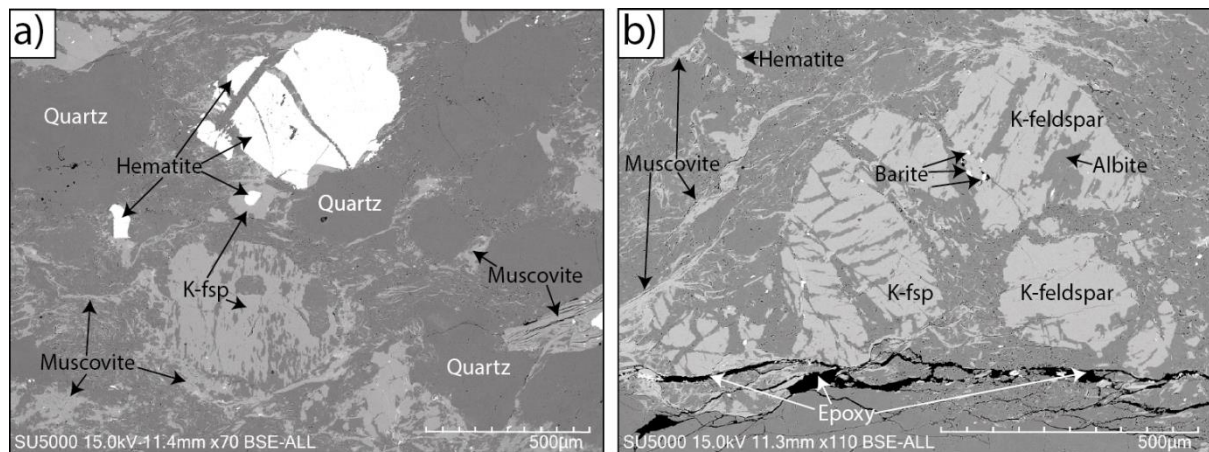
Figure 4.23: Examples from Facies 4, breccia, Ska 13-16. **a)** Large fractured hematite grain and smaller hematite grains, surrounded by quartz, K-feldspar and muscovite. **b)** Needles of muscovite in a quartz rich matrix, the grains are fractured. Barite is seen as very small white grains, in the middle of picture b.

Ring formation

Sample KIN 3-15 from the Ring Formation (Hedmark Group) was studied in SEM. Several perthite lamellas were observed, K-feldspar as the host grain with irregular albite lamellas, as seen in Figure 4.24b. Quartz-feldspar intergrowths were also observed in this sample. Chlorite acts as the pore filling material (Figure 4.24). In the Ring formation only rutile and monazite were identified. Iron oxides were found during SEM analysis and identified as hematite and ilmenite. Feldspar zonation was studied in detail, but no internal variation in chemical composition was found in the studied feldspar. The chlorite was further investigated during SEM and was found to be Fe-rich (Table 4.2).
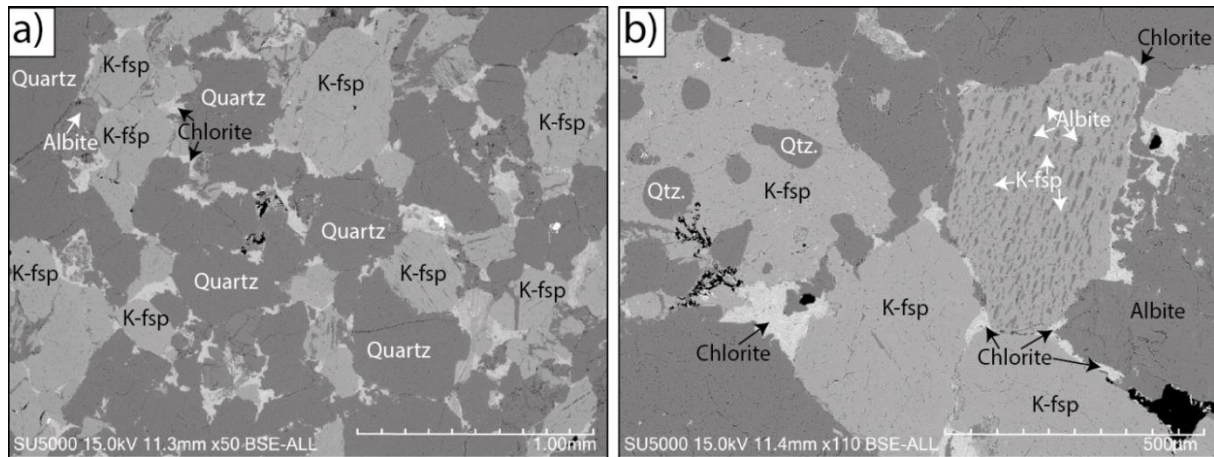
Figure 4.24: Backscatter photo of the studied sandstone from the Ring Formation, KIN3-15 (Hedmark Group). **a)** Shows the distribution of minerals in the sandstone with chlorite as the pore filling mineral. **b)** Shows a close up of an intergrowth of albite perthite lamella in a K-feldspar, seen towards the upper right corner. The chlorite is cementing the grains together and acts as pore filling.

Table 4.2: Mineral composition of chlorite from the Ring Formation sample, SEM analyses of KIN 3-15.

O	Mg	Al	Si	K	Fe
40.09	4.17	10.93	13.13	0.95	23.32
38.49	4.05	10.93	13.59	0.00	22.70
39.70	4.41	10.22	12.25	0.00	25.60
39.84	3.38	11.55	16.53	0.00	17.39
40.48	3.94	10.48	13.12	0.00	21.33
42.72	5.09	11.63	13.52	0.00	23.99
39.64	3.93	10.62	13.07	0.00	22.52
31.22	3.08	13.49	15.03	1.78	20.75

4.4.4 Heavy minerals

17 samples were sent to heavy mineral analyses and the results from Skarvemellen and the Hedmark Group are displayed in Table 4.3.The results from Rundemellen can be seen in Appendix E and are described by Sørhus (2017) in her master thesis (The Eocambrian Valdres Group at Rundemellen, Mellane).

The results from the heavy mineral analyses show that the Skarvemellen samples mostly contain stable minerals such as apatite, rutile, tourmaline and zircon (Table 4.3, Appendix E). The Hedmark Group contain occasional grains of unstable mineral phases such as pyroxene and amphibole. Zircon is the most abundant mineral in Skarvemellen, with an average percentage of 84 %. Ska 2-4-15 and Ska 10-9-16 are more apatite rich than the other

Skarvemellen samples, 28 % and 22 % respectively (Table 4.3). Tourmaline is found in two samples (Ska 10-9-16 and Ska 8-16) from Skarvemellen (Table 4.3) and some remnants are found in Ska 6-16. Rutile is only found in sample Ska 2-4-16 (Table 4.3).

In the Ring Formation sample (Ring 0) apatite is the most abundant mineral (74 %) (Table 4.3 and Appendix E). Ska 2-12-16, Ska 16-16 and BK 1 are not very representative since few heavy minerals were counted in these samples 22 %, 8 % and 24 % respectively.

Table 4.3: Results from the heavy mineral analyses. R=remnants, At (Anatas), Ap (Apatite), Ca (calcium amphibole), Cp (clinopyroxene), Ep (epidote), Gt (garnet), Mo (monazite), Op (orthopyroxene), Ru (rutile), To (Tourmaline). Ska = Skarvemellen, (Ska 2-4-16 = silyt to fine-grained sandstone, Ska 6-16, Ska 8-16, Ska 2-12-16 and Ska 16-16 = sandstones, Ska 10-9-16 = tillite. Ring 0 = Ring Formation, Rin 2-15 = Brøttum Formation, BK 1= Biri chalk from the Biri Formation, MB 1= Moelv Brygge representing the Moelv Tillite.

Samples	At	Ap	Ca	Cp	Ep	Gt	Mo	Op	Ru	Sp	To	Zr	total	count
Ska 2-4-16		27.5							0.5			72.0	100.0	200
Ska 6-16		1.0									R	99.0	100.0	200
Ska 8-16		17.0									5.0	78.0	100.0	200
Ska 10-9-16		21.5	R	R							2.5	76.0	100.0	200
Ska 2-12-16									4.5			95.5	100.0	22
Ska 16-16												(8)	0.0	8
Ring 0		73.5				1.5	0.5		R	R	1.0	23.5	100.0	200
Rin 2-15		49.0									1.0	50.0	100.0	200
BK 1		32.4	5.9						2.9		32.4	26.4	100.0	34
MB 1	0.5	75.5		R		R	R		0.5		0.5	23.0	100.0	200

5　Discussion

The depositional environment of the Skarvemellen section will first be discussed before a discussion around rift sedimentation and provenance area for the Valdres Group sedimentary rocks. Last, the Valdres Group, including Rundemellen and Skarvemellen, will be compared to the Ring Formation from the Hedmark Group based on e.g. correlation of the the Moelv Tillite to the tillite at Rundemellen and Skarvemellen. To interpret the depositional environment at Skarvemellen it will be compared with the Rendalen Formation (continental deposit of the Hedmark Basin).

5.1   Depositional environment

In this thesis the Eocambrian Valdres Group is represented by samples collected at Skarvemellen, Mellane. The Valdres Group was deposited in a continental rift basin on the western part of Baltoscandia (pers. com. J. P. Nystuen, 2017). The depositional environment described below is found to have similar characteristics as the braided stream deposits of the Rendalen Formation, from the eastern continental part of the Hedmark Basin.

5.1.1   Facies association 1 – Longitudinal bar deposits

Facies association 1 consists of conglomerates (Facies 1), sandstones (Facies 2) and silty- to fine-grained sandstones (Facies 3) (Figure 4.3). The conglomerates are grain supported, characterized by sub-rounded to sub-angular clasts ranging in size from coarse sand to cobble (0.5 cm to 10 cm) (Table 3.1, Appendix A). The matrix consists of medium to coarse sand (Appendix A). The roundness of the conglomerate clasts displays grain size relations, the largest grains, usually quartz, are in general more rounded than the smaller grains (usually feldspar). According to Boggs (2014) the degree of roundness is a function of grain size, grain composition, transport mechanism and distance. The variation in roundness within the samples may indicate that the transport distance has been longer for some grains. Well-rounded pebbles in ancient sedimentary rocks are generally an indicator of fluvial transport (Boggs, 2014).

The conglomerate matrix consists of sub-rounded to well-rounded grains, the sorting varies from well to very poor (Appendix A, Figure 4.11). The percentage of clasts and size of the clasts changes within the conglomerates; this may have been caused by changes in the supply, transport processes or distance from
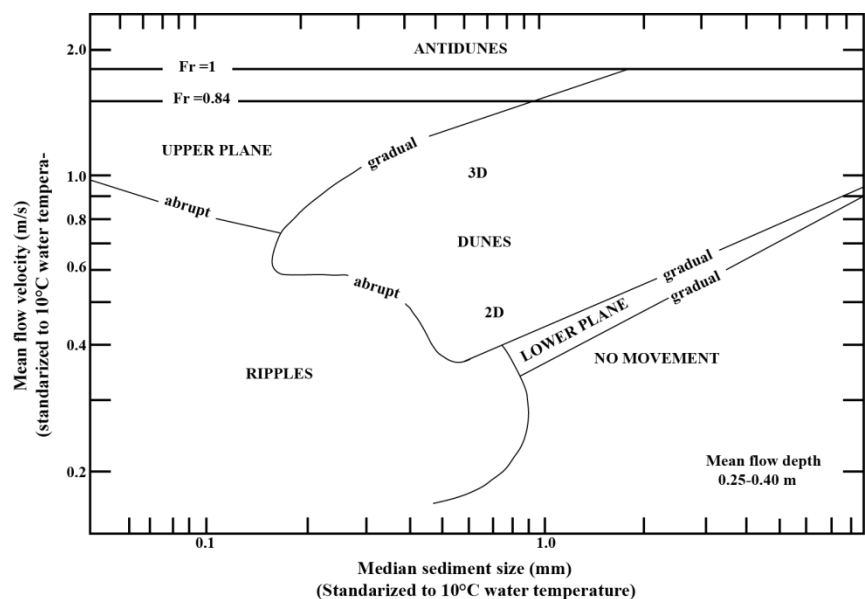
Figure 5.1: Plot of mean sediment flow (y-axis) against median sediment size (x-axis). Fr =Frouds number. From Southard and Boguchwal (1990).

the provenance area during deposition. The conglomerate matrices range in color from light pink to more red. The red color of the matrices may indicate the presence of red ferric oxides, which is typical for braided alluvial sediments (Selley, 1985). According to Turner (1980) the red coloring of the sediments occur during diagenesis, further discussion around ferric oxides is found in chapter 5.2.1 under Fe-oxides.

Sandstones of Facies 2 found in FA 1, can be divided into four separate sandstones, based on the sedimentological structures found; cross-bedded (2a), parallel laminated (2b), structureless (2c) and pebbly (2e) (Table 4.1). The parallel laminated and structureless sandstones are the two dominating sandstone units, the parallel laminated being more prominent in the lowermost part and the structureless dominating the upper part of FA1 (Figure 4.9). The cross-beds range in size between 15 to 30 cm, and no internal grain size variations have been discovered. They show only one transport direction indicating a uni-directional flow, towards E for Skarvemellen (Figures 4.1 and 5.9). The cross-bedding was developed within sand deposited during ripple or dune migration, they form in low or high flow velocity respectively (Figure 5.1) (Collinson et al., 2006).

Parallel laminated sandstones may have been deposited when grains settle from suspension, by traction transport or fluctuations in the depositional conditions (Collinson et al., 2006). These fine- to medium-grained parallel laminated sandstones probably deposited during low flow velocity (Figure 5.1). The structureless units could have been deposited during rapid settling of a suspension rich flow (Collinson et al., 2006). The grains probably settled so quickly that they were buried before any bedload movement occurred (Collinson et al., 2006). Pebbly sandstones (Facies 2e) occur in FA1 (Figures 4.8 and 4.9), the clasts are well-rounded to sub-rounded, ranging in size from 0.5 cm to 30 cm in diameter. The limiting factor of moving large particles are not the velocity of the stream, but the availability of particle size in the source area (McKee et al., 1967). If the available material were pebbly these would be transported during high flow velocity and deposited when the flow velocity decreased (pers. com. J. P. Nystuen, 2017). If the flow velocity was high but the available material was fine grained, the fine material would not reflect the velocity of the stream only the available material in the source area.

The silty- to fine-grained sandstone (Facies 3) found in FA 1, is characterized by alternating sequences of dark brownish-red and gray colored layers. The high silt content may point to a

low-energy environment, with possible fluctuations in energy of the fluvial stream in order to deposit these fine-grained particles from suspension. Generally climate highly effects the river discharge by seasonal variations, such as heavy rainfall and melting of snow (Richards, 1996), resulting in both dry periods or flooding stages. During a flooding stage the silty material of Facies 3 may have been deposited on the floodplains. The silty- to fine-grained layers (Facies 3) could also have been deposited during low-water stages or possibly in overbank areas (Smith, 1970).

FA1 can be interpreted to represent longitudinal bar deposit of a braided stream system as reflected in the grain size and sorting. Longitudinal bars consist of an accumulation of gravel with varying admixture of sand and finer materials (Figures 5.2 and 5.4) (Smith, 1970). Transverse bars on the other hand are composed of predominantly sand and finer-grained material (Figure 5.4) (Smith, 1970). FA1 may therefore interpreted as a longitudinal bar deposit as reflected in the coarse, gravely conglomerates with alternating layers of sand and finer
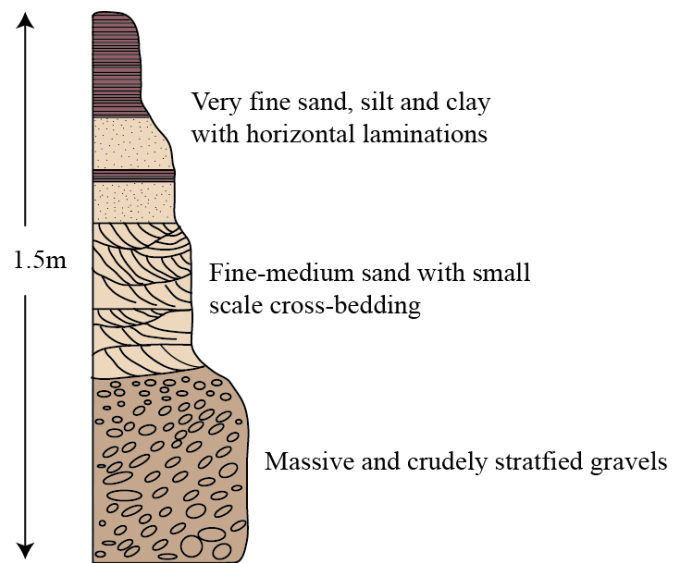
Figure 5.2: Longitudinal bar, displaying a fining upward sequence in a gravelly braided river. Modified from Turner (1980) and Williams and Rust (1969).

material as seen in Figure 4.9. Longitudinal bars tend to develop when the coarsest bedload material is deposited mid-channel (Leopold and Wolman, 1957). The longitudinal bars start to grow when finer material is deposited downstream and on top of the coarse bedload (Rust, 1977). The processes that act during formation and deposition of a longitudinal bar is not well understood (Turner, 1980). Studies of the Donjek River in Alaska by Williams and Rust (1969) and Rust (1972) show that cross-stratification in longitudinal bars tent to develop during low flow velocity when sand is separated from the gravelly bedload (Turner, 1980).

Longitudinal bars are bounded by active channels on both sides, they are typically gravel rich and more prominent in the proximal part of braided streams (Miall, 1977). Some sandy bars show similar characteristics as the longitudinal bars, this may be caused by erosion rather than deposition (Miall, 1977). The original bar type of the sandy bars may originally be quite different from longitudinal bars (Miall, 1977). The ratio of transverse bars to longitudinal bars should increase downstream because of the river
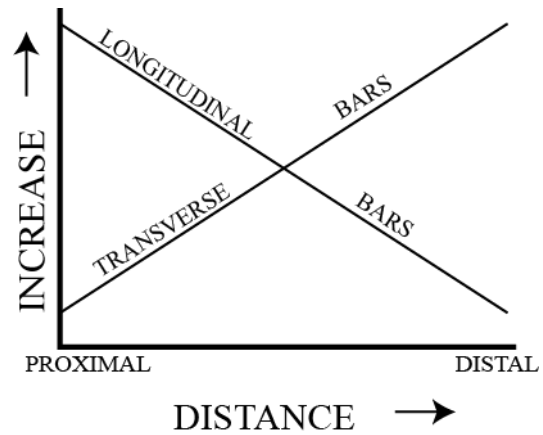
Figure 5.3: Show the distribution of longitudinal and transverse bars downstream a braided river, from Smith, 1970.

tendency to fraction its load into finer particles (Figure 5.3) (Smith, 1970). The impression of longitudinal bars is that they tend to develop in upwards fining sequences (Figure 5.2) (Turner, 1980) this trend is seen in FA 1 (Figure 4.9).

The conglomerate layers at Skarvemellen also support the theory of braided stream deposits. According to Miall (1977) the conglomerate facies found in braided streams consists mainly of coarse-grained and grain-supported conglomerates with a sandy or silty matrix that have filled the voids after deposition. In conglomerates originated from braided streams, upwards fining sequences are common (Nemec and Steel, 1984), this is found in all the conglomerates at Skarvemellen and supports the theory of deposition in a braided stream system. The conglomerates at Skarvemellen mainly suggests deposition of bedload from strong traction currents (Sundborg, 1956). Conglomerates of braided streams are often mature, this is probably a result of effective reworking of the clasts, strong channelized transport and continuous runoff (Nemec and Steel, 1984). The variation in clast size and amount may indicate varying river discharge and availability of material in the provenance area (Nemec and Steel, 1984).

Thin layers of very fine-grained material often occur in braided rivers on top of bars or interbedded/alternating in a sandstone sequence (Davis, 1983). Because of the flashy discharge in braided streams mud is kept in suspension and very fine-grained sediments are not abundant (Davis, 1983). The fine-grained material is often deposited in abandoned channels in shallow braided rivers when the river discharge decreases (Rust, 1977, Nemec and Steel, 1984). According to Smith (1970) the discharge in braided streams is highly variable

which leads to repeated reworking of the silty- to fine-grained material (Facies 3). The reworking of the layers may produce intra-clasts that are deposited as pebbles or clasts in the coarser sediments (Smith, 1970). These very fine-grained silty-layers possibly deposited in abandoned channels are diagnostic for braided stream deposits (Selley, 1985). Similar layers are found at Skarvemellen, as seen in (Figures 4.8 and 4.9)

5.1.2 Facies association 2 – Upwards fining channel fill depo

Facies association 2 represents an upwards fining development with grain sizes ranging between medium and coarse sand (0.41-0.75 mm) (Table 3.1). The sandstones are grain supported and moderately to well-sorted with a roundness ranging between sub-angular to sub-rounded (Figures 3.2 and 3.3, Appendix A). FA 2 consists of sandstones with varying sedimentary structures; cross-bedded (2a), parallel laminated (2b), structureless (2c), pebbly sandstone (2e) and thin layers of silty- to fine grained sandstone (Facies 3) (Figure 4.8). Parallel laminated and structureless sandstones are dominating in FA 2 (Figure 4.8), in the lowermost part structureless units are more common while parallel lamination dominates in the uppermost part (Figure 4.8). Cross stratification also becomes more prominent in the upper part of FA 2 (Figure 4.8). The depositional mechanism of the individual sedimentary structures is described in chapter 5.1.1.

FA 2 consists of upwards fining sandstone units with a silty- to fine-grained unit on top (Figure 4.8). The facies association has an overall upwards fining trend, which may reflect deposition in a fluvial environment. Paleocurrent measurements of the cross-bedded sandstones imply the same transport direction, towards East (Figure 16) which indicates a uni-directional flow during deposition.

The upwards fining trend of FA 2, points to a channel fill deposit. According to Reineck and Singh (1975) an upwards fining trends is often well developed in a channel fill sequence. The channel fill deposit may have been deposited by a rapid infill of the accommodation space due to increasing sedimentation rates and reduction in accommodation. The rate of sedimentation may be rapid in braided streams. After most of the available sediments have been deposited new sediments are only entered during overbank floods (Reineck and Singh, 1975). These sediments tent to be fine-grained, and in this case might represent deposits of Facies 3; silty- to fine-grained sandstones (Figure 4.8). The thickness of the fine grained deposits is

controlled by creation of new accommodation, in this case probably controlled by rifting events since the Skarvemellen sedimentary rocks were deposited in a rift controlled basin. The upwards fining sandstone units of FA 2 may also be deposited when the current velocity is decreasing and the channel is gradually filled with sediments (Selley, 1985).

FA 2 may represent several channel fill deposits stacked on top of each other (Figure 4.8) in a braided stream environment, based on the coarseness and structures of the succession at Skarvemellen. They may have been deposited when new accommodation space was created during an active tectonic phase or stacking of several channel fill sequences on top of each other. When the accommodation space was filled, the braided channels changed course to create new accommodation space to continue depositing material. Another interpretation is that
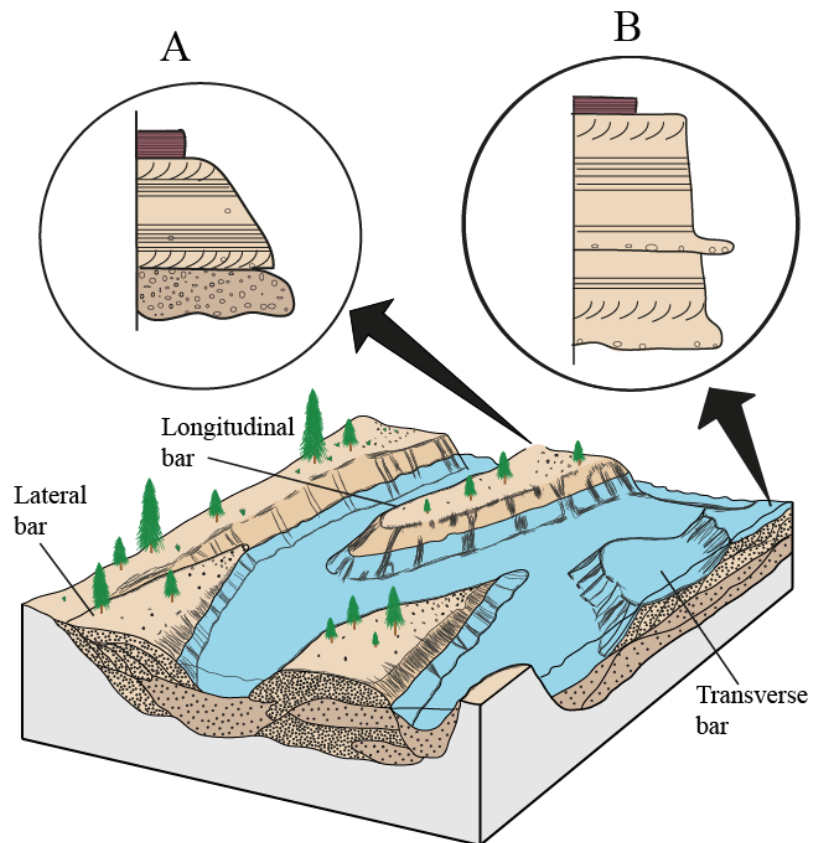
Figure 5.4: Depositional model for a low sinuosity braded river. Sequence **A** display a longitudinal bar deposit and sequence **B** a longitudinal bar. Modified from Galloway and Hobday (1996)

both channel fill deposits and transverse bars make up the succession in FA 2. Transverse bars (Figure 5.4) occur in zones of the river with low current energy (Davis, 1983), they may be stabilized by vegetation (transverse bars are further discussed in chapter 5.1.3). Due to lack of vegetation in Precambrian, the transverse bars probably migrated easy and had a low preservation potential.

5.1.3 Facies association 3 – Sandstone channel fill deposit or Transverse bar

Facies association 3 consists of sandstones with only small grain size and a slight upwards fining trend (Figure 4.8). The change from FA 2 to FA 3 is often abrupt. FA 3 consists of sandstones with different sedimentary structures; cross-bedded (2a), parallel lamination (2b), structureless (2c), trough cross-bedded (2d) and pebbly sandstone (2e). Structureless sandstone is the most abundant structure in the lowermost part of the facies, while cross-bedding is more abundant in the upper part, as seen in Figure 4.8. The depositional mechanisms of the individual sedimentary structures have been described in chapter 5.1.1. FA 3 reflects high fluctuations in river discharge; from the structureless sandstones deposited during high flow velocity to cross-bedded and parallel laminated sandstones deposited when the river discharge and flow velocity was lower. In general the river discharge appears to be gradually decreasing towards the top of FA 3, as seen in the frequent appearance of parallel laminated and cross-bedded sandstone and less sequences of structureless sandstones. FA 3 seems to have aggradational stacking patterns developed when the sedimentation rate is equal to the accommodation. The river discharge during FA 3 might have been less shifting than in FA2, since sandstones of FA 3 only show a small grain size variation and no silty- to fine-grained sandstones. These sandstones were likely deposited in channels when the current velocity was slightly decreasing and the channel gradually being filled with sediments simultaneously as new accommodation space were created (Selley, 1985). The river will need new accommodation space to continue depositing sediments in the current position or else the braided river will change its channel path/course. The creation of accommodation might in such a case be linked to an ongoing subsidence and extensive rifting of the continental rift basin.

Another interpretation of the deposition in FA 3 is a transverse bar deposit (Figure 5.4). According to Smith (1971) transverse bars can be formed when the sediments are deposited in an equilibrium profile where the sedimentation rates are equal to the rates of accommodation. This may have been the case for the Skarvemellen sandstones of FA 3 (Figure 4.8). Transverse bars are growing in the downstream direction and small scaled sedimentary structures are deposited on the active bar surface (Smith, 1971). These bars will consequently consist of predominantly well sorted sandy sediments, as seen in FA 3 at Skarvemellen, and primarily be deposited during low to intermediate water discharge. The channel is

transporting well sorted sandy sediments downstream and the transverse bar can be deposited when the stream encounter a depression (Smith, 1971), the sediment load will gradually build up from the channel floor.

5.1.4 Facies association 4 – Glacial deposit

Facies association 4 consists only of breccia (Facies 4) (Figure 4.8) and is found in a thin bed at Skarvemellen. It is represented by a poorly sorted, matrix supported deposit with angular clasts, classified as a diamictite. FA 4 may be an equivalent to the Moelv Tillite, representing a possible glacial deposit (Nystuen, 1976), this will be further discussed in chapter 5.5.1. The lithology of the breccia appears to be relatively homogenous, with predominantly feldspar clasts of varying size. Tillite is a lithified till deposited under a large continental ice sheet. Glaciers are able to transport large portions of poorly sorted material over a large distance, underneath the glacier (englacially), within the ice sheet or on the ice surface (supraglacial) (Eyles and Eyles, 2010). The poorly sorted, matrix supported breccia have similar characteristics as tillites, and in relation to the known glacial event of the Varangian Glaciation at the time, the breccia at Skarvemellen is therefore interpreted to represent a tillite deposit.

5.1.5 Braided stream deposits

The depositional systems described above seem to have similar characteristics to ancient braided river systems and might be comparable to the braided river deposits from the continental part of the Hedmark Basin (the Rendalen Formation). When looking at the studied Skarvemellen section the low variability in paleocurrent measurements (Figure 4.1), the coarseness of the sediments and the low abundance of fine-grained material all point to a low sinuosity braided stream deposit rather than a high sinuosity meandering stream deposit (Reineck and Singh, 1975). A typical feature of meandering deposits is the lack of gravely material and abundance of fine-grained sandy well sorted units (Davis, 1983). The Skarvemellen sedimentary rocks contain gravely conglomerate beds, coarse sandstones and some fine-grained layers, which is typical for a braided stream deposit not a meandering deposit (Smith, 1970). The Skarvemellen succession is therefore interpreted as a braided stream deposit with unstable river discharge and highly fluctuating channels

5.2   Mineralogical observations

5.2.1 Fe-oxides

Red beds occur under several environmental conditions e.g. desert, arid or seasonal climates, when iron is in the ferric oxide state. The red coloring is due to hematite (Fe_2O_3) formed by decomposition of ferromagnesian minerals and subsequently oxidation of Fe^{2+} to Fe^{3+} and precipitation of iron-oxides, where hematite is most abundant (Morton and Hallsworth, 1999). Fe-oxides are found as hematite (Fe_2O_3) in the Skarvemellen samples, which is confirmed by SEM analyses. The hematite mainly occurs in seams or clusters surrounded by heavy minerals. During formation of red beds dissolution of heavy minerals is an important process (Morton and Hallsworth, 1999). In red bed forming conditions the stability of other heavy minerals, as apatite, zircon and garnet, is not studied in detail and is therefore not known (Morton and Hallsworth, 1999). In ancient red beds apatite, zircon and garnet are generally abundant and is therefore thought to be stable under these conditions (Morton and Hallsworth, 1999). Apatite and zircon are the two most common heavy minerals found in the Skarvemellen samples (Table 4.3 and Appendix E).

5.2.2 Formation of sericite

Formation of sericite may be the result of mineral replacement due to hydrothermal activity or metamorphism (Que and Allen, 1996). When hydrothermal fluids reacts with the pore walls of plagioclase, sericitic muscovite starts to grow (Que and Allen, 1996). At Skarvemellen sericite was found during thin section analyses, appearing as mineral replacements caused by metamorphism and not hydrothermal reactions in replacing feldspar. No evidence of sericite replacement in the feldspar grains has been discovered, but sericite in the matrix replacing the mica was seen. During low grade metamorphism, in this case green schist facies, replacement of mica leads to the formation of sericite. During sericitization of mica, Al is replaced by Fe^{2+} and Mg (Dunoyer de Segonzac, 1970).

5.2.3 Heavy minerals

The heavy minerals found in the Skarvemellen samples are localized in seams. Zircon is the dominating mineral, with smaller amounts of phosphate minerals (apatite) and rutile. Phosphates are formed as secondary minerals, created by mineral replacement in low salinity

hydrothermal fluids in veins and pores (Morton and Hallsworth, 1994). The zircon grains in the Skarvemellen samples are often fractured and partially metamict. The heavy mineral content of the samples suggests a predominantly felsic igneous/metamorphic origin (further discussed in chapter 5.3.3), with hardly any garnet, rutile, monazite or spinel.

5.2.4 Undulatory quartz

Undulatory quartz is the most abundant mineral in most of the samples from Skarvemellen. Well-developed undulatory extinction is characteristic for metamorphic rocks, but is not only restricted to metamorphic rocks (Harvey and Christie, 1963). The development of undulatory quartz can be related to deformation when the quartz grains were subjected to pressure and temperature changes during burial or during tectonism. Post-depositional deformation processes may be the reason why the occurrence of undulatory quartz increase with age (Basu, 1985).

5.3   Environmental setting

5.3.1 Transport and maturity

The sedimentary successions at Skarvemellen consist of predominantly sub-rounded to rounded quartz and feldspar grains (Figure 4.18 and Appendix A). The high quartz and K-feldspar content (Appendix B and C) indicates a mature nature of the sedimentary rocks. Quartz and K-feldspar are according to Goldich (1938) (Figure 5.5)
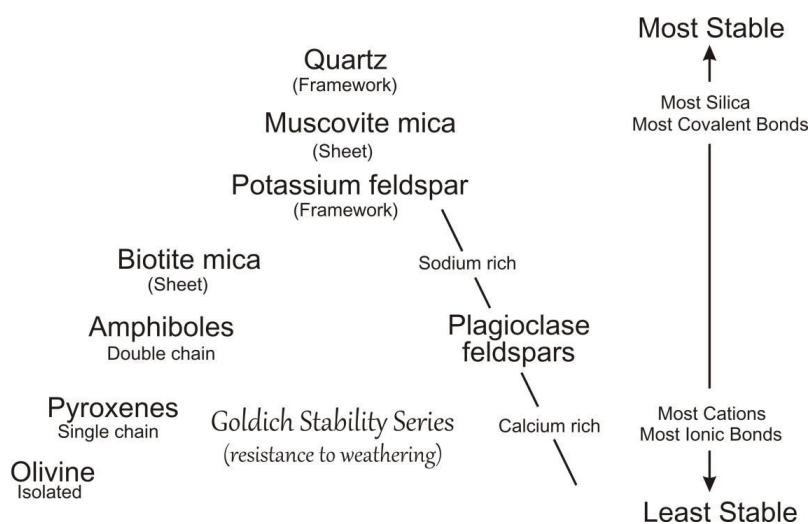
Figure 5.5: Goldich stability series, showing the stability of minerals during weathering. (Goldich, 1938).

the most stable minerals in terms of weathering and transport, suggesting a long transport. In the mature sediments there is an enrichment of stable minerals including quartz, muscovite and K-feldspar (Figure 5.5). Feldspar is a less stable and easier to erode during transport, resulting in low feldspar content in mature sediments. The feldspar preservation shows

correlation with grain size; large feldspar grains often with a better degree of preservation (Figure 3.4) than the smaller grains.

Quartz, K-feldspar and muscovite are the most abundant minerals in the Skarvemellen samples as seen from the XRD (Appendix C) and point counting results (Appendix B). The sedimentary rocks from Skarvemellen are found to be well sorted and sub-rounded to rounded, with a high quartz/feldspar ratio, indicating fairly mature sediments (Figure 5.6). The XRD and point counting results display a quite similar mineral content in the samples (Figure 5.6). The K-feldspar content is a slightly higher in the XRD than in the point counting results, this may indicate that some of the K-feldspar in the samples occurs in the matrix, and counted as matrix in the point counting results (Figure 5.6).
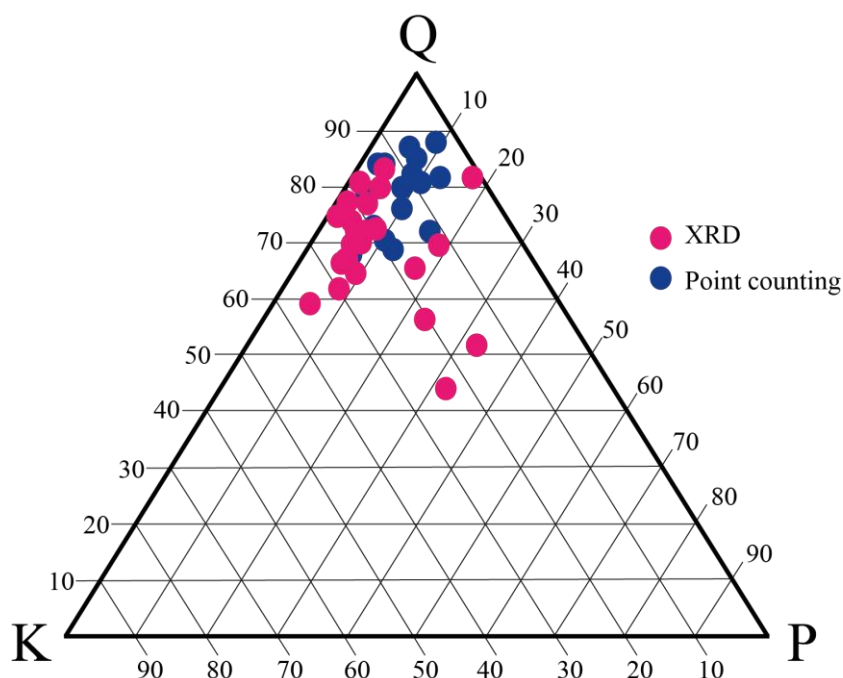
Figure 5.6: QAPF-diagram (Streckeisen, 1976) of the XRD (pink) and point counting (blue) results from Skarvemellen. The percentages of the quartz (Q), K-feldspar (K) and plagioclase (P) is calculated from the respective XRD and point counting results (Appendix B and C).

As seen in Figure 5.6 the Skarvemellen samples contain large amounts of quartz, followed by K-feldspar and plagioclase, all the samples show similar composition and plot close to the quartz corner (Figure 5.6), with minor variations. The high quartz/total feldspar reflect the maturity if the sediment composition which is a possible result of long to moderate sediment transport from the provenance area. The sedimentary rocks at Skarvemellen may already have been through several weathering cycles, consequently sedimentary rocks can be well sorted and mature without extensive transportation. As mentioned earlier the sorting may indicate a

moderate to long transport, but the roundness may show a different story. The sub-rounded to rounded grains might indicate a transport that is more moderate. They were probably not transported so far as indicated by the sorting. This may indicate mature rocks in the provenance area and the sediments were not necessarily transported too far to achieve the well sorting. Further discussion on the maturity of the provenance area is found in chapter 5.3.3.

The results from the heavy mineral analyses of the Skarvemellen sedimentary rocks show an abundance of zircon, followed by a small content of apatite and some remains of other heavy minerals such as rutile and tourmaline (Table 4.3 and Appendix E). Heavy mineral composition in sandstones are controlled by transport, deposition and diagenesis (Morton and Hallsworth, 1994). These processes affect all sediment components, not only the heavy minerals. The decrease in mineral diversity downstream have often been considered as an effect of abrasion (Morton and Hallsworth, 1999). However, studies of several major river systems, as the Mississippi (Russell, 1937), the Nile (Shukri, 1949) and Rhine (van Andel, 1950), with extremely long transport distance, show no clear-cut indication of decrease in mineral diversity downstream (Morton and Hallsworth, 1999). The abrasion effect on heavy minerals during transport is consequently thought to be negligible, but during special circumstances it may be of significance (Morton and Hallsworth, 1999, Morton and Hallsworth, 1994).

During transport and deposition heavy mineral behave different than quartz and feldspar, since they have a higher density (Morton and Hallsworth, 1999). In 1933 William Walden Rubey introduced the concept of hydraulic equivalent. He suggested that the velocity the grains settle is a function of the grain size and density of the grains. Small heavy mineral grains can settle with the same velocity as large quartz grains (Morton and Hallsworth, 1999). This is a useful concept, but is not always correct. At Skarvemellen heavy minerals are found occurring in seams or lamina, this settling is probably not explained in terms of the settling velocity "hydraulic equivalent" (Morton and Hallsworth, 1999), but rather by reworking of the minerals after deposition.

The most important factors controlling heavy mineral assemblage is hydraulics and diagenesis (Morton and Hallsworth, 1994). However, diagenesis is the most profound , which may cause partial or complete loss of heavy minerals (Morton and Hallsworth, 1994). During increasing burial, unstable minerals are lost through dissolution (Morton and Hallsworth, 1994). Zircon

is one of the most stable heavy minerals, in addition to rutile. Because of the stability of zircon, it is one of the last heavy minerals to dissolve during diagenesis. The sandstones at Skarvemellen contain large amounts of zircon, and small amounts of other heavy minerals (Table 4.3). Zircon, rutile and tourmaline are known to be stable under high pore fluid temperature conditions (Morton and Hallsworth, 1994). Three of the Skarvemellen samples contain considerable amounts of apatite found by heavy mineral analyses (Table 4.3, Appendix E) and as overgrowth in SEM analysis (Figure 4.22a). According to Morton and Hallsworth (1999) such overgrowths often appear at more than 4 km depth.

The heavy mineral diversity in the Skarvemellen samples is mainly related to tectonism and diagenesis, since transport/abrasion did not cause diversity in the heavy mineral assemblage. Since apatite overgrowth is common when the burial depth reaches 4 km, it is likely that the sediments at Skarvemellen have been exposed to pressure and temperatures similar such a depth. This increase in pressure and temperature was probably caused by the Jotun thrust sheet. The silty- to fine-grained samples from Skarvemellen contain more heavy minerals than the rest of the samples, according to Morton (1985) the composition of heavy minerals in channels may differ from the deposition on floodplains of the same river. Further discussion on the maturity of the provenance area is found in the following chapter 5.3.3.

5.3.2 Rift controlled basin

The Valdres Group sedimentary rocks were probably deposited during an active tectonic phase before the Varangian Glaciation and the sedimentary rock at Skarvemellen probably represent syn-rift sedimentation (pers. com. J. P. Nystuen, 2017). The succession was possibly tectonically reduced due to the Caledonian Orogeny (Loesche, 1967).

Several tectonic rift phases occurred after the formation of the Valdres Basin, resulting in basinal widening, which increased the accommodation. The sedimentary succession of Skarvemellen, indicate three largescale upwards fining sequences, as seen in Figure 5.11. The continental braided stream deposits of the Rendalen Formation in the eastern part of the Hedmark Basin, show similar trends. The upwards fining sequences of the Rendalen Formation (Figure 5.13) have been interpreted to be tectonically controlled, by variation in tectonic subsidence or rate of accommodation by movements along the marginal faults (Nystuen, 1987). In a rift controlled basin accommodation space is created due to rifting and

uplifted terrain is formed along the basin margins. This uplifted terrain is a possible sediment source for the basin. Reconstruction of the paleocurrent measurements from Skarvemellen indicates a transport direct from W towards E (Figure 4.1). The Skarvemellen sedimentary rocks are interpreted to represent deposits of a braided stream. Braided streams are formed in areas with high relief. It is therefore suggested that a highland area may have been the source for the Valdres Group sedimentary rocks. Based on the transport direction, the sediments originated from W which may reflect erosion of the southwestern basin margin of the Valdres basin (Figures 2.2 and 4.10). To obtain a constant sediment supply into the basin, erosion of the uplifted terrain was possibly maintained by block faulting (Nickelsen et al., 1985, Heim et al., 1977). The basin margins of the Valdres Basin are not present today because of erosion, this makes it hard or even impossible to reconstruct the geometry of the Valdres Basin (pers. com. J. P. Nystuen, 2017). Since the Hedmark Basin and Valdres Basin were located close to each other, it is reasonable to assume similarities between the tectonic developments of the basins. The upwards fining sequences at Skarvemellen may therefore be interpreted to be tectonically controlled and represent syn-rift sediments, similar to the Rendalen sedimentary rocks in the Hedmark Basin (Nystuen, 1987).

To get a reliable reconstruction of the transport direction several hundred measurements are required (Prothero and Schwab, 2004). It is therefore important to mention that this reconstruction is only based on 17 paleocurrent measurement. This needs to be taken into consideration when interpreting the transport direction of the sediments. But as seen in Figure 4.1 and Figure 5.9 the spread of the paleocurrent measurement at Skarvemellen is negligible and may therefor indicate a quite reliable reconstruction after all. As previously mentioned, it is important to notice that a horizontal fold axis have been assumed when reconstruction the paleocurrent measurements. If the fold axis were dipping the reconstruction of the measurements will deviate from those reconstructed in this thesis.

5.3.3 Provenance area

The composition of sedimentary rocks reflects the lithology of the source area, transport mechanisms and depositional processes (Morton and Hallsworth, 1999). The composition of the Valdres Group has been influenced by the processes occurring during the sedimentation cycle, from weathering of the source rock to deposition (transport, storage and climate etc.).

Secondary processes such as diagenesis, metamorphism during the Caledonian Orogeny, will also have an impact on the composition of the rocks found in the Valdres Group today.

The Sveconorwegian Orogen was formed during the formation of the supercontinent Rodinia during Mesoproterozoic times (Figure 1.3) (Lamminen et al., 2015). The Sveconorwegian Orogen probably functioned as the main sedimentary source for the Baltoscandian basins. The deposits in the Hedmark Group have been interpreted to have a Sveconorwegian source (Lamminen et al., 2015). This might also be the case for the Valdres Group deposits, since both basins were located close to each other on the western Baltoscandian margin.

The conglomerates at Skarvemellen consist of rhyolite-, granite- and quartzite clasts. These rock fragments may have originated from the Mesoproterozoic volcanic and sedimentary rocks of the so called Telemarkland ("Telemark Supracrustals"). The volcanic rocks of the Telemark area consist of rhyolite and basalt (Bingen et al., 2005b), while the Telemark sedimentary rocks consist of mature quartzites, sandstones, conglomerates and breccia (Bingen et al., 2005b). According to Loesche (1967) the volcanics (rhyolites) found at Mellane show great resemblance with volcanics from Telemark, Numedal and Hallingdal area. The frequent occurrence of quartz and quartzites at Skarvemellen also supports the theory of Telemark land as the provenance area for the Valdres Group sedimentary rocks (Loesche and Nickelsen, 1968). The heavy mineral content of the samples suggest a predominantly felsic igneous/metamorphic origin, with hardly any garnet, rutile, monazite or spinel (Table 4.3 and Appendix E). This also supports the theory of a Telemark origin of the sedimentary rocks at Skarvemellen. The quartzite grains found in the conglomerates and sandstones (Figure 4.10b), show internal polygonal simple boundaries and a large number of quartz crystals that are forming the grain. According to Walker and Pettijohn (1971) this is believed to indicate a metamorphic origin.

At Skarvemellen some perthites were found during SEM analyses, but they are not common (Figures 4.19 and 4.20b). Most of the perthites found occur as strings, films, veins or sponge formed perthites. Perhtites with similar characteristics as the Jotun perthites are found in very small amounts in some of the sandstone samples from Skarvemellen (Figure 5.7). The Jotun mesoperthites is quite special with tear, boat or spindle shape (Figure 5.7) (Englund, 1966, Dietrichson, 1953). Spindel-shaped mesoperthites are very typical for the Jotun igneous rocks (Dietrichson, 1953), and some mesoperthites are also found in the Valdres Group as clastic

grains (Loesche and Nickelsen, 1968). These mesoperthites have been used as evidence for a Jotun rock source area (Loesche and Nickelsen, 1968). The occurrence of Jotun mesoperthites makes it possible to believe that the Jotun rocks could have been the source material for the Skarvemellen and Valdres Group, since these perthites are so rare. Because of the low occurrence of Jotun mesoperthites found in the samples it is possible to believe that the Jotun rocks have not supplied the Valdres Group with much material (Loesche and Nickelsen, 1968, Loesche, 1967). The great resemblance between the rhyolite from the Valdres Group at Mellane and the Telemark, is thought to be from Telemark land and may therefore be interpreted as the provenance area for the Valdres Group sedimentary rocks (Loesche and Nickelsen, 1968). The assumption of mature Telemark land as a provenance area may explain the well-sorting and the maturity of the sedimentary rocks at Skarvemellen (Appedix A). To clarify the question of age and provenance for the Valdres Group at Skarvemellen the zircons needs to be examined further.
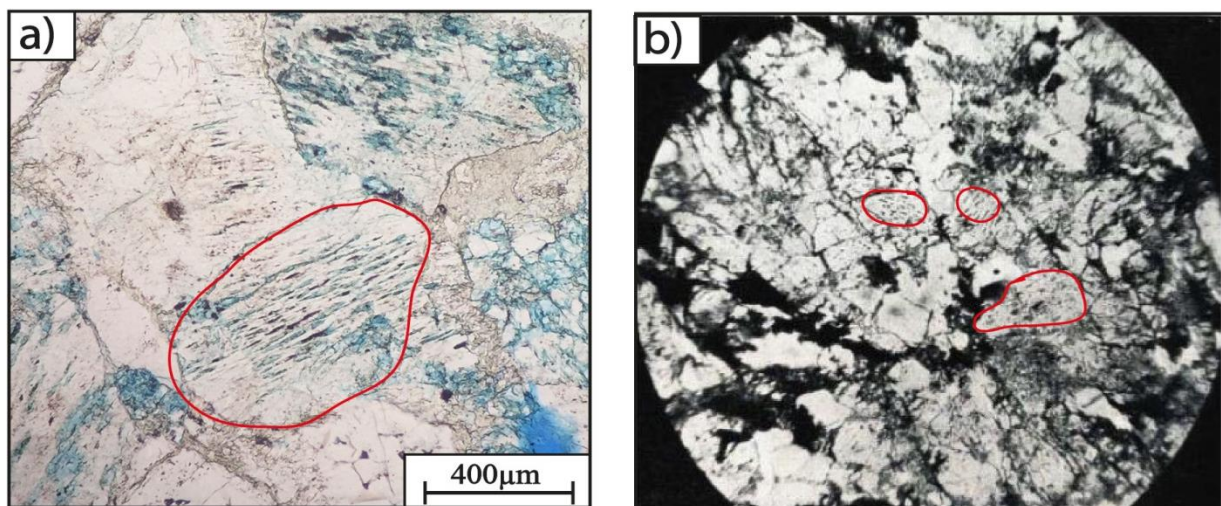
Figure 5.7: Examples of the Jotun perthite. **a)** Possible Jotun perthite (red circle) found in Ska 2-12-16 at Skarvemellen in ppl, b**)** Jotun micro-perhite (red circle) with tear shape, example from Dietrichson (1953), x50 in ppl.

Internal variations are seen when comparing petrographical composition of the Skarvemellen samples with the Rundemellen samples (Sørhus, 2017), they are quite similar but have some internal variatons, which is expected (Appedix A and B). Skarvemellen generally has more feldspar than Rundemellen. Rundemellen on the other hand contains more quartz (Appedix A and B). The paleocurrent measurements (Figure 5.9) imply that the transport direction was towards E, which implies a W source area for Skarvemellen, as described in the chapter above (5.3.2). The transport direction for Rundemellen indicates transport towards ESE with a source from WNW (Figure 5.9). According to Goldschmidt (1916) the provenance are for the

Valdres Group was about 7000 km^2, which is an important factor to consider when discussing the source area for the Valdres Group sedimentary rocks at Skarvemellen. Therefore, it is expected that the Valdres Group rocks have internal variation which is probably due to supply, sedimentary processes and petrographical composition of the source rocks (Loesche and Nickelsen, 1968).

5.4   Correlation with Rundemellen

Skarvemellen and Rundemellen are presently located approximately 2 km apart (Figure 1.1), both interpreted as braided stream deposits. The depositional environment at Rundemellen has been interpreted by Sørhus (2017). Skarvemellen and Rundemellen were probably deposited close to each other, but likely not in the same channel system since channels of braided streams are highly fluctuating. Even though the provenance area of Skarvemellen and Rundemellen (Sørhus, 2017) are thought to be the same, some minor variations in mineralogy are seen (Figure 5.8). This is expected since the mineralogy and transport direction in braided river systems can show large variations. The transport direction can vary as much as 180˚ (pers.com J.P. Nystuen, 2017).
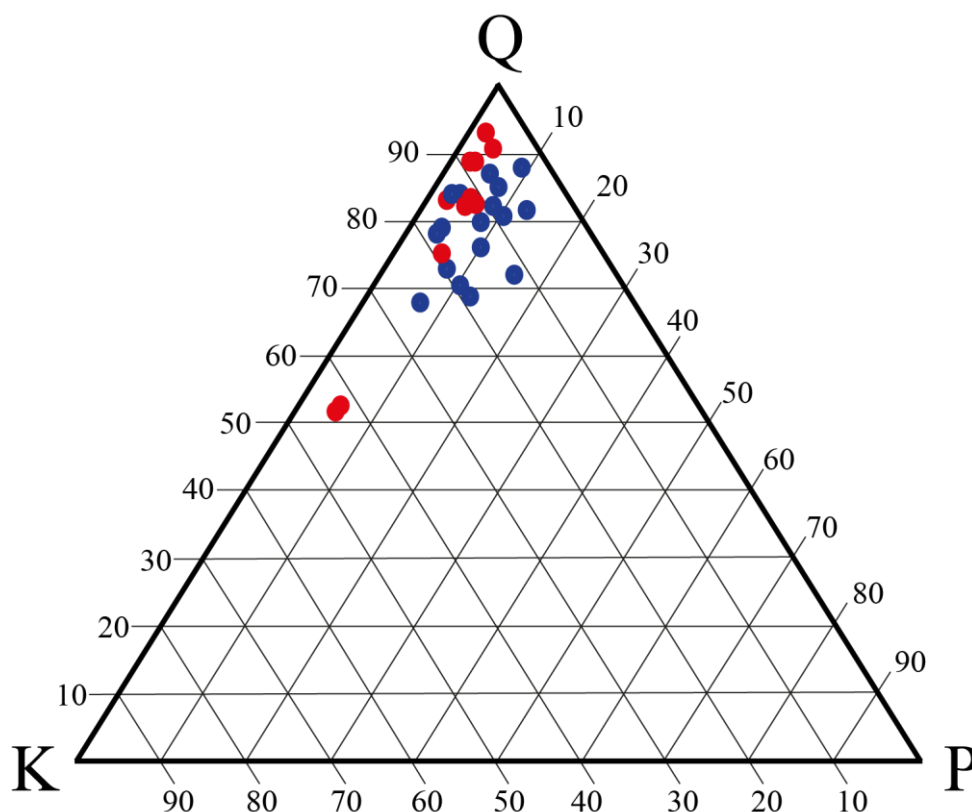
Figure 5.8: QAPF-diagram comparing the point counting results from Skarvemellen (blue) and Rundemellen (red). The percentages of the quartz (Q), K-feldspar (K) and plagioclase (P) is calculated from the respective point counting results (Appendix B).

The samples from Skarvemellen contain in general more feldspar than those from Rundemellen samples which contain slightly more quartz and are concentrated the top of the diagram (Figure 5.8). Only minor variations in mineralogy are seen (Figure 5.8, Appendix B and C), in the field and thin section they look quite similar in mineral content (Appendix A). In Figure 5.8, the two red dots that plot outside the cluster, is the breccia and one fine-grained sandstone from Rundemellen. The Skarvemellen samples show sandstones with sub-rounded to rounded grains, which indicate a moderate to long transport. The Rundemellen samples show sandstones with sub-angular to sub-rounded grains. The difference in roundness is too small to say anything certain about differences in length of transportation. The variation could be different interpretation of the roundness of the samples at Skarvemellen and Rundemellen. If only considering the mineralogy, the Rundemellen samples have slightly higher quartz content than Skarvemellen (Figure 5.8), which could be interpreted to representing slightly more mature sediments at Rundemellen. When looking at the big picture the sediments display a very similar maturity based on e.g. the quartz-feldspar content. Braided streams show large local variations, and therefore these minor discrepancies should not be taken into account in relation to length of transportation.
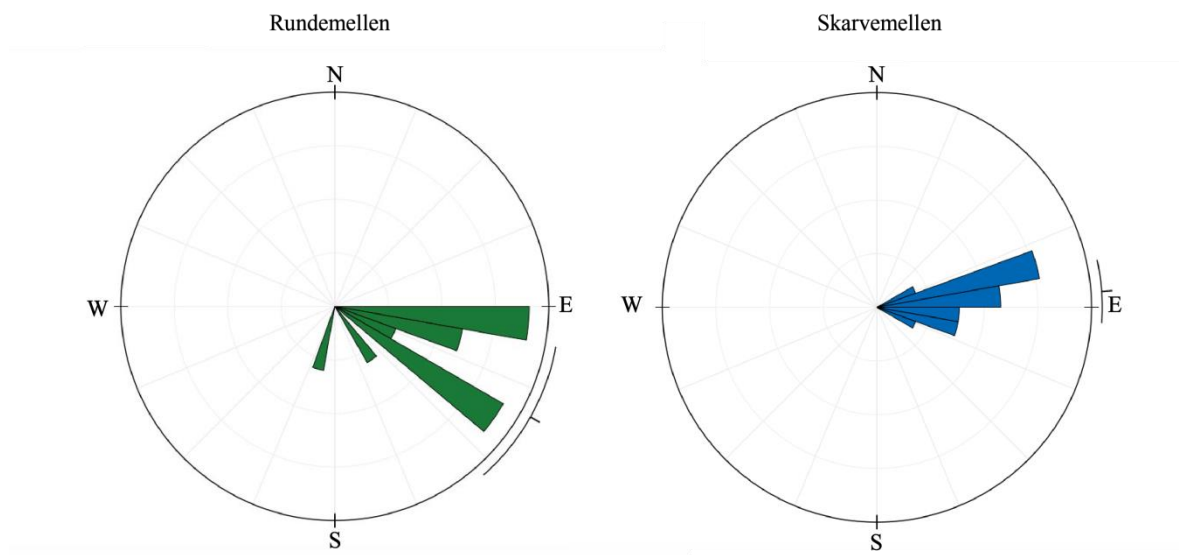
Figure 4.9: Reconstruction of the paleocurrent measurement of cross-bedding from Rundemellen (left) and Skarvemellen (right) presented in a Rose diagram, indicating a transport direction towards ESE for Rundemellen and E for Skarvemellen.

Skarvemellen indicating a transport towards E and Rundemellen a more ESE trend (Figure 5.9). The variation in transport directions are rather common when evaluating the highly fluctuating braided stream systems. Both sequences indicate a possible southwest provenance area. The variations in mineralogical composition of the two samples can be explained by minor differences in the drainage area or transport for Skarvemellen and Rundemellen. The provenance area of Telemark origin consisted of granites, gneisses, quartzites and volcanics such as rhyolite. The composition and occurrence of these rocks could be different for the drainage area for Skarvemellen and Rundemellen and could explain the minor differences in mineralogy, clast composition and clast size for the two areas (Figure 5.10) or in different channels with different flow velocity.
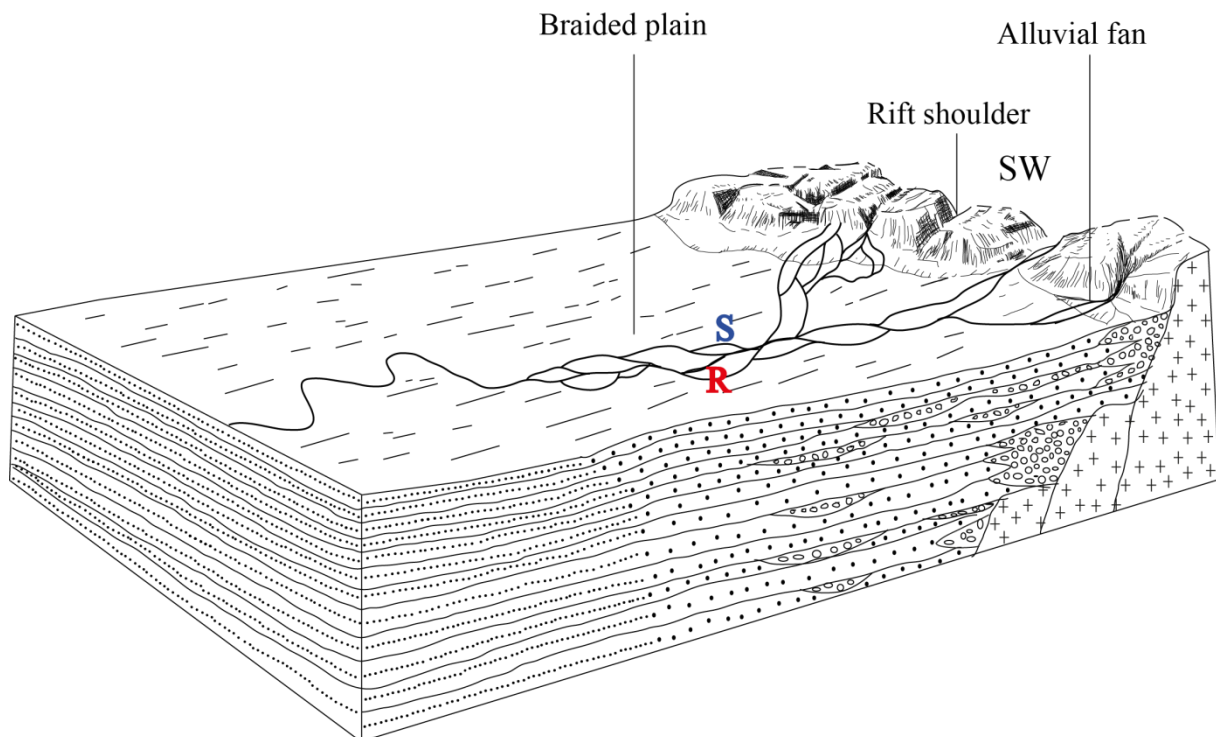
Figure 5.10: Sketch of the interpreted depositional setting of the Valdres Group succession in a continental rift basin, with the interpreted source area of the basin margin SW in the Valdres Basin and with the interpreted placement of Skarvemellen (S) and Rundemellen (R) succession in a braided stream environment in a rift setting. Modified from the continental part of the Hedmark Basin from Nystuen (1982).

Skarvemellen is located approximately 2 km from Rundemellen. The layers are overturned at both localities, which imply that they probably were situated on the same flank of the so called Skarvemellen recumbent anticline, dipping towards North (Nickelsen, 1967). If the localities are situated on the same flank of the fold, the distance between them today is close

to the same as before the Caledonian thrusting. If they were part of two different structural units or they were from two different limbs of parasitic folds, the distance between the localities during deposition may have been much larger that the distance of today. Another factor that supports the theory, that they are a part of the same overturned limb of the anticline is strike/dip measurements from field. Which show that the beds are dipping in the same direction towards north (Appendix F), at Rundemellen the layers show an average dip of 67° and at Skarvemellen a dip of 35° (Appendix F). The strike at Skarvemellen and Rundemellen is quite similar with an average of 254° and 259° respectively (Appendix F).

The Skarvemellen section (Figure 5.11) is comprised of more conglomerate units than the Rundemellen section (Figure 5.11). This may point to a different drainage area and possibly slightly different provenance than Rundemellen. Another explanation is different flow velocity in the channels, which leads to transport of different material downstream (Figure 5.10). Even though Skarvemellen seem to be slightly coarser grained than Rundemellen this might not be the case. It might be that Kathrine Sørhus and the author were more experienced when studying Skarvemellen, another explanation is that the two sections do not represent the exact same stratigraphic layer.

The breccia at Skarvemellen is found in outcrop, while at Rundemellen it is only found as several loose boulders, at a stratigraphically "correct" position. This unit is interpreted to be an equivalent to the Moelv Tillite (chapter 5.1.4). The tillite found at Skarvemellen and Rundemellen appear to be quite similar when studying them in the field, both are matrix supported, coarse grained, with angular clasts. Feldspar is the dominating clasts in both tillites, ranging in size from 0.3 - 4 cm. Based on this the tillites are thought to represent the same formation. The tillite layer is an important correlation bed in regards to correlation with other localities, as Rundemellen (Figure 5.11) and Hedmark Basin (chapter 5.5). This is based on the interpretation that the tillite is the same at both localities, deposited at the same time and at the same stratigraphic layer in the Valdres Basin, during the Varangian Glaciation.

The field observations and petrographic analyses of the tillite at Skarvemellen and Rundemellen show that both tillites consist of poorly sorted angular feldspar clasts floating in a greenish gray matrix (Appendix A).

S   N

Skarvemellen
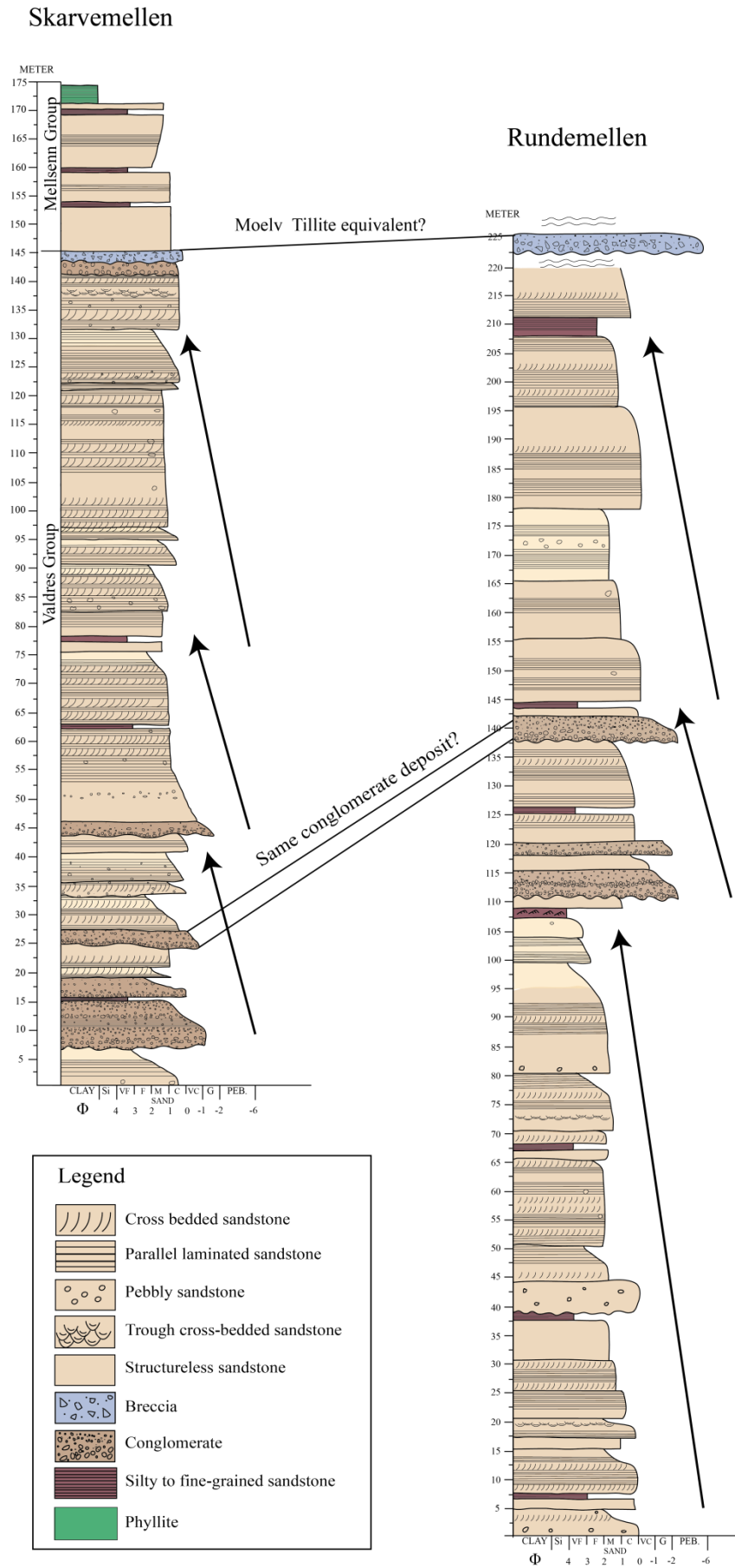
Rundemellen

Figure 5.11: Correlation of the Skarvemellen log (left) with the Rundemellen log (right), based on field observations and petrographic analyses. Arrows indicate large scale upwards fining units.

The point counting results show similar quartz content of the tillites, Skarvemellen with 32 % quartz and Rundemellen with 33.5 % (Appendix B). The XRD results indicate that Skarvemellen has 54 % quartz and Rundemellen only 25 % (Appendix C).This difference in XRD may be due to the high quartz content in the matrix at Skarvemellen, during point counting the quartz in the matrix was counted as matrix and not quartz grains. The total feldspar content on the other hand is quite different with 14 % in the Skarvemellen sample and 29 % at Rundemellen (Appendix B). The tillite samples analyzed from Skarvemellen is mainly from the matrix, and was found to consist of smaller grains than the Rundemellen tillite sample. The tillite sample from Rundemellen contained large K-feldspar clasts, which may explain the high feldspar content found during point counting. The difference between the tillite samples form Skarvemellen and Rundemellen are generally minor. Tillites are very heterogeneous and variation in composition is to be expected.
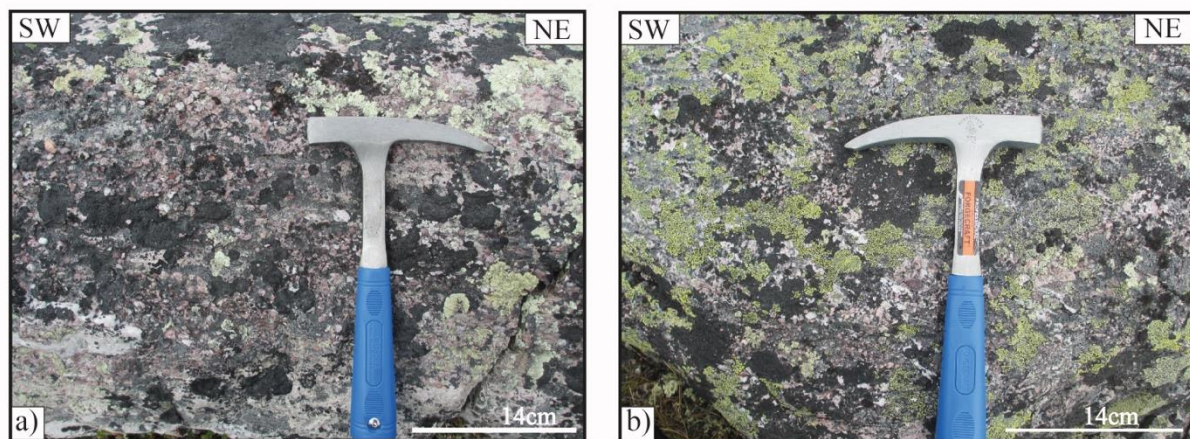
Figure 5.12: Pictures of the correlated conglomerates from Skarvemellen **(a)** and Rundemellen **(b).** The Skarvemellen conglomerate **(a)** found at level 25 meter in the sedimentary section from Skarvemellen (Figure 5.11) and Rundemellen **(b)** found at approximately level 140 meter in the Rundemellen section (Figure 5.11), the picture is not a good, but if looking closely towards left of the blue part of the hammer it may be possible to see some similarities between the two conglomerates. Both conglomerates have small clasts and appear similar in both mineralogy and appearance.

The correlation of the conglomerates in Figure 5.11, are mainly based on field observations. The grain supported conglomerates (Figure 5.12) from Skarvemellen and Rundemellen both contain small clasts. The matrix of the conglomerates and clasts seems to have the same mineralogy at both localities. Samples Ska 2-8-16 and Ska 2-13-16 represents the conglomerates of Skarvemellen and Rundemellen respectively. The Skarvemellen sample contain 57 % quartz based on XRD (Appendix C) and Rundemellen sample contain 71 % (Appendix C). In general, all the Rundemellen samples contain more quartz than Skarvemellen. The mineralogy of all the samples, as seen in Figure 5.8, is very similar and

further comparison of the petrographical analyses of the two samples does not give any additional correlation information.

The Valdres Group sedimentary rocks at both Skarvemellen and Rundemellen have been interpreted to represent braided stream deposits. Because of the close distance between the two localities, it is difficult to evaluate anything about the proximal- distal setting of the two sections in a braided stream environment. The sedimentary section at Skarvemellen contains more sedimentary structures than Rundemellen (Figure 5.11). This might be caused by more frequent changes in flow velocity/discharge at Skarvemellen than Rundemellen or more experience when Skarvemellen was studied.

5.5   Correlation with the Hedmark Basin

5.5.1 Mineralogical comparison with the Ring Formation

Chlorite and sericite was found to be the main pore-filling mineral in the Ring Formation during SEM (Figure 4.24) and thin section analyses; this is not the case in the Skarvemellen samples. In Skarvemellen muscovite is the dominating pore-filling mica mineral. The difference in mineralogical content of the Ring Formation and Skarvemellen might indicate that the samples have endured different degrees of metamorphism or had different provenance areas. Consequentially the mineral composition of the Ring Formation is quite similar to Skarvemellen, with quartz and feldspar as the dominating framework grains. When chlorite is precipitated, as described by Bjølykke (1998) a Fe and Mg source is required. Fe and Mg are typically found in clastic biotite, rock fragments and volcanic rocks (Bjølykke, 1998). Volcanic rocks are common in the Telemark land which is thought to be the provenance area for the Hedmark and Valdres basins. Chlorite is stable in sediments and metamorphic rocks, and to determine if the chlorite is formed diagenetic or metamorphic, coexisting minerals have to be identified (Winkler, 1979). When Fe-rich chlorite is found in contact with muscovite it is often an indicator of low grade metamorphism (Winkler, 1979). According to Bjørlykke (2015b) in high temperature metamorphic rocks Mg-rich chlorites are typical, Fe-rich chlorites are more common in diagenetic and low grade metamorphic rocks (Bjørlykke, 2015a, Winkler, 1979). During estimation of the mineral content in SEM the chlorites in the Ring Formation sample (KIN 3-15), were found to be iron-rich (Table 4.2). This may indicate that the chlorite in the Ring formation is formed diagenetically as a secondary mineral or

during low grade metamorphism. With increasing temperature and pressure, the chlorite becomes more Mg-rich and eventually disappears when transitioning into the Epidote-Amphibolite facies (Spear, 1993). In the Valdres Group sedimentary rocks at Skarvemellen there is no evidence of chlorite, only muscovite act as the pore filling mineral.

The heavy minerals in the Hedmark Group are generally the same heavy minerals as in the Skarvemellen samples, but in different quantities. Both basins contain the heavy minerals apatite, tourmaline and zircon (Table 4.3). The Skarvemellen samples contain more zircon than the Hedmark samples, but the Hedmark samples are more apatite rich than the Skarvemellen samples. Three of the Skarvemellen samples (Ska 2-4-16, Ska 8-16 and Ska 10-9-16) (Table 4.3) have a quite similar heavy mineral content to the Hedmark samples (Ring 0 and Rin 2-15) (Table 4.3). One reason for the apatite variations in Hedmark and Valdres samples is variability in the source area (Morton, 1986). This explanation is not very likely since apatite is a common mineral in the sedimentary rocks in the possible source area (Telemark land) for both basins. A more likely reason is loss of apatite through post-depositional dissolution in low-pH groundwater (Morton, 1986) in early diagenesis. This may indicate that apatite at Skarvemellen has been more dissolved that the apatite in Hedmark. To say this with more certainty, the apatite at Skarvemellen and Hedmark must studied to see if any etch features are visible on the apatite grains (Morton, 1986). Apatite overgrowth has been detected in SEM of the Skarvemellen samples, as described in chapter 5.3.1, interpreted to be caused by high pressure and temperature caused by the pressure of the overlying thrust sheet.

The provenance area for the Hedmark Group is interpreted to be Sveconorwegian, based on zircon dating performed by Lamminen et al. (2015). The provenance area for the Valdres Group is Sveconorwegian and most likely Telemark land (described in chapter 5.3.3) (Loesche and Nickelsen, 1968).

The Moelv Tillite in the Hedmark Basin has a wide regional extent with an erosional contact to the underlying sedimentary successions (Nystuen, 1982). The Moelv Tillite is interpreted to have been deposited by a regional glacial ice sheet, during the Varangian Glaciation (Nystuen, 1982). This Late Neoproterozoic glacial event has been recorded on most continents as glacial tillite/diamictite deposits (Bingen et al., 2005a). Which may imply a global glacial event the so called "Snowball Earth" (Bingen et al., 2005a). In Neoproterozoic successions around the

world the Neoproterozoic glaciations, Sturtian (750 – 700 Ma) and Varangrian (600-560 Ma), are well documented (Bingen et al., 2005a). The wide regional extent of this glacial deposit is the reason for its importance as a correlation bed. The glacier probably covered most of the Hedmark Basin (Nystuen, 1982). Because of the wide regional extent of the glaciation it is reasonable to believe that the Valdres Basin was covered with ice as well as the Hedmark Basin. It is therefore reasonable to believe that an equivalent to the Moelv Tillite is possible to find in the Valdres Basin. The breccia found at Skarvemellen has similar lithology and stratigraphic characteristics as the Moelv Tillite. This supports the interpretation that the breccia found in the Valdres Basin is an equivalent to the Moelv Tillite. At Mellane (including Skarvemellen and Rundemellen) the glacial deposit is thought to be deposited in a central position of the rift basin (Nystuen and Lamminen, 2011).

5.5.2 Correlation with the Rendalen Formation

The development of the eastern continental part of the Hedmark Basin is quite similar to the development of the continental succession of the Valdres Basin. The eastern part of the Hedmark Basin consists of fluvial deposits (Rendalen Formation). The depositional setting of the Valdres Basin is interpreted to represent similar depositional setting as the Rendalen Formation.

The Rendalen Formation, as seen in Figure 5.13, is composed of several coarse grained upwards fining units, interpreted to represent a braided stream environment on an alluvial plain (Nystuen, 1982). The abundance of coarse sand-gravel bars and the low spread in paleocurrent data in the Rendalen Formation favors a broad braided plain deposits, where the fining upwards units possibly originated from sheet floods or waning flood events (Nystuen, 1982).

In order to transport the coarse gravels found in the conglomerate units into the basin, the stream velocity must have been very high in the Rendalen Formation (Nystuen, 1982). This is probably also the case for the Valdres Group conglomerates at Skarvemellen and Rundemellen. According to Smith (1974) gravel bars studied in the Platt River, Nebraska, occur in abundance 250 km away from source area. The fining upwards units of Rendalen and Valdres are similar and both are possibly controlled by tectonic processes.

The Rendalen Formation and the Valdres Group have both been interpreted to be of Neoproterozoic age, but the Rendalen Formation is probably older than the Valdres Group sedimentary rocks at Skarvemellen. Further investigation of the Valdres Group and Rendalen Formation would probably make it possible to correlate the two sequences not only with respect to the depositional environment but also stratigraphically. Dating of the Valdres Group sandstones, conglomerates and tillite would be an interesting topic for further work in the area. Maybe correlation with the zircon ages of the Rendalen formation provided by Bingen et al. (2005a) or correlation with the Ring Formation.

Figure 5.13: Stratigraphy and sedimentology of the Rendalen Formation in three sections from Rendalsølen, Brennhammarean and Salsfjellet, modified from Nystuen (1982).

6 Conclusion

The Eocambrian Valdres Group at Skarvemellen is a medium to coarse grained siliciclastic succession deposited in the continental Valdres rift basin on the western margin of the continent Baltica. The Valdres Basin was tectonically displaced to its percent position in central southern Norway during the Caledonian Orogeny. The deformation from the Caledonian Orogeny is today represented in the elongated conglomerate clasts, partially deformed due to the pressure from the Jotun thrust sheet. The sediments display low metamorphic grade, possibly lower green schist facies.

The sedimentary succession at Skarvemellen is interpreted to represent longitudinal bar-, transverse bar- and channel fill deposits of a braided stream environment. The succession consists of conglomerates, medium to coarse grained sandstones and silty- to fine-grained sandstones, with an upwards fining trend characteristic for fluvial and braided stream deposits. The sedimentary input is probably tectonically controlled, representing syn-rift sediments. The breccia is interpreted to represent an equivalent to the Moelv Tillite probably deposited during the Varangian Glaciation.

The sediments have a characteristic red color, which is typical for braided sediments. Fe-oxides are found as hematite (Fe_2O_3) in the Skarvemellen samples, which is confirmed by SEM analyses. Hematite is most prominent in the silty-to fine-grained sandstones, found as enrichment in seams with heavy mineral or as clusters. The red coloring of the sediments is due to precipitation of iron-oxides where hematite is most abundant.

The sediments are sub-rounded to rounded with a high quartz and K-feldspar content indicating a mature nature of the sediments. The enrichment of stable minerals as quartz, K-feldspar and muscovite, in terms of weathering and transport suggests a moderate to long transport. The heavy mineral content, with an abundance of zircon, also indicate mature sediments. The apatite overgrowth indicates temperature and pressure equal to 4 km burial depth, probably caused by the pressure from the Jotun thrust sheet.

The conglomerates consist of rhyolite and gneisses, based on this and the predominant igneous/ metamorphic origin of the heavy mineral content. The provenance area is interpreted to be of Sveconorwegian origin, more precise Telemark land. The paleocurrent measurements indicate transport direction towards E, implying a sediment transport from W. This indicates an erosion and sediment transport from the southwestern basin margin of the Valdres Basin.

The Valdres Group is interpreted to represent braided stream deposits in a continental rift basin setting. This is based on the similarities between the sedimentary succession at Skarvemellen and the Rendalen Formation (continental part of the Hedmark Basin).

The Ring Formation (Hedmark Basin) and Valdres Group (Valdres Basin) at Skarvemellen are quite similar in mineral composition, with a high content of quartz. The only difference is that chlorite is found to be the pore filling mineral in the Ring Formation sample, at Skarvemellen muscovite is found to be pore filling. This might indicate a difference in diagenetic/metamorphic character of the two basinal deposits or slightly different provenance area. The provenance area for the Hedmark group is also interpreted to be of Sveconorwegian origin. The Moelv Tillite is deposited by the Varangian Glaciation, because of the wide regional extent of the glaciation the breccia at Skarvemellen is interpreted to be an equicalent to the Moelv Tillite.

Skarvemellen and Rundemellen are today located approximately 2 km apart, both interpreted to be braided stream deposits. They were probably deposited close to each other, but not in the same channel of the braided river system. The mineralogy of Skarvemellen and Rundemellen is quite similar, indicating fairly mature sediments. The Rundemellen samples also contain clasts of rhyolite and gneisses, and have a transport direction towards ESE indicating a possible source area of Telemark land origin and transport of material from the southwest basin margin. The close distance between the localities makes it difficult to say anything about the proximal- distal setting of the successions in a braided stream system. The breccia found at Skarvemellen and Rundemellen is both poorly sorted, matrix supported with angular clasts and is interpreted to be representing the same layer, deposited as till during the Varangian Glaciation.

References

Basu, A. 1985. Reading Provenance from detrital quartz. *In:* ZUFFA, G. G. (ed.) *Porvenance of Arenites* Reidel Publishing Company, 231-247

Bingen, B., Griffin, W., Torsvik, T. & Saeed, A. 2005a. Timing of Late Neoproterozoic glaciation on Baltica constrained by detrital zircon geochronology in the Hedmark Group, south-east Norway. *Terra Nova,* 17**,** 250-258.

Bingen, B., Skår, Ø., Marker, M., Sigmond, E. M. O., Nordgulen, Ø., Rangnhildstveit, J., Mansfeld, J., Tucker, R. D. & Liégeois, J.-P. 2005b. Timing of contiental building in the Sveconorwegian orogen, SW Scandinavia. *Norwegian Journal of Geology,* 85**,** 87-116.

Bjølykke, K. 1998. Clay mineral diagenesis in sedimentary basins - a key to the prediction of rock properties. Examples from the North Sea Basin. *Clay Minerals,* 33**,** 15-34.

Bjørlykke, K. 2015a. Compaction of sedimentary rocks: Shales, Sandstones and Carbonates *In:* BJØRLYKKE, K. (ed.) *Petroleum Geoscience* Springer.

Bjørlykke, K. 2015b. Sedimentary Geochemistry *In:* BJØRLYKKE, K. (ed.) *Petroleum Geoscience* Springer

Bjørlykke, K., Elvsborg, A. & Hoy, T. 1976. Late Precambrian sedimentation in the central sparagmite basin of south Norway. *Norsk Geologisk Tidsskrift,* 66**,** 1196-1230.

Bjørlykke, K. O. 1901. Overskyvninger i den norske fjerdkjæde. *Naturen, Kristiania (Oslo),* 5**,** 1-18.

Bockelie, J. F. & Nystuen, J. P. 1985. The southern part of Scandinavian Caledonides. *In:* GEE, D. G. & STURT, B. A. (eds.) *The Caledonian Orogen-Scandinavia and Related Areas.* J. Wiley & sons Ltd, 69-88.

Boggs, S. J. 2014. *Principles of Sedimentology and Stratigraphy*, Pearson Education, Inc. 564 p.

Bruker 2011. Diffrac.Suite. User Manual. Original Instructions. *Bruker AXS GMBH. 154 p.*

Collinson, J. D., Mountney, N. P. & Thompson, D. B. 2006. *Sedimentary Structures, third edition*, Harpended, Hertfordshire, England: Terra Publishing. 292 p.

Compton, R. R. 1962. Manual of Field Geology. *In Soil Science. .* New York: Wiley. 265 p.

Davis, R. A., Jr. 1983. *Depositional System; A Geinetic Approach to Sedimentary Geology*, Prentic-Hall Inc. 669 p.

Dietrichson, B. 1953. Pseudotachylit fra de kaledonske skyvesoner i Jotunheimens forgårder, Gudbrandsdalen, og deres dannelsesbetingelser. *Norges Geologiske Underskelser, Nr. 184*.

Dunoyer De Segonzac, G. 1970. The Transformation of clay minerals during diagenesis and low-grade metamorphism: A review. *Sedimentology,* 15**,** 281-346.

Englund, J.-O. 1966. Sparagmittgruppens bergarter ved Favang, Gudbrandsdalen: en sedimentologisk og tektonisk undersøkelse. *Studies on the latest Precambrian and Eocambrian rocks in Norway.* Universitetsforlaget.

Esmark, J. 1829. Reise fra Christiania til Tronhjem. *Cristiania (Oslo)***,** 81 p.

Eyles, C. H. & Eyles, N. 2010. Glacial Deposits. *In:* JAMES, N. P. & DALRYMPLE, R. W. (eds.) *Facies Models 4.* Geological Association of Canada, 73-105 p.

Fossum, K. 2012. *Sedimentology, petrology and geochemistry of the Kilimatinde Cement, central Tanzania.* Master Thesis, University of Oslo.

Galloway, W. E. & Hobday, D. K. 1996. Fluvial systems. *Terrigenous Clastic Depositional Systems* Springer Berlin Heidelberg

Gee, D. G., Fossen, H., Henriksen, N. & Higgins, A. 2008. From the Early Paleozoic Platforms of Baltica and Laurentia to the Caledonian Orogen of Scandinavia an Greenland. *Episodes* 31(1)**,** 44-51.

Gee, D. G., Kumpulainen, R. & Thelander, T. 1978. The Tåsjön Dècollement, central Swedish Caledonides *Sver. geol. Unders.,* C742**,** 1-35.

Goldich, S. S. 1938. A Study in Rock-Weathering *The Journal of Geology,* Vol. 46, No. 1**,** 17-58. DOI: 10.2307/30079586.

Goldschmidt, V. 1916. Konglomeraterne inden Høifjeldskvartsten. *Norges Geologiske Underskelser,* 77.

Goldstein, J., Newbury, D. E., Joy, D. C., Lyman, C. E., Echlin, P., Lifshin, E., Sawyer, L. & Michael, J. R. 2003. *Scanning electon microscopy and X-ray microanalysis*.

Google Maps. 2017. *Kartdata* [Online]. Available: https://www.google.no/maps/place/Norge/@60.3844329,8.581205,7z/data=!4m5!3m4!1s0x461268458f4de5bf:0xa1b03b9db864d02b!8m2!3d60.472024!4d8.468946 [Accessed 11.05 2017].

Harvey, B. & Christie, J. M. 1963. Undulatory extinction in quartz of igneous and metamorphic rocks and its significance in provenance studies of sedimentary rocks. *Sedimentary Petrology,* 33**,** 559-579.

Heim, M., Schärer, U. & Milnes, A. G. 1977. The nappe complex in the Tyin-Bygdin-Vang region, Central southern Norway. *Norsk Geologisk Tidsskrift* 57**,** 171-178.

Hillier, S. 2000. Accurate quantitative analysis of clay and other minerals in sandstones by XRD: comparison of a Rietveld and a reference intensitiy ratio (RIP) method and the importance of sample preperation. *Clay Minerals* 35**,** 291-302.

Holtedahl, O. 1959. Noen iakttagelser fra Grønsennknipa i Vestre Slidre, Valdres. *Norges Geol. Unders***,** 90-106.

Hossack, J. R. 1978. The correction of stratigraphic section for tectonic finite strain in the Bygdin area, Norway. *Geological Society, London,* 135**,** 229-241.

Hossack, J. R. & Cooper, M. A. 1986. Collision tectonics in the Scandinavian Caledonides. *In:* COWARD, M. P. & RIES, A. C. (eds.) *Collision Tectonics.* Geological society Special Publication, 19, 287-304.

Hossack, J. R., Garton, M. R. & Nickelsen, R. P. 1985. The geological section from the foreland up to the Jotun thrust sheet in the Valdres area, south Norway. *In:* GEE, D. G. & STURT, B. A. (eds.) *The Caledonide Orogen-Scandinavia and Related Areas.* John Wiley & Sons Ltd, 443-456.

Kartverket. 2017. *Norgeskart* [Online]. Available: http://www.norgeskart.no/?_ga=2.53548520.1151073586.1494512540-1546162589.1494512540#!?project=seeiendom&layers=1002,1014&zoom=13&lat=6786166.18&lon=190038.46&sok=skarvemellen [Accessed 11.05 2017].

Kjerulf, T. 1873. Sparagmittfjeldet. Universitetsprogram for andet Halvaar 1872. Christianai (Oslo), 85 pp. .

Kjerulf, T. 1879. Udsiget over det sydlige Norges geologi. *Christiania (Oslo), W. C. Faberitius, 262 pp*.

Kjerulf, T. & Dahll, T. 1866. Geologiske kart over det søndenfjeldske Norge, optaget 1858-1865. Christiania (Oslo).

Kulling, O. 1955. Den kaledonske fjällkedjans berggrund inom Väterbotters Iän. . *In:* GRAVELIN, S. & KULLING, O. (eds.) *Beskrivning till berglundskarta över Väterbottens län.* sver. geol. Unders., Ser. Ca. 37, 101-295.

Kulling, O. 1961a. On the age and tectonic position of the Valdres sparagmite. *Geol. Fören. Stockholm. Förh.,* 102, 531-550.

Kulling, O. 1961b. On the age and tectonic position of the Valdres Sparagmite *Geol. Fören. Stoch. Förh., 83, 210-214.*

Kumpulainen, R. 1980. Upper Proterozoic stratigraphy and depositional environments of the Tossåsfjället Group, Särv Nappe, southern Swedish Caledonides. *GFF,* 102**,** 531-550.

Kumpulainen, R. 1982a. Studies of late Proterozoic sedimentation and Caledonian tectonics in the central and southern parts of the Swedish Caledonides. *Abstracts of Uppsala Diss. Faculty Sci., 649,169-209.*

Kumpulainen, R. 1982b. The Upper Proterozoic Risbäck Group, Northern Jämtland and Southwestern Västerbotten, Central Swedish Caledonides. *Uppsala University, Institute of Geology, Department of Mineralogy and Petrology, Res. Report, 25, 60p.*

Kumpulainen, R. & Nystuen, J. P. 1985. Late Proterozoic basin evolution and sedimentation in the westernmost part of Baltoscandia. *In:* GEE, D. G. & STURT, B. A. (eds.) *The Caledonide Orogen-Scandinavia and Related Areas.* John Wiley & Sons Ltd, 213-231.

Lamminen, J., Andersen, T. & Nystuen, J. P. 2011. Zircon U-Pb ages and Lu-Hf isotopes from basement rocks associated with Neoproterozoic sedimentary successions in the Sparagmite Region and adjacent areas, South Norway: the crustal architecture of western Baltica. *Norsk Geologisk Tidsskrift,* 91**,** 35-55.

Lamminen, J., Andersen, T. & Nystuen, J. P. 2015. Provenance and rift basin architecture of the Neoproterozoic Hedmark Basin, South Norway inferred from U-Pb ages and Lu-Hf isotopen of conglomerate clasts and detrital zircons. *Geol. Mag. ,* 152**,** pp. 80 -105.

Leopold, L. B. & Wolman, M. G. 1957. River channel patterns: braided, meandering, and straight. *U.S. Geol. Survey. Prof. Paper 282-B. p. 39-85.*

Loesche, J. 1967. Zür Stratigraphie und Petrographie des Valdres-Sparagmites und der Mellsenn-Gruppe bei Mellane/Valdres (Süd-Norwegen). *Norges Geologiske Undersøkelser,* 243 A**,** 1-66.

Loesche, J. & Nickelsen, R. P. 1968. On the age and tectonic position of the Valdres Sparagmite in Slindre (Southern Norway). *Geological Paläont. Abh.,* 131**,** 337-367.

Mckee, E. D., Crosby, E. J. & Berryhill, H. L. 1967. Flood deposits, Bijou Creek, Colorado. *Jour. Sed. Petrology,* 37**,** 829-851.

Miall, A. D. 1977. A Review of the Braided-River Depositional Environment. *Earth-Science Reviews,* 13**,** 1-62.

Moore, D. M. & Reynolds, R. C. 1997. X-ray Diffraction and the Identification and Analysis of Clay Minerals. *Oxford: Oxford University Press***,** 378 p.

Morton, A. C. 1985. Heavy minerals in provenance studies *In:* ZUFFA, G. G. (ed.) *Provenance of Arenites.* NATO Scientific Affairs Division D. Reidel Publishing company

Morton, A. C. 1986. Dissolution of apatite in North Sea Jurassic Sandstones: Implications for the generation of secondary porosity. *Clay Minerals,* Vol. 21**,** p. 771-733.

Morton, A. C. & Hallsworth, C. R. 1994. Identifying provenance-specific features of detrital heavy mineral assemblages in sandstones *Sedimentary Geology,* 90**,** 241-256.

Morton, A. C. & Hallsworth, C. R. 1999. Processes controlling the composition of heavy mineral assemblages in sandstones *Sedimentary Geology,* 124**,** 3-29.

Nemec, W. & Steel, R. J. 1984. Alluvial and Costal Conglomerates: their significan features and some comments on gravelly mass-flow deposits *In:* KOSTER, E. H. & STEEL, R. J. (eds.) *Sedimentology of Gravels and Conglomerates* Canadian Society of Petroleum Geologists. Memoir 10, 1-31 p.

Nickelsen, R. P. 1967. The structure of Mellene and Heggeberg, Valdres. *Norges Geologiske Underskelser,* 243C**,** 99-121.

Nickelsen, R. P., Hossack, J. R., Garton, M. R. & Repetsky, J. 1985. Late Precambrian to Ordovician stratigraphy and correlation in the Valdres and Synnfjell thrust sheets of the Valdres area, southern Norwegian Caledonides; with some comments on sedimentation. *In:* GEE, D. G. & STURT, B. A. (eds.) *The Caledonian Orogen-Scandinavia and Related Areas.* J. Wiley and Sons Ltd, 369-375.

Nystuen, J. P. 1976. Late Precambrian Moelv Tillite deposited on a discontinuity surface associated with a fossil ice wedge, Rendal, southern Norway. *Norges Geologisk Tidsskrift,* 56**,** 29-56.

Nystuen, J. P. 1980. Stratigraphy of the Upper Proterozoic Engerdalen Group, Kvitvola Nappe, southeastern Scandenavian Caledonides. *Geol. Fören. Stoch. Förh., 102, 551-560.*

Nystuen, J. P. 1982. Late Proterozoic Basin Evolution in the Baltoscandian Craton: the Hedmark Group, Southern Norway. *Norges Geologiske Underskelser, Bulletin 67,* Nr. 375.

Nystuen, J. P. 1987. Synthesis of the tectonic and sedimentological evolution of the late Proterozoic-early Cambrian Hedmark Basin, The Caledonian Thrust Belt, southern Norway. *Norsk Geologisk Tidsskrift,* 67**,** 395-418.

Nystuen, J. P. Late Proterozoic to Cambrian of the Hedmark Basin, Sparagmite Region, Southern Norway. IAS 19th Regional European Meeting of Sedimentology, Excursion guide, Excursion B4, 1999. 123-144.

Nystuen, J. P., Andresen, A., Kumpulainen, R. A. & Siedlecka, A. 2008. Neoproterozoic basin evolution in Fennoscandia, East Greenland and Svalbard. *Episodes,* 31**,** 35-43.

Nystuen, J. P. & Lamminen, J. 2011. Neoproterozoic glaciation of South Norway: from continental interior to rift and pericratonic basins in western Baltica. *In:* ARNAUD, E., HALVERSON, G. P. & SHIELDS-ZHOU, G. (eds.) *The Geological Record of Neoproterozoic Glaciations* Geological Society, London: Memoirs, 36, 613-622.

Oberhardt, N. 2013. *Granite weathering, saprolitization and the formation of secondary clay particles, SW Bornholm. .* Master Thesis, University of Oslo.

Powers, M. C. 1953. A New Roundness Scale for Sedimentary Particles. *Journal of Sedimentary Petrology,* 23(2)**,** 117-119.

Prothero, D. R. & Schwab, F. 2004. *Sedimentary Geology - An Introduction to Sedimentary Rocks and Stratigraphy*, W. H. Freeman and Company New York, 557p.

Que, M. & Allen, A. R. 1996. Sericitization of plagioclase in the Rosses Granite Complex, Co. Donegal, Ireland *Mineraloical Magazine* 60**,** 927-936.

Reading, H. G. & Levell, B. K. 2009. Controls on the sediemntary rock records *In:* SONS, J. W. (ed.) *Sedimentary environments: processes, facies and stratigraphy.* Third edition ed.: Blackwell Publishing Ltd, 5-37 p.

Reineck, H.-E. & Singh, I. B. 1975. *Depositional Sedimentary Environments*, Springer-Verlag Berlin, Heidelberg, New York. 439 p.

Richards, K. J. 1996. Fluvial systems. . *In:* EMERY, D. & MYERS, K. (eds.) *Sequence Stratigraphy.* Blackwell Science Ltd, 111-133.

Rietveld, H. M. 1969. A profile refinement method for nuclear and magnetic structures *Journal of applied crystallography,* 2**,** 65-71.

Rubey, W. W. 1933. The size distribtuon of heavy minerals within a water-lain sandstone *Geological Society of American Bulletin,* 3**,** 3-29.

Russell, R. D. 1937. Mineral composition of Mississippi River sands *Geological Society of American Bulletin,* 48**,** 1307-1348.

Rust, B. R. 1972. Structure and process in a braided river. *Sedimentology.* Elsevier Publishing Company, Vol. 18, p. 221-245.

Rust, B. R. 1977. Depositional models for braided alluvium. *Canadian Society of Petroleum Geologists, Memoir 5*, p. 605- 625.

Selley, R. C. 1985. *Ancient Sedimentary Environments and their sub-surface diagnosis, third edition*, Chapman and Hall Ltd, 317 p.

Shukri, N. M. 1949. The mineralogy of some Nile sediments *Quarterly Journal of the Geological Society of London,* 105, 511-529.

Sietronics Pty Ltd 2017. Siroquant, V.4.

Smith, J. V. 1974. Intergrowth of Feldspar with Other Minerals *In:* SMITH, J. V. & SMITH, B. F. (eds.) *Feldspar Minerals: 2 Chemical and Textural Properties.* Springer-Verlag Berlin Heidelberg, New York.

Smith, N. D. 1970. The Braided Stream Depositional Environmen: Comparison of the Platt River with Some Silurian Clastic Rock, North-Central Appalachians. *Geological Society of American Bulletine* 81, 2993-3014.

Smith, N. D. 1971. Transverse Bars and Braiding in the Lower Platte River, Nebraska. *Geological Society of American Bulletine,* 82, 3407-3420.

Southard, J. B. & Boguchwal, L. A. 1990. Bed configuration in steady unidirectional water flows. Part 2. Synthesis of flume data. *Journal of Sedimentary Petrology,* Vol. 60, No.5, p. 658-679.

Spear, F. S. 1993. *Metamorphic Phase Equlibria ans Pressure-Temperature-Time Paths*, Mineralogical Society of America, Washington, D.C., p. 799.

Strand, T. 1959. Valdres-sparagmittens stratigrafiske stilling. *Norges Geologiske Underskelser,* no. 205, 184-198.

Streckeisen, A. 1976. To each plutonic rock its proper name. *Earth-Science Reviews,* 12, 1-33 p.

Sundborg, A. 1956. The River Klarälven: a study of fluvial processes. *Stockholm: Esselte Akiebolag* 38, 127-316.

Sørhus, K. 2017. *The Eocambrian Valdres Group at Rundemellen, Mellane* Master Thesis, University of Oslo.

Torsvik, T. H. 2003. The Rodinia jigsaw puzzle. *Science,* 300, 1379-1381.

Turner, P. 1980. *Continental Red Beds*, Elsevier Scientific Publishing Company, Amsterdam, Vol. 29, 562 p.

Törnebohm, A. E. 1882. Om Vemdalsqvartsiten och öfriga quartzitiska bildningar i Sveriges sydliga fjälltrakter. *Geol. Fören. Stoch. Förh., 6, 274-294.*

Törnebohm, A. E. 1888. Om fjällproblemet. *Geol. Fören. Stoch. Förh., 10, 328-336.*

Törnebohm, A. E. 1896. Grunddragen of det centrala Skandinaviens bergbygnad. *Kongl. Svenska Vetenskapsakad. Handl., 28 , 210 pp.*

Törnebohm, A. E. 1973. Ueber die Geognosie der schwedischen Hochgebirge. *Kongl. Svenska Vetenskapsakad. Handl. bih. 1, (12), 59 pp.*

Van Andel, T. H. 1950. Provenance, Transport and Deposition of Rhine Sediments *Veenman, Wageningen*.

Walker, J. D., Geissman, J. W., Bowring, S. A. & Babcock, L. E. 2012. *GSA Geological Time Scale v. 4.0* [Online]. The Geological Society of America Available: https://www.geosociety.org/documents/gsa/timescale/timescl.pdf [Accessed 20.02 2017].

Walker, R. G. & Pettijohn, F. J. 1971. Archaean Sedimentation: Analysis of the Minnitaki Basin, Northwestern Ontario, Canada *Geological Society of American Bulletin,* Vol. 82, p. 2099-2130.

Wentworth, C. K. 1922. A scale of grade and class terms for clastic sediments. *Journal of Geology,* 27, 377-392.

Williams, P. F. & Rust, B. R. 1969. The sediemtology of a braided river. *Journal of Sedimentary Research,* Vol. 39, No. 2**,** p. 649-679.

Winkler, H. G. F. 1979. *Petrogenesis of Metamorphic Rocks* Springer-Verlag New York Inc., p. 348.

Appendix A – thin section analysis

Table A.1: Thin section description of the Skarvemellen samples, displayed according to facies. Facies 1= Congomerates, Facies 2=Sandstones, Facies 3= silty- to fine-grained sandstones, Facies 4= breccia (tillite). Qtz=quartz, K-fsp=K-feldspar, Plag=plagioclase, Seric= sericite, Hem= hematite, Opq=opaque grains, R.F.=Rock fragments.

Facies	Sample	Lithology	Dominating framework configuration	Average of the 10 largest grains	Average grain size (mm)	Most common grain shape	Sorting	Mineral content		Feldspar preservation		Remarks/Comments
								1.	2.	K-fsp.	Plag.	
1	Ska 11-16	Conglomerate	Grain supported	2.27 mm	Coarse 0.65 mm	Sub-rounded	Poor	Qtz. K-fsp. Plag. Mica Seric.	Hem. R.F Opaq.	III	II	Rock Fragments: Rhyolite, Granite and quartzite. Rock fragments are the largest grains in the sample. Mica is pore filling.
	Ska 10-16	Conglomerate	Grain supported	1.48 mm	Coarse 0.88 mm	Sub-rounded	Well	Qtz. K-fsp. Plag. Mica	Hem. R.F Opaq	III	III	Rock Fragments: Rhyolite, Granite and quartzite. Small amounts of pore filling mica. Fractured grains, filled with epoxy, mica or polycrystalline quartz.
	Ska 2-9-16	Conglomerate	Grain supported	1.22 mm	Coarse 0.55 mm	Sub-rounded to rounded	Well	Qtz. K-fsp. Plag. Mica	Hem. R.F Opaq	III	III	Rock Fragments: Rhyolite, Granite and quartzite. Mica is pore filling.
	Ska 2-8-16	Conglomerate	Grain supported	4.84 mm	Very coarse 1.94 mm	Sub-rounded to rounded	Poor	Qtz. K-fsp. Plag.	Opq. R.F			Rock Fragments: Rhyolite, Granite and quartzite. Largest rock fragments are the quartzites in this sample. Rhyolite and granite occur as small grains in the matix.
	Ska 2-7-16	Conglomerate	Grain supported	0.54 mm	Medium 0.46 mm	Sub-rounded	Well	Qtz. K-fsp. Plag. Mica	Hem Opaq.	III	III	Represents the conglomerate matrix.
	Ska 2-5-16	Conglomerate	Grain supported	4.47 mm	Very coarse 1.16 mm	Sub-rounded	Moderat	Qtz. K-fsp. Plag. Mica	R.F Hem Opaq	II/III	II	Rock fragments of rhyolite, granite and quartzite are the largest grains in the sample.

Facies	Sample	Lithology	Dominating framework configuration	Average of the 10 largest grains	Average grain size (mm)	Most common grain shape	Sorting	Mineral content		Feldspar preservation		Remarks/Comments
								1.	2.	K-fsp.	Plag.	
2	Ska 9-16	Arkose	Grain supported	2.31 mm	Coarse 0.58 mm	Sub-rounded	Moderat	Qtz. K-fsp. Plag. Mica	Hem. Opaq	II	II	Fracturing of the grains, especially the quartz grains.
	Ska 8-16	Arkose	Grain supported	0.61 mm	Medium 0.41 mm	Sub-angular to sub-rounded	Moderat	Qtz. K-fsp. Plag. Mica Seric.	Hem. R.F Opaq	III	III	Fracturing of the grains. Mica is pore filling.
	Ska 6-16	Arkose	Grain supported	0.71 mm	Medium 0.50 mm	Sub-angular	Well	Qtz. K-fsp. Plag. Mica Seric.	R.F. Hem Opaq.	III	II	The grains are fractured.
	Ska 4-16	Arkose	Grain supported	1.11 mm	Medium 0.46 mm	Sub-rounded	Well	Qtz. K-fsp. Plag. Mica Seric.	Hem. Opaq	III	II	Deformation cracks, filled with polycrystalline quartz.
	Ska 2-13-16	Arkose	Grain supported	1.00 mm	Coarse sand	Angular	Well	Qtz. K-fsp. Plag. Mica Seric.	Hem. R.F Opaq	II/III	III	
	Ska 2-12-16	Arkose	Grain supported	1.01mm	Coarse 0.54 mm	Sub-rounded to rounded	Well	Qtz. K-fsp. Plag. Mica Seric.	R.F Opaq	II/III	II/III	Mica is pore filling.

Facies	Sample	Lithology	Dominating framework configuration	Average of the 10 largest grains	Average grain size (mm)	Most common grain shape	Sorting	Mineral content		Feldspar preservation		Remarks/Comments
								1.	2.	K-fsp.	Plag.	
3	Ska 7-16	Green fine-grained sandstone	Grain supported	0.74 mm	Medium 0.40 mm	Sub-rounded	Moderate	Qtz. K-fsp. Plag. Mica Seric.	Hem. R.F Opaq	III	II	Mica is pore filling. Wavy zone in the thin section is filled with mica and heavy minerals.
	Ska 5-16	Grey fine-grained sandstone	Matrix supported	0.52 mm	Medium 0.28 mm	Angular to sub-angular	Poor	Qtz. K-fsp. Plag. Mica Seric.	Hem. Opaq	II/III	II/III	Fractured grains scattered, some filled with mica. Mica is pore filling.
	Ska 2-11-16	Fine-grained sandstone with a small green layer on top	Matrix supported	0.71 mm	Medium 0.37 mm	Sub-rounded to rounded	Medium to poor	Qtz. K-fsp. Plag. Mica Seric.	Hem. Opaq	II/III	II/III	Mica is pore filling. Quartz more rounded and larger than the feldspar grains.
	Ska 2-4-16	Red silty layer	Matrix supported	0.87 mm	Fine 0.25 mm	Sub-angular	Very poor	Qtz. K-fsp. Plag. Mica	Hem. Opaq	III	II	Mica occur in zones, with an enrichment of hematite In these zones.
	Ska 2-2-16	Red silty layer	Matrix supported	0.72 mm	Fine 0.20 mm	Sub-rounded	Poor	Qtz. K-fsp. Plag. Mica	Hem. Opaq	III	III	Alternating zones of fine-grained and coarser grained material. Fractures through the entire thin section.
4	Ska 13-16	Breccia	Matrix supported	3.54 mm	Very coarse	Sub-angular to angular	Poor	Qtz. K-fsp. Plag. Mica	R.F Opaq	II	III	Rock fragments of quartzite.
	Ska 10-9-16	Breccia	Grain supported		Coarse – very coarse	Sub-angular to sub-rounded	Poor	Qtz. K-fsp. Plag. Mica Seric.	R.F Opaq	II	II	Large amounts of polycrystalline quartz. Rock fragments of quartzite.

Table A.2: Thin section description from Sørhus (2017) of the Rundemellen samples, displayed according to facies. Facies 1= Congomerates, Facies 2=Sandstones, Facies 3= fine-grained sandstones, Facies 4= breccia (tillite). Qtz=quartz, K-fsp=K-feldspar, Plag=plagioclase, Seric= sericite, Hem= hematite, Opq=opaque grains, R.F.=Rock fragments.

Facies	Sample	Lithology	Dominating framework configuration	Average size of the 10 largest grains (mm)	Average grain size	Most common grain shape	Sorting	Mineral content 1.	Mineral content 2.	Feldspar preservation K-fsp.	Feldspar preservation Plag.	Remarks/Comments
1	Rund 1-13-16	Conglomerate	Grain supported	1.82	Coarse sand	Sub-rounded	Poorly-moderate	Quartz K-fsp. Plag. Mica Hem.	Seric. Opaq.	II/III	II/III	Coarse clastic conglomerate. Quartz is the most abundant mineral, and also represents the largest grains in the matrix. Rock fragments are present in the matrix together with K-feldspar, plagioclase and mica. Traces of hematite.
	Rund 1-14-16	Conglomerate	Grain supported	4.04	Very coarse	Angular to sub-rounded	Poorly sorted	Quartz K-fsp. Plag. Mica Hem.	Seric. Opaq.	II	II/III	Coarse clastic conglomerate. Quartz is the most abundant mineral, and also represents the largest grains in the matrix. A large amount of the quartz grains are polycrystalline. Rock fragments are present in the matrix together with K-feldspar, plagioclase and mica. Traces of hematite.
	Rund 1-15-16	Conglomerate	Grain supported	5.26	Gravel	Sub-angular	Very poorly sorted to poorly sorted	Quartz K-fsp. Plag. Mica Hem.	Seric. Opaq.	IV	V	Coarse clastic conglomerate. Quartz is the most abundant mineral and represents the largest grains in the matrix. Rhyolite, quartzite and granite make up a large part of the clasts in the conglomerate together with K-feldspar and illite. Rock fragments are present in the matrix together with K-feldspar, plagioclase and mica. Traces of hematite.
2	Rund 1-6-16	Sandstone	Grain supported	1.05	Medium sand	Sub-angular to sub-rounded	Well sorted	Quartz K-fsp. Plag. Mica	Seric. Opaq.	III	II	
	Rund 1-7-16	Sandstone	Grain supported	1.05	Coarse sand	Sub-angular to sub-rounded	Well sorted	Quartz K-fsp. Plag. Mica Hem.	Seric. Opaq.	III	III	

Facies	Sample	Lithology	Dominating framework configuration	Average size of the 10 largest grains (mm)	Average grain size	Most common grain shape	Sorting	Mineral content		Feldspar preservation		Remarks/Comments
								1.	2.	K-fsp.	Plag.	
2	Rund 1-9-16	Sandstone	Grain supported	1.21	Coarse sand	Sub-angular to sub-rounded	Very well sorted	Quartz K-fsp. Plag. Mica	Seric. Opaq.	III	III	
	Rund 1-10-16	Sandstone	Grain supported	1.07	Coarse sand	Sub-rounded	Well sorted	Quartz K-fsp. Plag. Mica	Seric. Opaq.	III	II/III	
	Rund 1-12-16	Sandstone	Grain supported	2.84	Very coarse sand	Sub-angular	Moderately sorted	Quartz K-fsp. Plag. Mica		IV	IV	
	Rund 2-1B-16	Sandstone	Grain supported	1.12	Coarse sand	Sub-angular to sub-rounded	Well sorted	Quartz K-fsp. Plag. Mica	Seric. Opaq.	II	III	
	Rund 2-2-16	Sandstone	Grain supported	1.01	Coarse sand	Angular to sub-angular	Well sorted	Quartz K-fsp. Plag. Mica	Seric. Opaq.	III	III	
	Rund 2-5-16	Sandstone	Grain supported	0.93	Medium sand	Sub-angular to sub-rounded	Well sorted	Quartz K-fsp. Plag. Mica	Seric. Opaq.	II	III	

Facies	Sample	Lithology	Dominating framework configuration	Average size of the 10 largest grains (mm)	Average grain size	Most common grain shape	Sorting	Mineral content		Feldspar preservation		Remarks/Comments
								1.	2.	K-fsp.	Plag.	
2	Rund 2-6-16	Sandstone	Grain supported	1.00	Coarse sand	Angular to sub-angular	Moderately to well sorted	Quartz K-fsp. Plag. Mica	Seric. Opaq.	III	III	
	Rund 2-8A-16	Sandstone	Grain supported	1.01	Medium sand	Sub-rounded	Moderately sorted	Quartz K-fsp. Plag. Mica	Seric. Opaq.	II	II	
	Rund 2-8-16	Sandstone	Grain supported	1.17	Coarse sand	Sub-angular	Well sorted	Quartz K-fsp. Plag. Mica	Seric. Opaq.	II/III	II	
3	Rund 1-11-16	Sandstone	Matrix supported	0.82	Fine-grained sand	Sub-rounded	Moderately sorted	Quartz K-fsp. Plag. Mica Hem.	Seric. Opaq.	II/III	II/III	High content of mica and sericite, which makes up large parts of the matrix. The largest grains in the sample are quartz, mostly undulating. High content of opaque grains.
	Rund 2-3-16	Sandstone	Matrix supported	0.69	Fine-grained sand	Angular to sub-angular	Poorly sorted	Quartz K-fsp. Plag. Mica Hem.	Seric. Opaq.	II/III	II/III	High content of mica and sericite, which makes up large parts of the matrix. The largest grains in the sample are quartz, mostly undulating. High content of opaque grains.
	Rund 2-7B-16	Sandstone	Matrix supported	0.61	Fine-grained sand	Sub-angular to sub-rounded	Very poorly to poorly sorted	Quartz K-fsp. Plag. Mica Hem.	Seric. Opaq.	II/III	II/III	High content of mica, which makes up large parts of the matrix. The largest grains in the sample are quartz, mostly undulating. High content of opaque grains.
4	Rund 1-5-16	Breccia	Matrix supported	4.53	Gravel to very coarse sand	Angular	Very poorly sorted	Quartz K-fsp. Plag. Mica Hem.	Seric. Opaq.	II/III	II	Matrix supported breccia with K-feldspar clasts of varying size. The matrix consists of mica and small grains of quartz, K-feldspar, plagioclase and hematite. Opaque mineral grains are abundant.

Appendix B - Point counting results

Table B.1: Results obtained from point counting of the chosen samples from Skarvemellen. Displayed according to facies. Und. = Undulatory extinction, K-fsp = K-feldspar, R.F = Rock fragment, H.M =Heavy minerals, OPQ = Opaque mineral grains, M= Mellsenn Group

Skarvemellen

| | Samples | Monocrystalline | | Polycrystalline | | Feldspar | | | | | | | | |
		Und.	Non. Und.	Undulatory	Total Qtz.	K-fsp.	Plagioc lase	Total Fsp.	R.F	Matrix	Hematite	HM/ OPQ	Porosity	Other
Facies 1	Ska 10-16	32,0 %	15,0 %	19,5 %	66,5 %	5,0 %	5,3 %	10,3 %	9,0 %	14,3 %	0,0 %	0,0 %	0,0 %	0,0 %
	Ska 2-9-16	52,5 %	5,0 %	8,8 %	66,3 %	7,5 %	7,5 %	15 %	2,3 %	12,8 %	1,5 %	1,3 %	0,8 %	0,30 %
	Ska 2-8-16	34,3 %	3,0 %	19,3 %	56,5 %	7,8 %	2,5 %	10,3 %	0,5 %	25,3 %	3,3 %	3,8 %	0,5 %	0,0 %
	Ska 2-7-16	26,0 %	8,0 %	9,0 %	43,0 %	11,3 %	3,8 %	15,0 %	6,3 %	31,3 %	1,5 %	2,8 %	0,0 %	0,3 %
	Ska 2-5-16	36,5 %	1,5 %	24,3 %	62,3 %	6,5 %	6,3 %	12,8 %	4,5 %	20,5 %	0,0 %	0,0 %	0,0 %	0,0 %
Facies 2	Ska 18-16 (M)	26,8 %	1,5 %	43,5 %	71,8 %	16,8 %	3,3 %	20,0 %	3,8 %	4,5 %	0,0 %	0,0 %	0,0 %	0,0 %
	Ska 16-16 (M)	22,5 %	5,0 %	35,3 %	62,8 %	13,5 %	3,8 %	17,3 %	1,5 %	18,3 M	0,3 %	0,0 %	0,0%	0,0 %
	Ska 9-16	29,8 %	10,5 %	5,8 %	46,0 %	17,0 %	4,0 %	21,0 %	2,5 %	29,8 %	0,0 %	0,0 %	0,8 %	0,0 %
	Ska 8-16	44,8 %	11,0 %	6,5 %	61,8 %	2,8 %	6,0 %	8,8 %	7,8 %	19,0 %	1,5 %	0,0 %	1,0 %	0,3 %
	Ska 7-16	24,8 %	14,8 %	10,5 %	50,0 %	8,8 %	7,8 %	16,5 %	1,3 %	31,3 %	1,0 %	0,0 %	0,0 %	0,0 %
	Ska 6-16	37,0 %	13,0 %	5,3 %	55,3 %	5,3 %	3,8 %	9,0 %	5,5 %	25,3 %	1,8 %	2,0 %	1,0 %	0,3 %
	Ska 4-16	31,3 %	5,5 %	11,8 %	48,5 %	8,3 %	9,5 %	17,8 %	4,3 %	27,0 %	0,5 %	0,8 %	0,5 %	0,8 %
	Ska 2-13-16	12,8 %	37,8 %	14,0 %	64,5 %	10,0 %	5,8 %	15,8 %	6,3 %	12,3 %	0,0 %	0,0 %	0,8 %	0,5 %
	Ska 2-12-16	39,8 %	8,3 %	10,0 %	58,0 %	10,5 %	6,8 %	17,3 %	5,8 %	14,8 %	0,3 %	2,5 %	1,3 %	0,3 %
Facies 3	Ska 5-16	16,0 %	5,8 %	1,0 %	22,5 %	5,8 %	3,5 %	9,3 %	0,5 %	64,0 %	1,3 %	1,0 %	1,5 %	0,0 %
	Ska 2-11-16	28,0 %	3,8 %	4,0 %	35,8 %	3,0 %	2,5 %	5,8 %	2,0 %	54,0 %	1,3 %	1,0 %	0,5 %	0,0 %
	Ska2-4-16	17,8 %	5,8 %	0,8 %	24,3 %	1,8 %	3,5 %	5,3 %	1,0 %	45,3 %	22,3 %	1,5 %	0,0 %	1,0 %
Facies 4	Ska 13-16	20,0 %	1,0 %	11,0 %	32,0 %	9,0 %	5,3 %	14,0 %	6,0 %	44,8 %	0,3 %	3,0 %	0,0%	0,0%

Table B.2: Point counting results from Sørhus (2017) of the chosen samples from Rundemellen. Displayed according to facies. Und. = Undulatory extinction, K-fsp = K-feldspar, R.F = Rock fragment, H.M =Heavy minerals, OPQ = Opaque mineral grains.

Rundemellen

	Samples	Monocrystalline		Polycrystalline		Feldspar								
		Und.	Non. Und.	Undulatory	Total Qtz.	K-fsp.	Plagio clase	Total Fsp.	R.F	Matrix	Hematite	HM/ Opaque	Porosity	Other
Facies 1	Rund 1-13-16	57,0 %	6,0 %	7,7 %	70,7 %	6,5 %	2,5 %	9,0 %	2,0 %	17,2 %	0,0 %	0,2 %	0,2 %	0,5 %
	Rund 1-14-16	59,5 %	10,0 %	15,5 %	85,0 %	4,7 %	0,2 %	4,9 %	5,0 %	3,7 %	0,0 %	0,2 %	1,2 %	0,0 %
Facies 2	Rund 1-7-16	43,5 %	6,3 %	7,0 %	56,8 %	9,0 %	3,2 %	12,2 %	7,0 %	21,5 %	0,0 %	1,5 %	0,0 %	0,2 %
	Rund 1-10-16	52,5 %	7,3 %	15,5 %	75,3 %	7,2 %	1,5 %	8,7 %	2,5 %	13,0 %	0,0 %	0,5 %	0,0 %	0,0 %
	Rund 1-11-16	37,5 %	6,5 %	3,5 %	47,5 %	12,0 %	3,7 %	15,7 %	1,2 %	33,5 %	0,0 %	0,2 %	1,7 %	0,2 %
	Rund 2-8-16	45,3 %	7,8 %	17,7 %	70,8 %	10,2 %	2,0 %	12,2 %	0,5 %	16,5 %	0,0 %	0,0 %	0,0 %	0,0 %
	Rund 2-6-16	43,0 %	8,0 %	6,5 %	57,5 %	8,1 %	3,0 %	11,1 %	6,7 %	22,0 %	0,0 %	2,5 %	0,2 %	0,0 %
	Rund 2-5-16	51,2 %	3,3 %	6,0 %	60,5 %	3,5 %	2,5 %	6,0 %	3,2 %	27,7 %	0,7 %	1,2 %	0,5 %	0,2 %
	Rund 2-2-16	52,5 %	7,7 %	7,7 %	67,9 %	12,0 %	2,2 %	14,2 %	3,5 %	14,2 %	0,0 %	0,2 %	0,0 %	0,0 %
Facies 3	Rund 2-7B-16	9,4 %	2,4 %	0,2 %	11,8 %	9,5 %	0,7 %	10,2 %	0,2 %	70,2 %	0,7 %	6,2 %	0,7 %	0,0 %
	Rund 2-3-16	15,8 %	4,2 %	0,7 %	20,7 %	3,2 %	1,0 %	4,2 %	0,7 %	66,7 %	0,0 %	7,7 %	0,0 %	0,0 %
Facies 4	Rund 1-5-16	17,0 %	4,0 %	12,5 %	33,5 %	26,6 %	2,7 %	29.3 %	2,5 %	24,0 %	0,3 %	9,7 %	0,7 %	0,0 %

Appendix C – XRD%

Table C.1: Skarvemellen mineral estimation from XRD, in weight %, displayed stratigraphically.

Samples	Wt.% Quartz	Wt.% K-Feldspar	Wt.% Plagioclase	Wt.% Mica	Wt.% Illite	Wt.% Hematite	Wt.% Chlorite	Wt.% Rutile	% Sum
Ska 21-16	28,5	0,0	5,7	51,7	0,0	0,0	11,2	2,9	100,0
Ska 18-16	70,6	23,2	5,4	0,8	0,0	0,0	0,0	0,0	100,0
Ska 16-16	64,1	25,4	7,9	2,6	0,0	0,0	0,0	0,0	100,0
Ska 15-16	66,2	11,5	17,4	4,9	0,0	0,0	0,0	0,0	100,0
Ska 13-16	54,1	20,1	20,3	4,2	0,0	1,3	0,0	0,0	100,0
Ska 11-16	43,3	13,2	28,1	15,4	0,0	0,0	0,0	0,0	100,0
Ska 10-16	62,2	15,9	16,5	5,4	0,0	0,0	0,0	0,0	100,0
Ska 9-16	53,6	15,8	2,4	28,1	0,0	0,1	0,0	0,0	100,0
Ska 8-16	47,7	13,8	4,0	20,7	10,2	3,6	0,0	0,0	100,0
Ska 7-16	41,9	8,2	1,9	48,0	0,0	0,0	0,0	0,0	100,0
Ska 6-16	56,4	20,0	4,2	15,4	0,0	4,0	0,0	0,0	100,0
Ska 5-16	46,3	12,4	0,5	40,8	0,0	0,0	0,0	0,0	100,0
Ska 4-16	58,6	24,2	5,0	12,2	0,0	0,0	0,0	0,0	100,0
Ska 2-13-16	60,3	28,9	7,4	3,4	0,0	0,0	0,0	0,0	100,0
Ska 2-12-16	65,5	24,5	7,5	2,5	0,0	0,0	0,0	0,0	100,0
Ska 2-11-16	38,9	12,7	0,1	47,0	0,0	1,3	0,0	0,0	100,0
Ska 2-9-16	70,5	19,5	6,0	3,1	0,0	0,9	0,0	0,0	100,0
Ska 2-8-16	63,5	20,9	5,3	10,3	0,0	0,0	0,0	0,0	100,0
Ska 2-7-16	50,4	19,7	4,3	20,7	0,0	4,9	0,0	0,0	100,0
Ska 2-5-16	75,4	17,4	3,2	4,0	0,0	0.0	0,0	0,0	100,0
Ska 2-4-16	41,5	7,1	0,7	29,3	16,3	5,1	0,0	0,0	100,0
Ska 2-2-16	39,3	8,6	0,0	49,1	0,0	3,0	0,0	0,0	100,0

Table C.2: Rundemellen mineral estimation from XRD, in weight %, displayed stratigraphically. Results from Sørhus (2017).

Samples	Wt.% Quartz	Wt.% K-Feldspar	Wt.% Plagioclase	Wt.% Mica	Wt.% Hematite	% Sum
Rund 1-5-16	24,9	38,7	8,3	17,3	10,8	100,0
Rund 2-7B-16	27,0	16,6	0,0	53,6	2,8	100,0
Rund 2-3-16	35,5	22,9	0,5	33,9	7,2	100,0
Rund 1-11-16	44,0	24,0	2,0	30,0	0,0	100,0
Rund 1-12-16	70,9	20,5	3,6	4,8	0,2	100,0
Rund 2-5-16	52,7	21,3	0,0	26,0	0,0	100,0
Rund 1-8-16	53,0	25,8	3,5	17,7	0,0	100,0
Rund 1-7-16	54,1	25,9	6,8	13,2	0,0	100,0
Rund 1-3-16	57,4	23,6	6,5	12,5	0,0	100,0
Rund 2-8-16	58,7	15,9	0,0	23,3	2,1	100,0
Rund 2-6-16	60,7	21,0	0,0	18,3	0,0	100,0
Rund 1-6-16	63,3	21,1	6,6	9,0	0,0	100,0
Rund 2-8A-16	63,5	16,8	0,0	19,7	0,0	100,0
Rund 2-2-16	74,6	19,5	3,2	2,4	0,3	100,0
Rund 1-9-16	67,7	23,8	6,2	0,0	2,3	100,0
Rund 1-13-16	74,3	18,2	2,1	5,4	0,0	100,0
Rund 2-1B-16	74,7	20,5	2,6	2,0	0,2	100,0
Rund 1-15-16	78,1	14,2	3,3	4,4	0,0	100,0
Rund 1-14-16	86,8	7,6	3,9	1,7	0,0	100,0
Rund 1-10-16	60,7	27,8	5,5	6,0	0,0	100,0

Appendix D – Quartz/total feldspar content

Table D.1: Values for the quartz/total feldspar content (Figure 4.17) based on XRD analyses (Appendix C) from Skarvemellen.

Sample	Quartz/total feldspar
Ska 21-16	5
Ska 18-16	2,5
Ska 16-16	1,9
Ska 15-16	2,3
Ska 13-16	1,3
Ska 11-16	1,0
Ska 10-16	1,9
Ska 9-16	2,9
Ska 8-16	2,7
Ska 7-16	4,2
Ska 6-16	2,3
Ska 5-16	3,6
Ska 4-16	2,0
Ska 2-13-16	1,6
Ska 2-12-16	2,0
Ska 2-11-16	3,0
Ska 2-9-16	2,8
Ska 2-8-16	2,4
Ska 2-7-16	2,1
Ska 2-5-16	3,7
Ska 2-4-16	5,3
Ska 2-2-16	4,6

Appendix E – Heavy minerals

Table E.1: Results from the heavy mineral analyses. R=remnants, At (Anatas), Ap (Apatite), Ca (calcium amphibole), Cp (clinopyroxene), Ep (epidote), Gt (garnet), Mo (monazite), Op (orthopyroxene), Ru (rutile), To (Tourmaline). Skarvemellen: Ska 2-4-16 = fine-grained sandstone, Ska 6-16, Ska 8-16, Ska 2-12-16 and Ska 16-16 = sandstones, Ska 10-9-16 = breccia. Rundemellen (results from Sørhus, 2017): Rund 1-5-16= breccia, Rund 2-5-16, Rund 2-6-16, Rund 1-7-16, Rund 1-8-16 and Rund 2-8-16 = sandstone. Hedmark Group: Ring 0 = Ring Formation, Rin 2-15 = Brøttum Formation, BK 1= Biri chalk from the Biri Formation, MB 1= Moelv Brygge representing the Moelv Tillite.

Samples	At	Ap	Ca	Cp	Ep	Gt	Mo	Op	Ru	Sp	To	Zr	total	count
Ska 2-4-16		27,5							0,5			72,0	100,0	200
Ska 6-16		1,0									R	99,0	100,0	200
Ska 8-16		17,0									5,0	78,0	100,0	200
Ska 10-9-16		21,5	R	R							2,5	76,0	100,0	200
Ska 2-12-16									4,5			95,5	100,0	22
Ska 16-16												(8)	0,0	8
Rund 1-5-16		2,0				0,5			1,5			96,0	100,0	200
Rund 2-5-16			0,5	0,5	1,0		R					98,0	100,0	200
Rund 2-6-16		2,0	1,0					1,0			0,5	95,5	100,0	200
Rund 1-7-16		4,0									0,5	95,5	100,0	200
Rund 1-8-16			1,0		2,9	1,0						95,1	100,0	105
Rund 2-8-16					1,8							98,2	100,0	55
Ring 0		73,5				1,5	0,5		R	R	1,0	23,5	100,0	200
Rin 2-15		49,0									1,0	50,0	100,0	200
BK 1		32,4	5,9						2,9		32,4	26,4	100,0	34
MB 1	0,5	75,5		R		R	R		0,5		0,5	23,0	100,0	200

Appendix F – Strike/dip

Table F.1: Strike/dip measurements collected from Skarvemellen

Skarvemellen	
Strike/dip	**Strike/dip**
243/38	255/36
248/33	258/33
250/31	256/33
253/35	257/33
260/38	258/29
250/32	262/30
247/30	253/34
256/30	270/30
250/33	258/32
250/33	258/35
248/30	248/41
254/32	255/38
248/35	250/42
247/30	260/45
254/31	252/35
355/32	260/54
252/30	256/30
253/34	247/31
250/30	263/54
252/30	257/38
252/32	260/32

Table F.2: Strike/dip measurements collected from Rundemellen

Rundemellen	
Strike/dip	**Strike/dip**
260/88	263/80
265/82	267/77
267/78	255/80
260/60	264/66
265/58	265/63
261/70	267/72
259/60	263/70
259/50	258/80
259/65	249/68
258/67	250/40
254/60	254/63
261/52	247/49